uOttawa

L'Université canadienne
Canada's university

FACULTÉ DES ÉTUDES SUPÉRIEURES ET POSTOCTORALES

uOttawa

L'Université canadienne
Canada's university

FACULTY OF GRADUATE AND POSDOCTORAL STUDIES

Mo´mena Dawood

AUTEUR DE LA THÈSE / AUTHOR OF THESIS

M.Sc. (Cellular and Molecular Medicine)

GRADE / DEGREE

Department of Cellular and Molecular Medicine

FACULTÉ, ÉCOLE, DÉPARTEMENT / FACULTY, SCHOOL, DEPARTMENT

Studies on the Molecular and Functional Analysis of Tail-Anchored Membrane Associated Protein (SLMAP) in Drosophila melanogaster

TITRE DE LA THÈSE / TITLE OF THESIS

Dr. B. Tuana

DIRECTEUR (DIRECTRICE) DE LA THÈSE / THESIS SUPERVISOR

CO-DIRECTEUR (CO-DIRECTRICE) DE LA THÈSE / THESIS CO-SUPERVISOR

EXAMINATEURS (EXAMINATRICES) DE LA THÈSE / THESIS EXAMINERS

Dr. J. Copeland

Dr. M. Ekker

Dr. M. Sonnerfeld

Gary W. Slater

Le Doyen de la Faculté des études supérieures et postdoctorales / Dean of the Faculty of Graduate and Postdoctoral Studies

Studies on the Molecular and Functional Analysis of Tail-Anchored Membrane Associated Protein (SLMAP) in *Drosophila melanogaster*

By

M'omena A. Dawood

Department of Cellular and Molecular Medicine
Faculty of Medicine
University of Ottawa
Ottawa, Ontario, Canada

September 10, 2006

This thesis is submitted as a partial fulfillment of the M.Sc. degree program in the Department of Cellular and Molecular Medicine

Your file Votre référence
ISBN: 978-0-494-25761-6
Our file Notre référence
ISBN: 978-0-494-25761-6

This work is dedicated to my parents.

ACKNOWLEDGEMENTS

It is a pleasure to acknowledge the encouragement, help and cooperation of my mentors, Dr. Balwant Tuana, for his sound guidance, tremendous support and help in presenting this project and Dr. Margaret Sonnenfeld who has given me constant encouragement and advice. I owe a dept of gratitude to Maysoon Salih for her continuous support and helpful suggestions that made a difference in this project.

I would also like to thank my colleagues; Joseph Byers, Puneet Singh, Moni Nader, Xuetao Sun, Lunde Huang, Tatiana Morozova, Helina Tadesse and Nasrin Habibi for their on going support during my graduate studies.

Lastly I wish to thank my parents for their continued encouragement and support throughout my academic research. Special thanks to my sister Mai and my brothers Bashar and Tariq, and special thanks to Hazim and his family.

ABSTRACT

Previous work in our lab identified a novel gene encoding a unique family of tail-anchored α-helical coiled-coil proteins termed SLMAPs (sarcolemmal membrane associated proteins) that were highly conserved in rodents and humans. Alternative splicing yields three SLMAP isoforms: a ubiquitously expressed isoform (SLMAP3), and two tissue-specific variants (SLMAP1 and SLMAP2). The salient features of SLMAP are a hydrophobic C-terminal sequence, which targets membranes, a central coiled-coil structure and N-terminal fork head associated domain (FHA). A sequence in fruit flies (corresponding to CG17494 in flybase) was identified that shares 28.6% identity with the full-length mammalian SLMAP3 amino acid sequence. However, a 55.9% identity was identified at the fork head associated domain of *Drosophila* and SLMAP3 isoform, whereas a 25% identity was shared at the C-terminal transmembrane domain. The rest of the protein was predicted to form a coiled-coil structure. In view of these similarities with the mammalian SLMAP3 isoform, this *Drosophila* gene was designated *Dslmap*.

In situ hybridization on whole mount embryos revealed a ubiquitous expression of *Dslmap* mRNA throughout various stages of embryonic development. To study the function of *Dslmap* during embryonic development, a GAL4-driven hairpin-induced RNA interference (RNAi), as well as overexpression experiments were performed. The Gal4/UAS binary system was used to allow hairpin RNA to conditionally silence *Dslmap* expression in *Drosophila*. A pan-neuronal driver (*Elav*-Gal4) that expresses GAL4 in every cell of the nervous system from embryogenesis onward was mated to transgenic flies carrying the activatable *Dslmap* RNAi vectors. The resulting phenotypes revealed dramatic defects in the development of axon scaffold in the fly central nervous system

(CNS) with particular structural defects within the longitudinal connectives and commissures. An overexpression construct was also made using pUAST vector carrying the full length *Dslmap* cDNA in frame with a yeast upstream activator sequence (UAS) to generate transgenic lines. Overexpression in the transgenic lines was activated by mating with the CNS Gal4 lines, which resulted in phenotypes that revealed similar defects in the CNS to those observed in the RNAi lines. These data revealed that the *Drosophila* genome contains a SLMAP homologue, which is ubiquitously expressed and plays a critical role in developing neurons and glia.

TABLE OF CONTENTS

CHAPTER THREE

LIST OF FIGURES

Page x missing.

LIST OF ABBREVIATIONS

Arm	Armadillo
BLAST	Basic Local Alignment Search Tool
CIP	Calf Intestinal Phosphatase
cnn	Centrosomin gene
CNS	Central nervous system
Dslmap	*Drosophila* sarcolemmal membrane associated protein
E-C	Excitation-contraction
EGFP	Enhanced Green Fluorescent Protein
ELAV	Embryonic lethal abnormal vision
ER	Endoplasmic Reticulum
FHA	Fork head associated domain
Gcm	Glial cells missing
IR	Inverted Repeat
Ln	line (pertaining to certain fly lines)
M1	1st initiating methionine
M2	2nd initiating methionine
MTOC	Microtubule organizing center
PCR	Polymerase Chain Reaction
PNS	Peripheral nervous system
PTGS	Post Transcriptional Gene Silencing
pUAST	Upstream activating sequence transformation vector

pWIZ	White intron zipper vector
RdRP	RNA dependent RNA polymerase
Reg	Region
RISC	RNA induced silencing complex
RNAi	RNA interference
RT	Room Temperature
siRNA	short interfering RNA
SLMAP	Sarcolemmal Membrane Associated Protein
SMART	Simple Modular Architecture Research Tool
SNAREs	*s*oluble *N*-ethylmaleimide-sensitive factor attachment protein receptor
TA	Tail-anchored
TMD	Transmembrane Domain
UAS	Upstream activating sequence
Wt	Wild type
XNP	X-linked nuclear protein

INTRODUCTION

1.1 Genes in Development

Major advances have been made in developmental biology due to the ability to manipulate genes that control embryonic development. In order to establish a clear picture of the precision with which the embryo develops and progresses to the generation of the adult phenotype, we still need to identify those genes that are critically involved in controlling development. Development is regulated by the temporal activation of distinct genes which are essential for growth, patterning, and cell differentiation; all are key events in the establishment of organized structures from an initially very simple group of cells. In order to define the function of novel genes, various model systems have been established. In vertebrates, the frog *Xenopus*, the mouse, the chick, and currently the zebrafish, are the key model systems now studied. Among invertebrates, the fruit fly *Drosophila melanogaster* and the nematode worm *Caenorhabditis elegans* are currently the best models in understanding developmental genetics due to the ease of performing genetic manipulations.

Each developmental model system has its own advantages and disadvantages. For example, the chick embryo has been an excellent model system to investigate the mechanisms underlying pattern formation in the central nervous system of vertebrates (Tufan *et al.*, 2004). This was accomplished due to the availability of fertile eggs, and the ability to access the embryo outside the mother along with the fact that it is well suited for embryological manipulation such as, transplants of limbs, notochord or neural crest (Storey *et al.*, 1995). However, a disadvantage of this system stems from the fact

that it is difficult to perform genetic manipulations and as a consequence little is known about the chick's developmental genetics. A closer model organism to humans is the mouse, where a great deal of genetics is known and many developmental mutations have been identified. However, like all mammals, the mouse embryo develops inside the mother, making it difficult to carry out experimental embryonic manipulation; additionally the mutations of interest can be lethal at an early embryonic stage. Further complications arise from the high genetic redundancy in vertebrates, which may mask the effects of mutations in single genes (Carroll *et al.*, 2003). Due to the limitations associated with the mouse model, alternative model systems, with less similarity to humans, are utilized where genetic manipulations can be more easily applied. The *D. melanogaster* and *C. elegans* in particular serve this purpose and continue to play an essential role in the functional analysis of developmental genes. *Drosophila* has the greatest wealth of genetic studies combined with the ease of genetic and microsurgical manipulations making it one of the most famous invertebrates studied. In addition, there is a high degree of molecular similarity between flies and mammals (Adams *et al.*, 2000; Rubin *et al.*, 2000). For example, most of the major neurotransmitters and the channels for neurotransmission that are identified in mammals and flies share a high level of similarity (Littleton and Ganetzky, 2000; Lloyd *et al.*, 2000). An example to illustrate this point is netrins and the netrin receptors, which have been shown to be conserved in *C. elegans*, *D. melanogaster* and mice (Kennedy *et al.*, 1994). Mutations in the function of genes encoding netrins and the netrin receptors result in a similar phenotype in all three species. These mutations consisted of misrouting of commissural axons and their

failure to be attracted toward the midline as well as a failure of some longitudinal axons to avoid the midline (Keleman and Dickson, 2001; Serafini *et al.*, 1996).

1.2 Fruit fly as a model organism

D. melanogaster has been widely used to study genetics and developmental biology. It has the longest history of any model organism and as a result an immense volume of data has accumulated about fly biology. In addition, the short life cycle of fruit fly has made it more practical and convenient to use as a model system. The life cycle of *Drosophila melanogaster* produces new adults in two weeks; eight days in the egg and larval stages, and six days in the pupal stage. During the two week period and once the embryo has completed cleavage and gastrulation, the embryo becomes segmented and hatches out as a larva. The larva has two molting periods (3 instars), which result in the shedding of cuticle, mouth, hooks, and spiracles. In the final stage, the third instar forms a pupa which undergoes metamorphosis to generate the adult fly (Fig. 1).

Over the years, *D. melanogaster* has contributed to many scientific discoveries including: the creation of the first chromosome maps in 1913 by Alfred H Sturtevant, the discovery that X-rays cause increased rates of mutations in 1926 by H.J. Muller, the 1995 Nobel prize for pattern formation (Nüsslein-Volhard and Wieschaus), and the identification of many genetic pathways such as those involved in the Notch signaling pathway. The Notch pathway regulates genes involved in multiple differentiation processes during the development of *Drosophila* and *C. elegans* (Greenwald, 1998; Simpson, 1997). Mutations in components of the Notch pathway result in notching of the

Figure 1. Life cycle of the fruit fly.

The developmental period for *Drosophila melanogaster* takes 2 weeks at 25°C. The Females lay around 400 eggs (embryos), which are about 0.5 millimeters long. Twenty four hours after fertilization and upon completion of cleavage and gastrulation, the embryo develop and hatch into a worm-like larva. The larva eats and grows continuously through two molts (3 instars). After two days as a third instar larva, an immobile pupa forms which undergoes metamorphosis for four days after which the adult fly emerges. Adapted from Wolpert *et al.*, 2002.

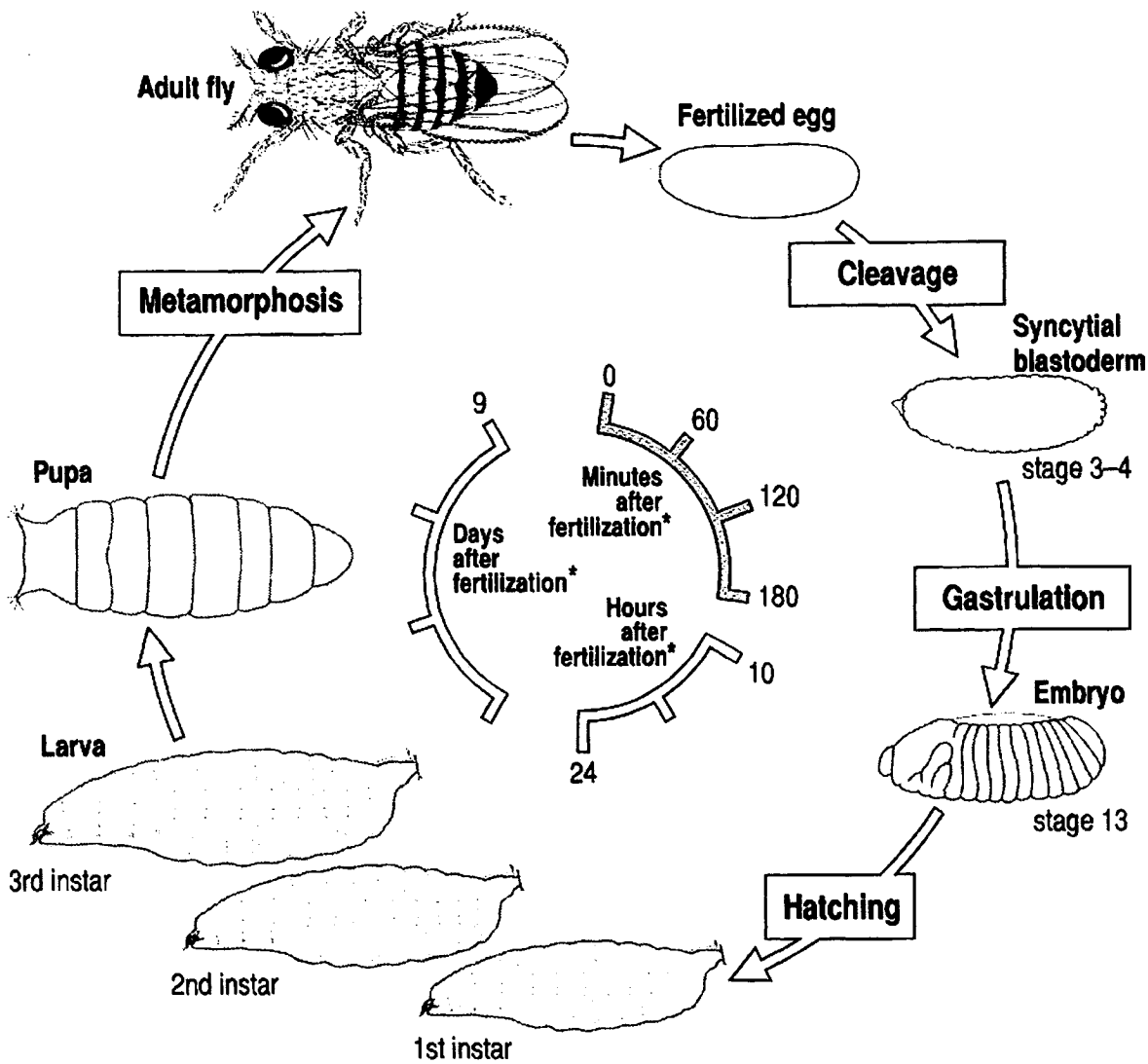
Adult fly
Fertilized egg
Cleavage
Syncytial blastoderm
stage 3–4
Gastrulation
Embryo
stage 13
Hatching
1st instar
2nd instar
3rd instar
Larva
Pupa
Metamorphosis
0
60
120
180
10
24
9
Minutes after fertilization*
Hours after fertilization*
Days after fertilization*

wing margin in flies (Irvine, 1999; Wu and Rao, 1999). However, in vertebrates, reductions in the ligand Delta3 component of this pathway result in defects that include axial skeletal malformations (e.g. spondylocostal dysostosis) (Conlon *et al.*, 1995). Therefore, it is not necessary for the phenotypes observed in vertebrates and invertebrate to be similar; the only critical aspect of the invertebrate model is that it identifies essential components acting as part of a common molecular pathway.

In this thesis, the fruit fly model system was utilized to establish a role for a tail-anchored membrane protein termed (SLMAP) which has been identified in mammals and whose function remains to be elucidated.

1.3 Tail-anchored membrane proteins

Tail-anchored (TA) membrane proteins represent a distinct class of integral membrane proteins that possess a single hydrophobic transmembrane segment at their C-terminus (Wattenberg and Lithgow, 2001). This transmembrane segment ranges from 15-22 amino acids in length, and has the capacity for post-translational integration into a target membrane such that the majority of the protein faces the cytosol (Abell *et al.*, 2003; Wattenberg and Lithgow, 2001). TA proteins perform a variety of functions, such as regulation of apoptosis, metabolism, membrane fusion and signal transduction (Cory and Adams, 2002). Examples of TA proteins include: the SNARE proteins of the Vamp/synaptobrevin and syntaxin families, TOM translocase components of mitochondria, cytochrome P450, monoamine oxidase, and the apoptotic proteins Bcl-2 and Bax (Watternberg and Lithgow, 2001).

TA proteins play an important role in membrane fusion, an essential process involved in diverse cellular events such as fertilization and neurosecretion (Robinson and

Martin, 1998). A family of C-terminal tail-anchored membrane proteins collectively known as SNAREs (*s*oluble *N*-ethylmaleimide-sensitive factor attachment protein receptor) mediates the fusion of intracellular transport vesicles (Sollner *et al.*, 1993; Bajjalieh, 1999). This is an essential step in the transport of macromolecules between organelles and in exocytosis (Knecht and Grubmuller, 2003). There is one SNARE (v-SNARE), which is tail-anchored into the membranes of transport vesicles, and two or more SNAREs (t-SNAREs) which are tail-anchored in the membranes of target compartments (Xue and Zhang, 2002). The assembly of the t- and v- SNAREs into a stable trans-SNARE complex brings the vesicle close to the target membrane and promotes membrane fusion (Xue and Zhang, 2002; Knecht and Grubmuller, 2003). Membrane fusion is also essential in synaptic transmission which is the primary form of communication in the central nervous system (CNS) (Kidokoro, 2003). Most of our understanding of synaptic transmission comes from mutational analysis of the SNARE proteins in *Drosophila* (Kidokoro, 2003) which highlights the significance of the invertebrate model system in developmental biology.

The TA proteins in the Bcl-2 family are key regulators of apoptosis. Members of the Bcl-2 family in mammals include: the anti-apoptotic members such as Bcl-2 and Bcl-X which promote cell survival and the pro-apoptotic members promoting programmed cell death e.g. Bax, Bad and Bak (Corey and Adams, 2002). The anti-apoptotic proteins (Bcl-2 and Bcl-X) are tail-anchored via their C-terminal transmembrane domain to the membranes of mitochondria and the endoplasmic reticulum (ER) (Nguyen *et al.*, 1993; Lithgow *et al.*, 1994). The targeting of these proteins ultimately results in the sequestering of different apoptotic regulatory molecules from the cytoplasm to their site

of action indicating the importance of tail-anchors in apoptosis. A Bcl-2 pro-survival like protein has been identified in *Drosophila*, referred to as *Buffy* (Quinn *et al.*, 2003). *Buffy* shares several conserved motifs with the mammalian Bcl-2 including the C-terminal hydrophobic membrane anchor which suggests once again the importance of the hydrophobic anchor (Quinn *et al.*, 2003). Ablation of *Buffy* by RNA interference (RNAi) results in ectopic apoptosis, whereas overexpression of Buffy leads to inhibition of programmed cell death (Quinn *et al*, 2003).

Thus tail-anchored membrane proteins regulate distinct functions ranging from membrane fusion in the developing CNS to the regulation of apoptosis. In view of the importance of this class of molecules we propose to define whether a novel tail-anchored membrane protein termed SLMAP, has an orthologue in *D. melanogaster*.

1.4 Sarcolemmal Membrane Associated Proteins (SLMAPs)

In order to define the molecular components of membrane junctions in myocardium that may be involved in intracellular signaling, an expression screen was devised that resulted in the isolation of a cDNA encoding Sarcolemmal Membrane Associated Proteins (SLMAPs). The mammalian SLMAP gene spans over 122 kb of genomic DNA, and consists of twenty-four exons (Guzzo *et al.*, 2004). Intron sizes range from 87-bp to over 50.5 kb of genomic DNA, whereas SLMAP exons range in size from 51-bp to over 1.8 kb (Guzzo *et al.*, 2004). There are three different SLMAP isoforms: SLMAP3 is the longest isoform whereas SLMAP1 begins at exon XIV and SLMAP2 begins at exon IX relative to SLMAP3 (Fig. 2). The three distinct SLMAP transcripts encode two muscle specific variants (SLMAP1 and SLMAP2) and a ubiquitously expressed isoform (SLMAP3) (Wigle *et al.*, 1997) (Fig. 3). Fluorescence *in situ*

hybridization indicated that a single gene located on the short arm of human chromosome 3 (3p14.3-21.2) encodes SLMAP (Wigle *et al.*, 1997; Wielowieyski *et al.*, 2000). Analysis of the structural features of the three SLMAP transcripts revealed a common carboxyl terminal sequence that is generated by alternative splicing with divergent amino-terminal sequences (Wielowieyski *et al.*, 2000) as depicted in Figure 3.

Two distinct trans-membrane domains, TMD1 and TMD2 within the extreme carboxyl terminus of all three SLMAPs and are encoded by alternative exon XXIII and exon XXIV of SLMAP3 (Wielowieyski *et al.*, 2000). Each SLMAP variant is predicted to express a single trans-membrane domain, either TMD1 or TMD2. TMD2 is only expressed if TMD1 is removed by alternative splicing, due to the presence of an in frame stop codon in the TMD1 (Wielowieyski *et al.*, 2000). Exons XX and XXI encode two leucine zipper motifs in specialized regions of the coiled-coil structure in the common carboxyl portion of SLMAPs (Wielowieyski *et al.*, 2000). The fork head associated domain is encoded by exon I of SLMAP3 (Guzzo *et al.*, 2004). Two in-frame start codons (ATG1; M1) and (ATG2; M2) are present in the full length cDNA sequence of the rabbit SLMAP3 isoform (Wigle *et al.*, 1997). The first initiating methionine (ATG1) is encoded in exon I, whereas the second initiating methionine (ATG2) resides in exon II (Guzzo *et al.*, 2004) (Fig. 2).

1.4.1 Features of the tail-anchored membrane protein SLMAP

SLMAPs possess several interesting structural features (Fig. 4). A central alpha-helical coiled-coil region containing two leucine zipper motifs; and a carboxyl-terminal TM domain make up the predominant structural features of SLMAPs (Wigle *et al.*,

Figure 2. Genomic Organization of the SLMAP gene.

A schematic illustrating that the mammalian SLMAP gene is composed of twenty four exons and introns spanning over 122 kb of genomic DNA. Regular (un-spliced) exons are shown in orange, alternatively spliced exons are shown in green and the intronic regions are shown in yellow. Trans-membrane domains are encoded by exon XXIII and exon XXIV. Exon XX and exon XXI encode the leucine zipper motifs. The Fork Head Associated (FHA) domain is encoded by exon I. ATG1 (M1; green arrow) is encoded in exon I whereas ATG2 (M2; red arrow) is present in exon II. SLMAP3 begins at the start site (green arrow) of SLMAP, whereas SLMAP2 begins at exon IX and SLMAP1 begins at exon XIV relative to SLMAP3. Arrows indicate the transcription start sites of every exon.

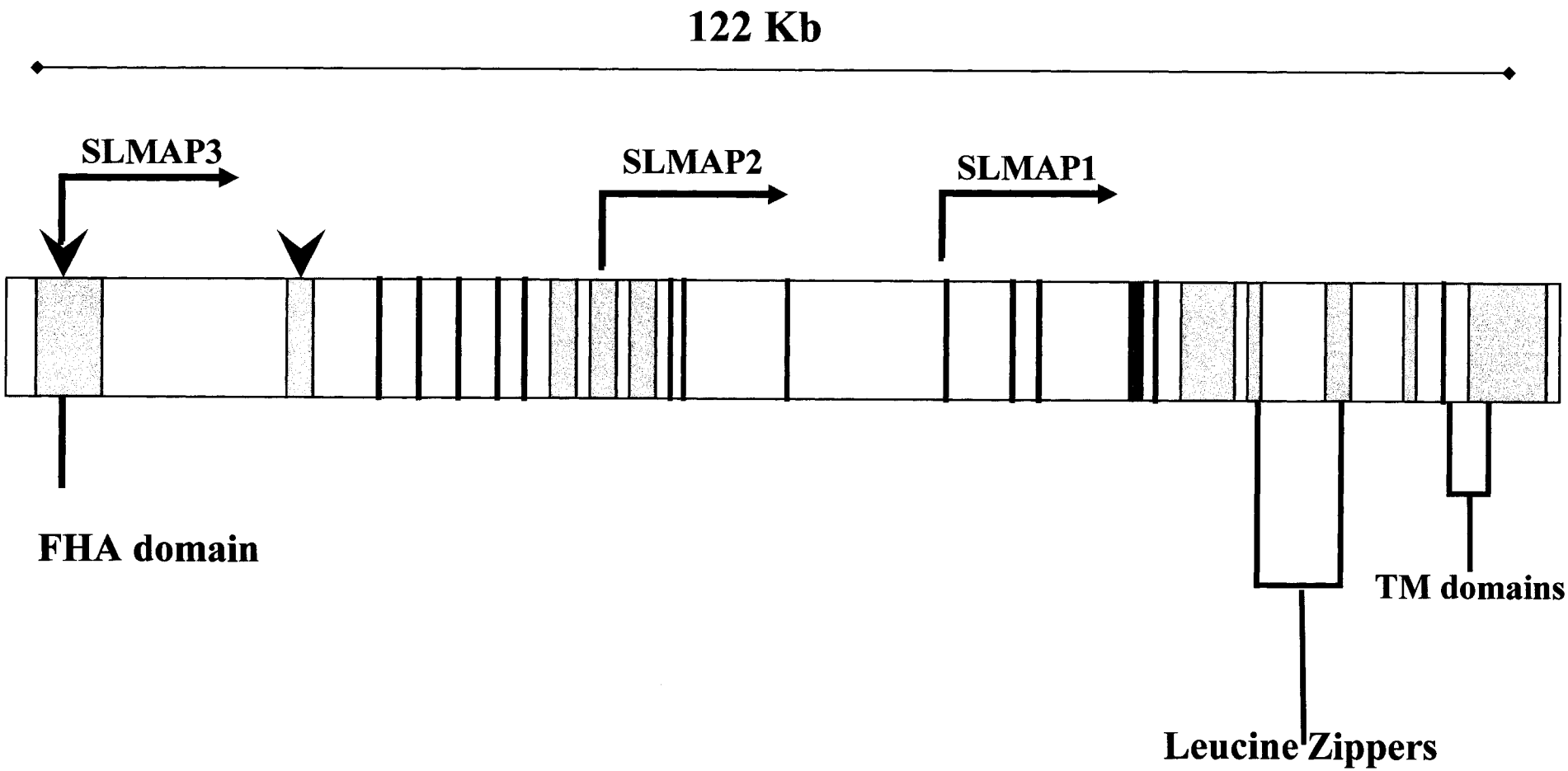
122 Kb
SLMAP3
SLMAP2
SLMAP1
FHA domain
TM domains
Leucine Zippers

Figure 3. Domain structure of the mammalian SLMAP isoforms.

Alternative splicing of a single gene econding SLMAP resulted in three distinct mRNA species. A C-terminal transmembrane domain and coiled-coil regions are common in all three isoforms. SLMAP3 is widely expressed, whereas SLMAP 1 and 2 are muscle specific variants. SLMAP3, as demonstrated by previous *in vitro* transcription-translation experiments, is generated by the utilization of one of two in-frame initiating methionines (M1 and M2). A PEST motif, which generally confers susceptibility to proteolysis is present in SLMAP3 and SLMAP2.

Adapted from Guzzo, R.M. (2003).

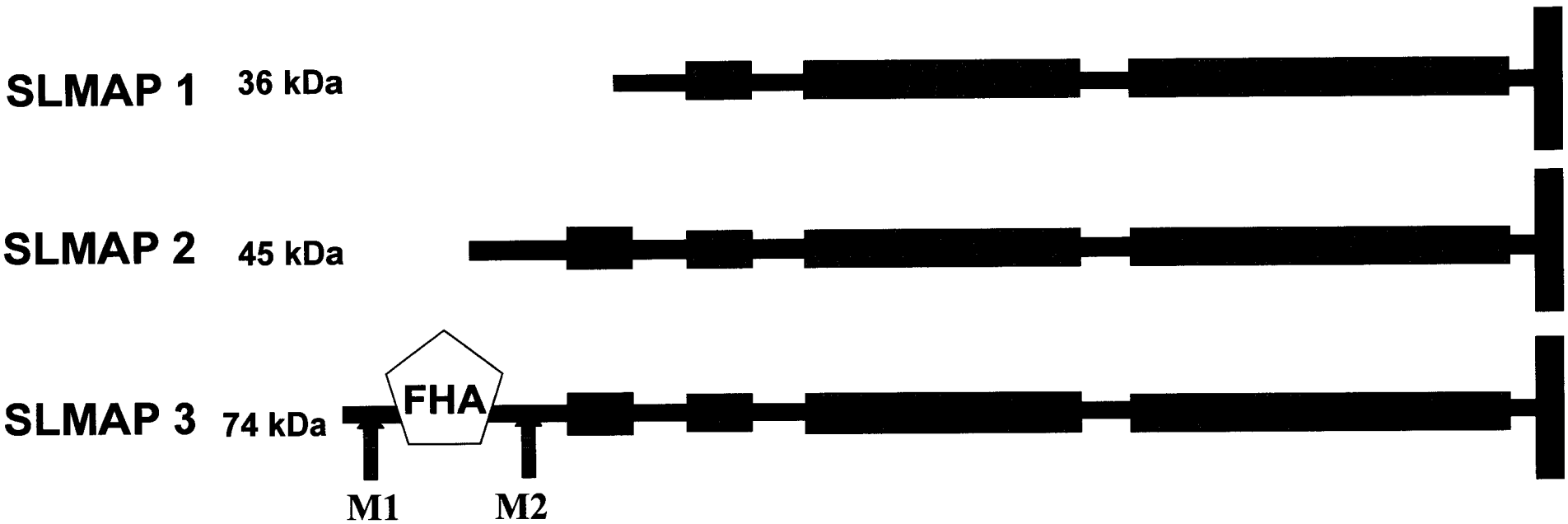

Fork head associated domain

PEST domain

Coiled coil domain

TM domain

1997). Secondary structural analysis of SLMAP predicts that the protein forms alpha-helical coiled-coil structures comprised of two leucine zipper motifs identified within the common carboxyl core of SLMAPs (Wigle *et al.*, 1997; Guzzo *et al.*, 2004). The presence of leucine-rich coiled-coil regions in SLMAP are essential for SLMAP oligomerization and were shown to mediate SLMAP-SLMAP interactions (Guzzo *et al.*, 2004). Coiled-coil structures are 2 to 5 stranded bundles of α-helices which are stabilized by hydrophobic and other interactions (Engel, 1996). Coiled-coil domains are widely used in extracellular matrix molecules to connect subunits in oligomeric proteins and confer protein stability by directing subunit oligomerization (Procopio *et al.*, 1999). Proteins that withstand considerable cellular stress such as motor proteins (myosins), extracellular proteins (laminin) and cytoskeletal components (α-keratin) harbor coiled-coil motifs (Burkhard *et al.*, 2001). Furthermore, the coiled-coil structure is a general feature in some of the proteins that are targeted to the centrosome. For example, the centrosomin protein identified in *Drosophila* is rich in coiled-coil regions and contains three predicted leucine zippers, one near the amino terminus, one in the central region of the protein and one near the carboxyl terminus. Centrosomin is a novel type of structural protein that localizes to the centrosome and plays a role in the process of midgut morphogenesis in *Drosophila* (Heuer *et al.*, 1995). Coiled-coil regions are also found in proteins that mediate membrane fusion such as SNAREs. The SNARE proteins assemble into alpha helical coiled-coil structures that bridge the gap between the synaptic vesicle and the plasma membrane. This drives membrane fusion, an essential process required for the release of neurotransmitter (Kweon *et al.*, 2003). Leucine zipper motifs are also present in various classes of proteins including: enzymes such as acetyltransferase-1

Figure 4. Structural Features of SLMAPs.

A modified schematic drawing adapted from Guzzo, R.M (2003) showing an overview of the structural features of SLMAPs and the functions associated with these features.

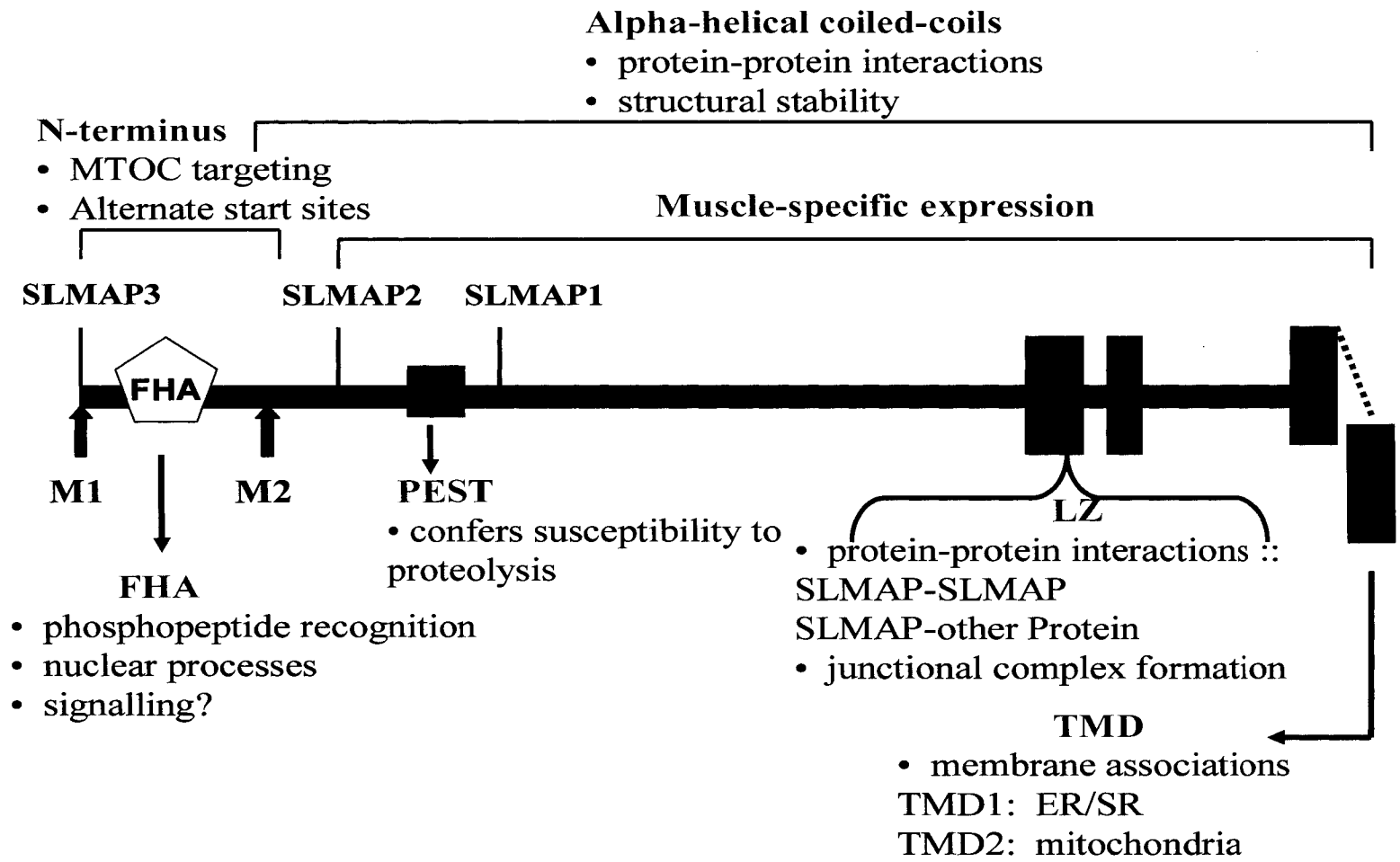
Alpha-helical coiled-coils
• protein-protein interactions
• structural stability
N-terminus
• MTOC targeting
• Alternate start sites
Muscle-specific expression
SLMAP3
SLMAP2
SLMAP1
FHA
M1
M2
PEST
• confers susceptibility to proteolysis
LZ
• protein-protein interactions ::
SLMAP-SLMAP
SLMAP-other Protein
• junctional complex formation
FHA
• phosphopeptide recognition
• nuclear processes
• signalling?
TMD
• membrane associations
TMD1: ER/SR
TMD2: mitochondria

(Ahmad *et al.*, 2001), glucose-transporter glycoproteins (Buckland and Wild, 1989) and voltage-gated Ca^{2+} channels (White and Weber, 1989). The coiled-coil region of SLMAP was demonstrated to be important in protein-protein interactions (Guzzo *et al.*, 2004). Protein-protein interaction assays revealed that SLMAP proteins can self associate and that these interactions are mediated by the leucine-rich coiled-coil motifs (Guzzo *et al.*, 2004). Overexpression of SLMAP deletion mutants defective in the homodimerization domain also compromised the fusion of myoblasts (Guzzo *et al.*, 2004).

An important aspect of cell biology concerns the mechanism involved in targeting novel proteins such as SLMAP to their proper subcellular location. The extreme C-terminus shared by all SLMAP isoforms is understood to perform this function (Wielowieyski *et al.*, 2000). SLMAPs have also been implicated in forming associations with membrane structures in cardiac cells as well as in cultured cells, and are speculated to serve a role in membrane processes (Wigle *et al.*, 1997; Wielowieyski *et al.*, 2000). The mammalian SLMAPs possess two mutually exclusive TMD (TMD1 and TMD2) at the extreme C-terminus. TMD1 targets SLMAPs to the ER whereas TMD2 targets SLMAPs to the mitochondria (Guzzo *et al*, 2004). Detergent-extraction studies have also revealed that the bulk of SLMAPs are oriented within the cytosol which confirms that SLMAPs are integral membrane proteins (Wigle *et al.*, 1997).

Another interesting feature of SLMAP is the presence of the fork head associated (FHA) domain at the extreme N-terminus of the SLMAP3 isoform encoded by exon I. The FHA domain is a phosphopeptide recognition motif known to be important in the control of transcription, DNA repair and cell cycle progression (Pike *et al.*, 2001). The

FHA domain is found in many regulatory proteins and is thought to mediate protein-protein interactions (Durocher *et al.*, 2000; Sun; *et al.*, 1998). It has also been characterized in a number of proteins of diverse function including: kinases such as Rad53 (Pike *et al.*, 2001), transcription factors (Kim *et al.*, 2002), metabolic enzymes (Durocher and Jackson, 2002), and kinesins such as the KIF1A kinesin motor protein which transports synaptic vesicle precursors in neuronal axons (Lee *et al.*, 2003). The FHA domain was revealed to target the SLMAP3 variant to the centrosome, also known as the microtubule organizing center (MTOC) (Guzzo *et al.*, 2004). This centrosomal localization of SLMAP3 suggests a fundamental role in cell division and mitosis.

The tissue-specific expression of the SLMAP isoforms suggests an important role for these proteins in regulating different developmental and molecular physiological processes. The SLMAP3 (5.9 kb) transcript was revealed to have a broad tissue expression, as its mRNA was detected in: cardiac tissue, fast and slow twitch skeletal muscle, smooth muscle, liver, pancreas, kidney, spleen, and brain (Wigle *et al.*, 1997). Whereas the SLMAP1 (3.5 kb) transcript and the SLMAP2 (4.5 kb) transcript exhibited muscle-specific expression and were solely expressed in: cardiac tissue (atria, ventricles), slow twitch skeletal muscle and smooth muscle tissue isolated from the aorta, uterus, esophagus and stomach (Wigle *et al.*, 1997). The molecular mechanism responsible for generating muscle-specific SLMAP1 and SLMAP2 expression remains to be resolved; however, the abundance of SLMAP transcripts in muscle suggests that SLMAPs perform important functions in muscle physiology. In addition, the ubiquitously expressed SLMAP isoform (SLMAP3) may serve a fundamental role in cell biology. SLMAP3 was also found to be expressed in areas of the rat brain that undergo neurogenesis and

migration such as the neonatal hippocampus, and olfactory bulbs (Wigle, 1997). SLMAP3 expression also appeared to be highly localized in the Mueller glial cells in the rodent retina and in neonatal migratory neurons (Wigle, 1997).

The abundance of SLMAP transcripts in muscle and the central nervous system led us to speculate that SLMAPs may fulfill specialized functions in the physiology of these tissues. This pattern of expression suggests a role for SLMAPs in myoblast fusion, during the process of myogenesis, and in the membrane biology of excitation-contraction (E-C) coupling in developing muscles. The expression of SLMAP *in vivo* is initiated early in skeletal myogenesis and as development progresses, SLMAP proteins become distributed within specialized membrane systems involved in calcium signaling (Guzzo *et al.*, 2004). The de-regulation of SLMAP by ectopic expression in myoblasts compromised the ability of these cells to fuse into myotubes under differentiation promoting conditions (Guzzo *et al.*, 2004). Guzzo *et al* (2004) proposed that the cardiac-specific expression of SLMAPs that can be targeted to different membrane systems, self associate, and interact with the myofibril may have a potential role in the structural arrangement of the E-C coupling apparatus. This was an important finding which may offer insights into heart disease. As identifying the molecular components necessary for the organization and stabilization of the cardiac membrane architecture would advance our understanding of cardiomyocyte function.

Since the precise function of SLMAP is unknown, we propose to use the *Drosophila* system as a model to investigate the role of SLMAP in development. We will first determine if a homologue of the mammalian SLMAP is present in fruit flies and then attempt to determine the function of this homologue using two approaches. One

utilizes an *in vivo* RNAi approach which has been applied successfully to generate a reduction-of-function phenotype while the other alternative approach will rely on gain-of-function to overexpress the *Drosophila* SLMAP *in vivo*.

1.5 RNA interference

Under most circumstances, RNA is present in a cell as a single-stranded molecule. Messenger RNA (mRNA) is synthesized in the cell nucleus and transported to the ribosomes in the cytoplasm as a single strand. Double-stranded RNA (dsRNA), in which the sense and the antisense complementary strands pair up, is normally present only in circumstances that pose a threat to the cell (Soutschek *et al.*, 2004). The mechanism of RNA interference (RNAi) is common in several posttranscriptional gene-silencing processes (PTGS) that are induced by dsRNA like co-suppression, quelling, and transgene induced silencing (Napoli *et al.*, 1990; van der Krol *et al.*, 1990). RNAi is based on an ancient defense mechanism developed by plants and invertebrates to protect against viruses, which utilizes dsRNAs to induce degradation of homologous mRNAs by endogenous enzymes (Ruiz *et al.*, 1998; Roman, 2004).

The mechanism of RNAi involves essential molecules functioning in a five step process (Fig. 5). Introduction of dsRNA into the cell can be achieved by either viral infection or micro-injection and acts as a silencing trigger. In the first step, referred to as the initiation step, an RNase III-like enzyme, termed DICER, acts through an ATP dependent process to cleave the dsRNA into 21-23 nucleotide fragments referred to as short interfering RNAs (siRNA) (Fig. 5, step 1) (Bernstein *et al.*, 2001; Ketting *et al.*, 2001; Knight and Bass, 2001). In the effector step, the siRNA duplex is unwound in an ATP dependent process by a helicase associated with the RNA-induced silencing

complex (RISC) (step 2) (Nykänen *et al.*, 2001). One strand of the siRNA duplex is incorporated into RISC which guides it to its homologous cellular sense mRNA (step 3) (Nykänen *et al.*, 2001). The bound sense mRNA is then cleaved by an RNA dependent RNA polymerase (RdRP) (Fig. 5, step 4). In the final step, RISC is released from the cleaved mRNA and recycled back into step 3 (Fig. 5, step 5).

Dslmap is one of a number of genes whose sequence is known but its function is still unknown. Moreover, no mutation in *Dslmap* has been reported so far, making it difficult to determine its function *in vivo*. However, thanks to the RNAi technology, it is now possible to study the function of any gene of interest. Furthermore, RNAi analysis has become more convenient by introducing the GAL4/UAS binary system, which targets hairpin-loop RNA in any spatial or temporal specific pattern. Currently, a wide variety of approaches have been adopted and shown to be successful in the directed expression of dsRNA constructs (Giordano *et al.*, 2002; Kalidas and Smith, 2002; Nagel *et al.*, 2002; Piccin *et al.*, 2001; Reichhart *et al.*, 2002; Schmid *et al.*, 2002; van Roessel *et al.*, 2002). The dsRNAs produced from these constructs were capable of mediating gene-specific RNAi silencing. Only a few molecules of dsRNA per cell are required to silence the expression of a gene, and the silencing effect can be transmitted through the germ line for several generations (Piccin *et al.*, 2001).

The effect of RNAi on gene expression occurs after the creation of mRNA during transcription, thus the term posttranscriptional gene silencing (PTGS) referring to the interruption of translation of the mRNA (Matzhe *et al.*, 2001). However, since RNAi may not totally abolish the expression of a gene, it is referred to as reduction-of-function, making it easier to distinguish it from procedures in which the DNA sequences encoding

Figure 5. A model for the proposed mechanism of RNA interference.

(Step 1) The initial dsRNA is cleaved into small interfering RNAs (siRNAs) by a nuclease called Dicer. The siRNAs associate with the RNA-induced silencing complex (RISC). (Step 2) RISC will be activated through unwinding of the siRNA duplex and displays nuclease activity toward mRNA. (Step 3) The altered complex would then search for its homologous cellular mRNA based upon the sequence of the antisense RNA. (Step 4) After annealing of a cellular sense mRNA strand, the complex would mark the sense mRNA for degradation. (Step 5) In the final step, RISC is liberated from the cleaved mRNA and is recycled to step 3 to continue the cycle again.

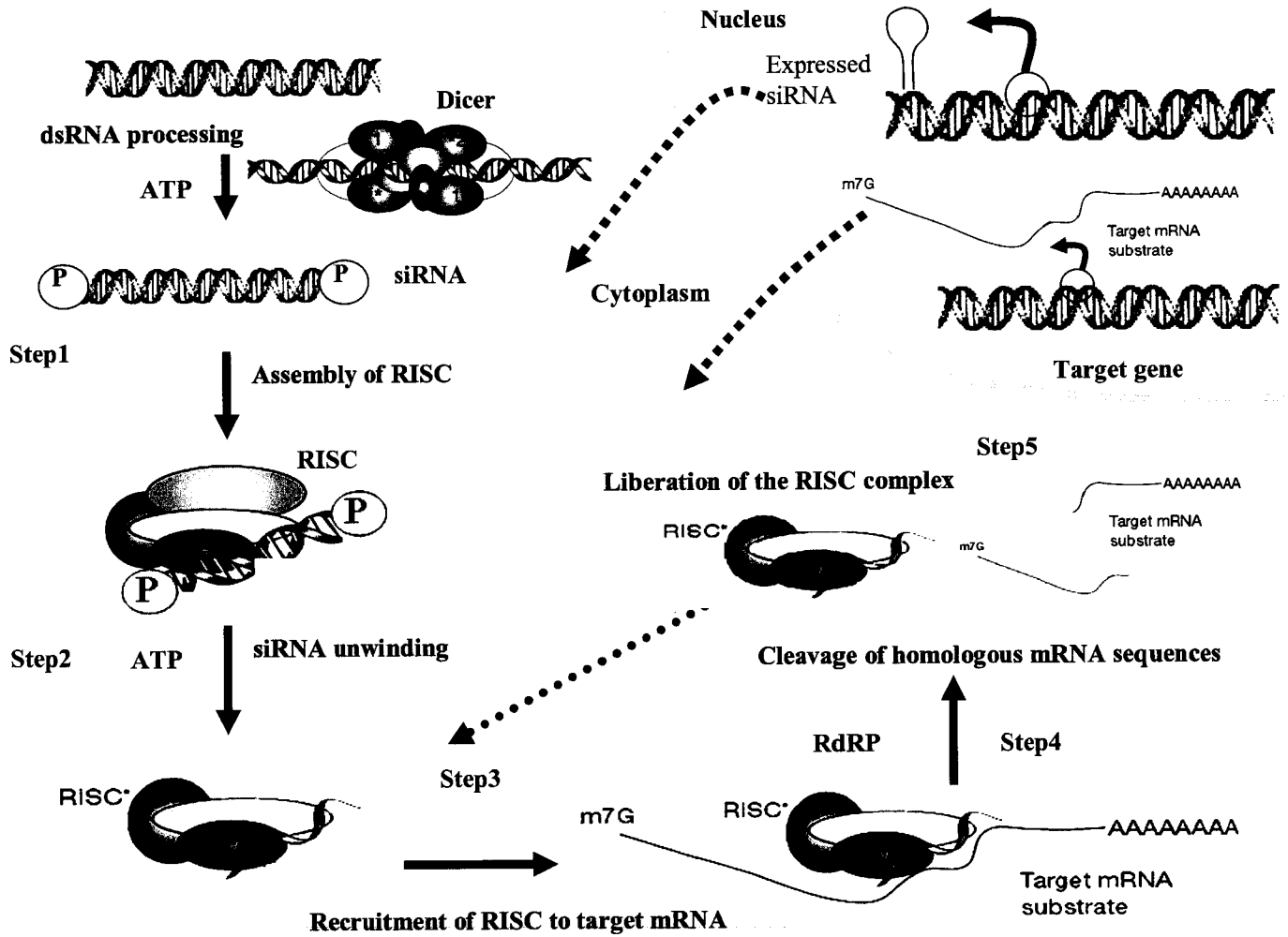
Nucleus
Expressed siRNA
Dicer
dsRNA processing
ATP
siRNA
Cytoplasm
m7G
AAAAAAAA
Target mRNA substrate
Target gene
Step1
Assembly of RISC
RISC
Step5
Liberation of the RISC complex
Step2
ATP
siRNA unwinding
Cleavage of homologous mRNA sequences
RdRP
Step4
Step3
Recruitment of RISC to target mRNA

a gene have been removed. The RNAi technique can be applied to a wide variety of species including: the nematode *C. elegans* (Gönczy *et al.*, 2000), *Drosophila* (Giordano *et al.*, 2002) and in some plant species (Elmayan *et al.* 1998). PTGS produces a general systemic effect in plants and *C. elegans* with some exceptions, the neurons in *C.elegans* and the guard cells in plants (Fire *et al.*, 1998; Palauqui *et al.*, 1997; Voinnet *et al.*, 1998). However, in *Drosophila* the RNAi effect is generally a cell-autonomous process, allowing mRNA transcripts to be targeted only in the cells where the RNAi transgene is expressed via the Gal4/UAS binary system (Kalidas and smith, 2002; Reichhart *et al.*, 2002; Enerly *et al.*, 2002; Roessel *et al.*, 2002).

The RNAi technique can be performed in a variety of ways. The most common method in RNAi relies on the micro-injection of dsRNA into embryos which results in the RNAi being present throughout the cell body (Schindelholz *et at.,* 2001; Dzitoyeva *et al.*, 2001 and 2003). However, micro-injection of dsRNA has some disadvantages that limit its usefulness including a transient effect and the fact that it is not inherited in the next generation (Kennerdell and Carthew, 1998; Misquitta and Paterson, 1999).

To overcome the limitations associated with dsRNA injection, new methods have been developed to express stable dsRNA *in vivo* by the targeted expression of an inverted repeat (IR) transgene. Transgenes that have an IR configuration are able to produce dsRNA as extended hairpin structure (Lam and Thummel, 2000; Martinek and Young, 2000; Roessel *et al.*, 2002). This method combined with the Gal4/UAS binary system has been successfully applied to determine the function of novel genes, including the identification of a novel role for Notch in chemosensory startle behavior (Presente *et al.*, 2002).

1.6 The GAL-4/UAS Binary System: *targeted gene expression*

In order to determine the role of any gene *in vivo* both gain-of-function and reduction-of-function approaches can be utilized (Yang *et al.*, 2005; Penny and McCabe, 2005; Dzitoyeva *et al.*, 2003). However, in order to determine the precise function of a gene in a specific structure or system, the two approaches need to be targeted in a cell or tissue specific manner. The GAL4/UAS binary system can be used for this purpose (Brand and Perrimon, 1993). For example, studying Huntington's and Parkinson's diseases in fruit flies relied greatly on the availability of certain neuronal Gal4 lines (Bonini and Fortini, 2003; Lee *et al.*, 2004; Warrick *et al.*, 1999). The strength of perturbations introduced through the GAL4/UAS system has been characterized mainly by examining the phenotypic effects. However, Goentoro *et al.* (2005) examined the strength of the GAL4/UAS binary system using a fluorescence-based quantitative analysis. An assay was developed using a panel of four GAL4 lines and three UAS-transgenic lines to determine the relative level of expression in *Drosophila* oogenesis. Target proteins were tagged with the enhanced green fluorescent protein (EGFP). For each set of GAL4/UAS pairs being examined, the GFP-based measurement of the relative protein levels correlated well with the relative overall transcript levels. Furthermore, it correlated with the biological effects of the Gal4 lines (Goentoro *et al.*, 2005). This study in addition to several others (Fischer *et al., 1988*; Kakidani and Ptashne, 1988; Webster *et al.*, 1988) gave an indication of the strength and importance of the GAL4 lines in the functional analysis of genes.

1.6.1 Mechanism of the binary system

Many Gal4 lines express the yeast GAL4 protein in a wide variety of cells/tissues at various stages of the fly life cycle (Brand and Perrimon, 1993). GAL-4 encodes a galactose induced transcriptional factor isolated from the yeast *Saccharomyces cerevisiae* (Laughon *et al.*, 1984; Laughon and Gesteland, 1984; Oshima, 1982). The system's key feature is that the Gal-4 gene and the UAS-target gene are initially present in two distinct separate lines (Fig. 6). In the Gal-4 line, the activator protein is present, but has no target gene to activate. In the UAS-target gene line, the target gene is silent in the absence of the activator. The target gene is turned on only in the progeny of a cross between the two parental lines allowing reduction-of-function or gain-of-function phenotypes to be analyzed in cell and tissue specific manner. The binary system is very convenient since it allows the activation of the target gene only within cells where GAL-4 is expressed. Currently there are a large collection of GAL-4 lines which include: a ubiquitous driver (*arm*-GAL-4 and *Da*-GAL4), a pan-neuronal driver (*Elav*-GAL-4) and a glial driver (*Gcm*-GAL-4) (Duffy, 2002). In the GAL4/UAS binary system, expression of *Dslmap* is controlled by the presence of the UAS element, comprised of five tandemly arrayed and optimized GAL4 binding sites (Fig. 6).

1.6.2 Advantages of the binary system

The binary system where the Gal4 line and the UAS-target gene line are maintained as separate parental lines has numerous strengths. First, transgenic lines can be generated for gene products that are toxic, lethal, or have reduced viability when expressed (Duffy, 2002). Current transgenic lines include: the toxic gene *ricin a*, the apoptotic gene *reaper* and oncogenes such as *braf* (Aplin and Kaufman, 1997; Brand and

Figure 6. Mechanism of the GAL4/UAS binary system

In transgenic flies, a yeast transcription factor, GAL4 can activate the expression of any coding sequence downstream of a yeast upstream activating sequence (UAS) sequence (red circles). Two types of transgenic flies are required, one carries a GAL4 transgene fused to a promoter that has specific expression pattern and the other one carries a coding sequence for the target gene, cloned downstream of the UAS sequence. Both strains are transcriptionally inactive and phenotypically normal. The gene cloned downstream of UAS will only be expressed when GAL4 is present. The first generation (F1) offspring of a cross between GAL4 strains and UAS strains carry both transgenes and will express the UAS downstream gene in all cells that express GAL4.

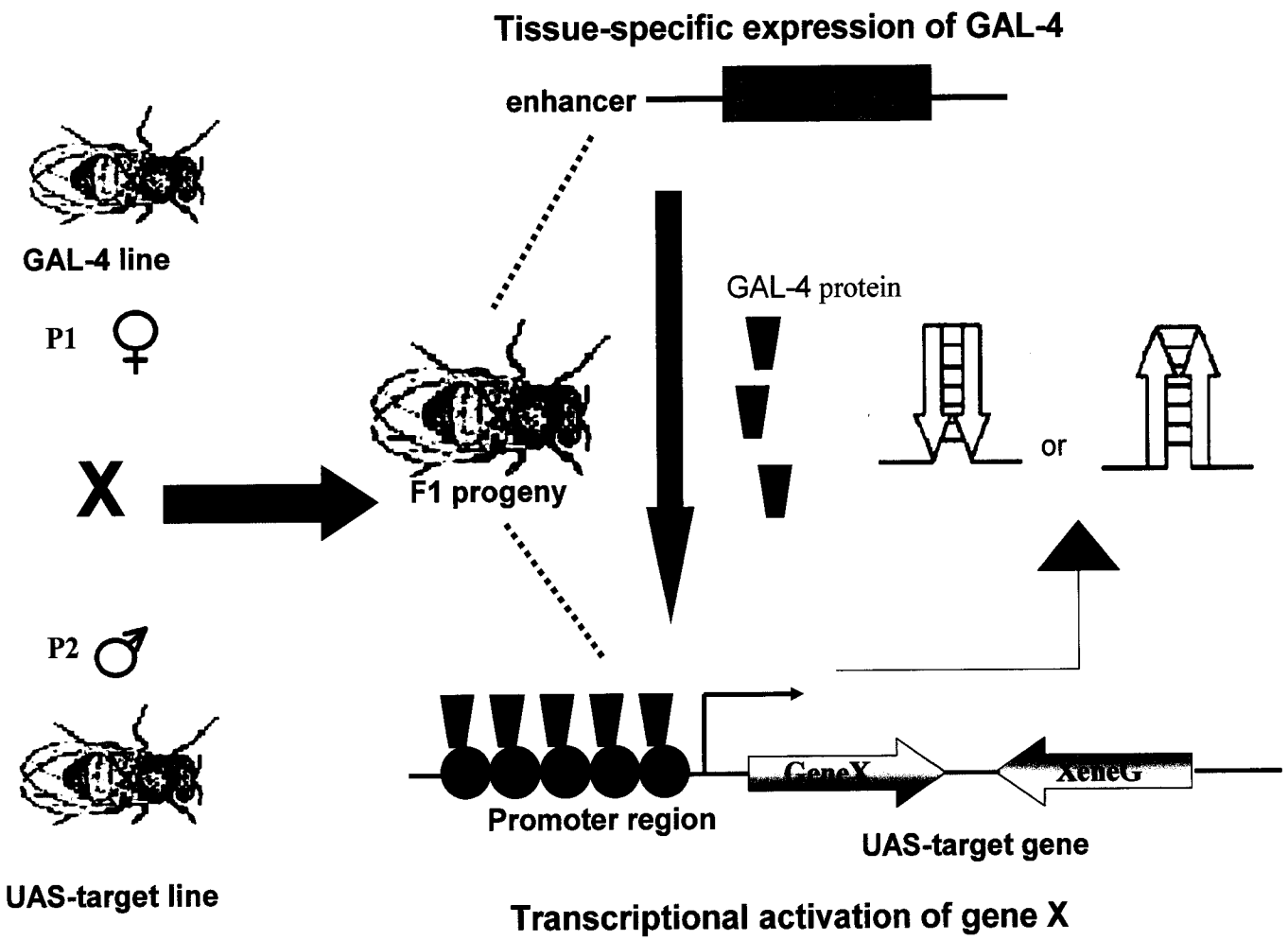
Tissue-specific expression of GAL-4
enhancer
GAL-4 line
P1
GAL-4 protein
or
F1 progeny
X
P2
Promoter region
GeneX
XeneG
UAS-target gene
UAS-target line
Transcriptional activation of gene X

Perrimon, 1994; Zhou *et al.*, 1997). Another advantage of the system arises from the ability to target expression of the desired gene in a variety of ways using GAL4 lines with specific spatial and temporal expression patterns.

1.7 Rationale and statement of the Problem

Many of the biological problems associated with the use of vertebrate model systems have been circumvented by complementary studies which exploit the genetic simplicity of invertebrate organisms. The recognition that vertebrates seem to have well-defined sequences encoding the SLMAP gene stimulated a search for ancestral sequences in invertebrates such as *Drosophila.* The *Drosophila* genome has been an abundant source for finding related genes in vertebrates. The fruit fly harbors only 13,500 genes, some of which may have essential functions in fly development and behavior. In this project, reverse genetics have been applied to analyze the function of SLMAP in *Drosophila* (*Dslmap*) using RNAi and overexpression approaches.

1.7.1 Hypothesis

SLMAP is a novel member of the tail-anchored super family of proteins which serve diverse roles in development and cellular functions. In view of the molecular features of SLMAP and its cell biology we propose that it may play significant roles in development and cell function.

1.7.2 Objectives

1. Identify the mammalian SLMAP homologue in fruit flies and determine its expression pattern.

2. Construction of vectors containing an IR sequence of the *Dslmap* cDNA to down-regulate SLMAP transcript *in vivo* using targeted approach coupled with the GAL4/UAS binary system.

3. Construction of vector containing full length *Dslmap* cDNA to overexpress SLMAP *in vivo* using the GAL4/UAS binary system.

4. Analyze reduction-of-function and gain-of-function phenotypes.

MATERIALS AND METHODS

2.1 Identification of the SLMAP homologue in fruit flies

The rabbit SLMAP cDNA sequences was entered into a Basic Local Alignment Search Tool (BLAST) (Altschul *et al.*, 1990) and resulted in the identification of a related SLMAP sequences present in fruit flies with accession No. CG17494 or LD47843 found in FlyBase Genome Annotation Database (http://www.flybase.bio.indiana.edu/annotl) (Adams *et al.*, 2000). The *Drosophila* clone ID No. UG56C12 was ordered from Open Biosystems and was sequenced to confirm its identity. Structural analysis was performed using Simple Modular Architecture Research Tool (SMART) at http://smart.embl-heidelberg.de/ (Schultz *et al.* 1998). Multiple sequence alignments were performed with CLUSTAL X (1.81) (Thompson, Higgins, and Gibson, 1994) available from the Gene Jockey II software package at http://www2.ebi.ac.uk/clustalw/. Subsequently, the sequences were run on WEB-based BoxShade program, (http://bioweb.pasteur.fr/seqanal/interfaces/boxshade.html#letters) and manually adjusted in Microsoft word 98. The Coiled-coil prediction was performed using the Coils program developed by Lupas and coworkers (Lupas *et al.* 1991) at http://www.ch.embnet.org/software/COILS_form.html.

2.2 Fly Stocks and Genetics

Flies were raised on cornmeal molasses/yeast/agar medium with both Tegosept and proprionic acid at room temperature. The following stocks were obtained from the Bloomington *Drosophila* Stock Center at Indiana University: w^{1118}, *yellow white* (*YW*), *elav*-Gal4, *arm*-Gal4, *paired*-Gal4, *gcm*-Gal4, and lab stock UAS *Rhum E.*

2.3 Construction of *Dslmap* probes for *in situ* hybridization

2.3.1 Construction of RNA riboprobes:

Regions 1, 2 and 3 of SLMAP were PCR amplified to generate 520, 530, and 374-bp PCR fragments respectively (Table I), which were subcloned into pCR 4-TOPO vector using conditions listed in the Invitrogen manual. All three constructs were confirmed by restriction digest with the appropriate restriction enzymes. The DNA plasmid constructs were linearized with the appropriate restriction enzymes: *PstI* for sense probes and *NotI* for antisense probes. The digested DNA plasmids were purified using the Qiagen PCR purification kit. To create the RNA strands, (Rnase-free conditions), 1μg of resuspended DNA was incubated for 2 hours in the following reagents provided in Genius 4 RNA labeling Kit (Roche): 2μl NTP 10X labeling mixture, 2μl 10X transcription buffer, 2μl Rnase inhibitor, 1μl T3 or T7 RNA polymerase for antisense and sense probes respectively, and DEPC treated water up to 20μl total volume. The T3 and T7 reaction mixture was incubated in a 37°C water bath for 2 hours.

After the synthesis of the RNA strands, the reaction was terminated by adding 2 μl of 200mM EDTA solution to stop the transcription reaction. The RNA was precipitated with 0.1 volume of 4M LiCl and 2.5-3.0 volume of 100% chilled ethanol. The reaction mixture was mixed and incubated for 2 hours at -70°C and was later thawed briefly at room temperature and centrifuged at 13,000 rpm for 15 minutes at 4°C. Pellets were washed again with 100μl of 70% ethanol, centrifuged again at 13,000 rpm for 15 minutes at 4°C. Finally the pellet was allowed to dry at room temperature (RT) and was resuspended in 150μl of Hybridization A solution. Riboprobes were stored indefinitely at -80°C.

Table I: Primers used to amplify various regions of *Dslmap* cDNA.

List of primers used to amplify three regions and one full length region of *Dslmap* cDNA to generate RNAi and overexpression constructs respectively. Middle column represent the sizes of the amplified regions. The exons encoded in each of the amplified regions are listed in the last column.

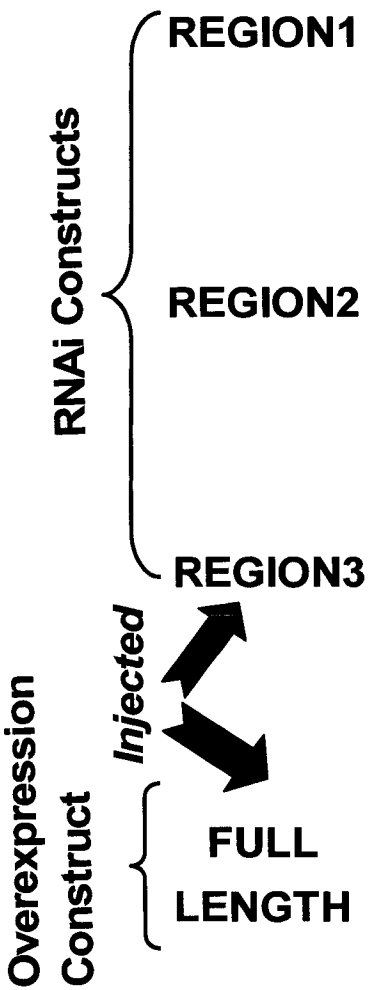

	Primers	Size	Exons
REGION1	**F-PRIMER:** *EcoRI* TAGTAGGAATTCGTTGATGAAGACC AGACGTCAAGT **R-PRIMER:** *AvrII* TAGTAGCCTAGGCACTGAAGAGACT TGTAAAGTGCC	520bp	**Exon II** CAAGTTCATTATCGCCGACG…… ….AGGTGGCATCGGAATGCG
REGION2	**F-PRIMER:** *XhoI* TAGTAGCTCGAGTATGGCGATATTGT GAAGTTCGGC **R-PRIMER:** *BglII* TAGTAGAGATCTTTTTCAGAAGTGGC GTAGGCCATC	530bp	**Exon II + Exon III** GTTGAGGTAATTGAGAATTC….. ……AAATGCTCTCTAAGATGGA
REGION3	**F-PRIMER:** *AvrII* TAGTAGCCTAGGGGAAGCTAAAACT AAGTAATCCCG **R-PRIMER:** *EcoRI* TAGTAGGAATTCCCTCAACGTCTACA AGCTTTTCCT F-PRIMER:	374bp	**ExonIV** ATTTAGAAGAAGGCAATTAT…….. ……..TTGTCAGCCCCTAATGCG
FULL LENGTH	**F-PRIMER:** *EagI* CTGCGGCCGTTGTTTGGATGTAAAGT AATG **R-PRIMER:** *EagI* GGACGGCCGTTAAATTCGACTGGAA ACAAA	2711bp	**Exons II-IV** ATGGTCTTGGTGTGCA……. ……..CATATATTTTCTTT

2.3.2 Construction of DNA probes

Digoxigenin-labeled DNA probes were made for three regions of *Dslmap* using the Genius 1 DNA Labeling and Detection Kit (Roche). PCR amplification of all three regions was performed, followed by heat denaturation in a boiling water bath for 10 minutes and quickly chilled on dry ice for 30 seconds before use. The following reagents were added to a sterile microfuge tube (on ice) in the following order: 3μg DNA template, 2μl Hexanucleotide mixture (10X), 2μl dNTP labeling mixture (10X), ddH2O up to 19μl, and 1μl Klenow enzyme (100 units/ml). The reaction tube was then incubated in a 37°C water bath overnight. The following day, 2μl of 200mM EDTA was added to terminate the reaction. Labeled DNA was precipitated with 0.1 volume of LiCl and 2.5-3.0 volumes of chilled ethanol, the reaction was mixed and incubated at -70°C for 30 minutes. The reaction tube was allowed to thaw briefly at RT and centrifuged at 13,000 rpm for 15 minutes. Ethanol was removed and pellets were washed with 100μl of 70% ethanol, centrifuged again at 13,000 rpm for 5 minutes. Pellets were dried and resuspended in 30μl TE buffer. DNA probes were stored at -20°C.

2.4 Embryo collection and fixation for *in situ* hybridization

Embryos were collected on apple juice agar plates and transferred into a reaction vial comprised of a sieve. Embryos were washed with double distilled water and dechorionated in 25% commercial bleach (Chlorix) in water for about 2-3 minutes. Embryos were later transferred into a glass scintillation vial containing 6 ml heptane and 1 ml fixation solution (4% formaldehyde in 1X PBS pH 7.4), which were shaken on a

nutator for 15-20 minutes. The lower phase was removed with a glass pipette and 8 ml methanol was added. The vial was shaken vigorously for 10 seconds to burst the vitelline membrane and cause the fall of devitellinized embryos to the bottom. Embryos were transferred into a reaction vial and washed twice with methanol. Embryos were stored at this stage in the refrigerator for a few weeks at –20°C.

2.5 In *situ* hybridization of DIG-labeled probes to tissues

In situ hybridization is a method of localizing and detecting specific mRNA sequences in morphologically preserved tissue sections or cell preparations by hybridizing the complementary strand of a nucleotide probe to the sequence of interest. The following protocol was modified from the Nüsslein-Volhard lab. All materials used in the making of RNA riboprobes were cleaned with RNAase free solution to reduce contamination with Rnase. All solutions were made in DEPC water.

Embryos stored at –20°C were thawed at room temperature, washed 2X for 10 minutes in PBT [998.5 ml 1X PBS; 500ul DEPC; 0.1% (v/v) Tween 20]. Embryos were post-fixed in 1ml PBT, 4% formaldehyde for 15 minutes then washed 5X for 5 minutes in PBT and incubated in 0.05% Proteinase K in PBT for 5 minutes. Proteinase K digestion was terminated by incubating embryos for 2 minutes in 2mg/ml glycine in PBT, which were further washed 2X for 5minutes in PBT. Embryos were again fixed in 1ml PBT, 4% formaldehyde for 20 minutes and were washed again 5X for 5 minutes in PBT. Embryos were later washed in hybridization B solution [hyb B: 50% (V/V) formamide; 25% (v/v) 20X SSC; 25% (v/v) DEPC in H2O] for 5 minutes and prehybridized in hybridization A solution [50% (v/v) formamide; 25% (v/v) 20X SSC; 10 mg/ml sonicated salmon sperm DNA; 20 mg/ml tRNA; 100 mg/ml heparin, pH 5.0] for 1 hour in a water

bath at 70°C (55°C for DNA probes). Most of the liquid was removed, leaving about 2 mm of solution above the surface of settled embryos. 2µl of the probe was added to 60µl of hybridization A solution containing the embryos. Hybridization was carried out at 70°C water bath overnight (55°C for DNA probes). Several washes 2X for 15 minutes with hybridization B solution were made followed by serial washes in hybridization solution in PBT for 10 minutes at RT, which were followed by several washes in PBT 3X for 10 minutes.

The anti-DIG antibody conjugate was prepared freshly and was preabsorbed the 1st day of this protocol against fixed embryos in order to remove any unspecifically binding material. The final working dilution of the antibody conjugate is 1: 2000 in PBT. Embryos were incubated for 2 hours in 1.2 ml of the diluted, preabsorbed anti-DIG antibody complex. Embryos were washed 3X for 20 minutes in PBT, and then washed again 2X for 20 minutes in staining buffer [1M MgCl2; 5M NaCl; 1M Levamisol; 20% Tween 20; 0.1M Tris-HCl, pH 9.5]. 15 ml staining buffer containing [2.56% (v/v) NBT/BCIP] was prepared and 1ml of the staining solution was added to embryos. The color was allowed to develop in the dark by covering the tube containing the embryos with aluminum foil. The staining reaction was allowed to proceed until sufficient staining was observed under dissecting microscope. The staining reaction was stopped by washing with PBT. Embryos were washed 2X for 10 minutes in PBT, and 2X for 10 minutes in water on the nutator. The dehydration process proceeded through a series of steps that include treatment with increasing ethanol concentrations starting with only 70% ethanol followed by inverting the tube several times and allowing the embryos to settle down. The ethanol was removed and the embryos were treated with a mix of 70%

ethanol and 100% ethanol followed by inversion of the tube several times. The dehydration process ends by adding two final rounds of 100% ethanol alone and leaving it on the bench for 5 minutes. Embryos were stored in 80% glycerol at RT.

2.6 RNAi Experiments:

To generate RNAi constructs, a multipurpose RNAi vector that employs spliced hairpin RNA was used. The pWIZ (pWIZ, for White Intron Zipper) vector (Lee and Carthew, 2003) is derived from a pUAST transformation plasmid (Brand and Perrimon, 1993; *Drosophila* genomics resource center). Three regions of the full length *Dslmap* cDNA corresponding to 520, 530 and 374-bp fragments of Regions (Reg) 1, 2 and 3 respectively were PCR amplified twice, using primers containing *XbaI* restriction sites for 1st insert and directional restriction sites for 2nd insert (Table I). For efficient digestion we added an extra six nucleotides to the five prime and three prime side of each primer restriction site. The PCR-amplified fragments containing the *XbaI* restriction sites were digested 1st with *XbaI* and PCR purified, then ligated to *NheI* digested, CIP (Calf Intestinal Phosphatase) treated and PCR purified pWIZ vector, to give pWIZ/1st insert of Reg 1, 2 and 3 (see Fig. 14 in results). This clone was then digested with restriction enzymes corresponding to each of the restriction sites available on the 2nd amplified PCR fragments of the three regions listed in Table I. The digested clone was later ligated to the 2nd PCR amplified fragments which are first digested with the same restriction enzymes used to cut the 1st clone (pWIZ/1st insert of Reg 1, 2 and 3) to produce three inverted repeat (IR) constructs corresponding to the three regions of the full length *Dslmap* cDNA.

Transformation of the three RNAi constructs was done by adding 2.5µl of the ligation product to 50µl of thawed competent DH5 α cells. The cells were incubated on ice for 30 minutes followed by heat shock for 20 seconds in 37°C water bath, and finally 2 minutes on ice. Then 950µl of LB broth was added to the transformed mix which was incubated for 1 hour at 37°C rotating incubator (250 rpm) to allow the expression of the antibiotic resistance markers. 250µl and 150µl of each transformation reaction were added to LB + ampicillin plates and a bent glass rod was used to spread the cells. Plates were placed inverted at 37°C for at least 18 hours. QIA prep Spin Miniprep Kit (Qiagen) was used to perform all minipreps. The miniprep DNA was stored at -20°C. Maxipreps were required in order to obtain higher concentration and larger amounts of the constructs to send for micro-injection. The constructs were confirmed by restriction digest. The DNA was dissolved in 300µl of sterile water instead of TE buffer and was sent to transgenic services for micro-injection into stage 1 or 2 embryos (Fig. 7).

2.7 Overexpression Experiments:

The UAS-*Dslmap* transgene was constructed by inserting the full length *Dslmap* cDNA in frame into the multiple cloning site behind the UAS element of the P-expression vector, pUAST (*Drosophila* genomics resource center). The full length *Dslmap* cDNA was amplified using primers with *EagI* restriction sites at the end. A 2.7 kb fragment was generated, gel extracted, then subcloned into pCR 4 TOPO vector. The ligation reaction continued for 20 minutes at RT as in the TOPO vector instruction manual (Invitrogen). Colonies were selected and digested with *EagI* to release a 2.7 fragment with sticky ends, which was blunt treated with DNA blunting ligation kit [Fermentas Life Sciences]. The 2.7 Kb blunt fragment was later ligated into the CIP

Figure 7. Injection procedure.

Injection procedure was carried out by transgenic services in Sudbury MA. Two constructs were sent for micro-injection into stage 1 or 2 embryos. One RNAi construct (Reg3-*Dslmap*-pWIZ) and one over expression construct of full length *Dslmap* cDNA (*Dslmap*-UAS). Seven transgenic RNAi lines and twelve overexpression lines were generated that required a pair-wising process.

Injection Procedure

50µg of *Dslmap* Qiagen purified maxiprep DNA dissolved in water is sent for micro-injection

Micro-injection

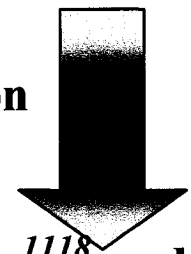

Stage 1 or 2 w^{1118} embryos (180 embryos)
Kept on O_2 for 5 days at 18 °C

10 days

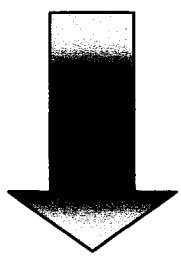

60-80 single crosses to males or virgins of w^{1118}

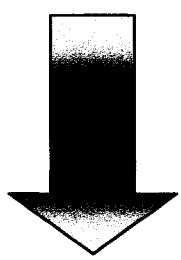

Screen the progeny for orange to red (W^+) eyes
(7 Reg3-pWIZ-*Dslmap* W^+
& 12 *Dslmap*-UAS W^+)

treated and blunt-ended *KpnI* site of the pUAST vector following the manufacturer instructions on the kit (DNA Blunting Ligation Kit from Fermentas Life Sciences).

2.8 Immunohistochemistry

2.8.1 Embryo fixation

Embryos from various stages of embryonic development were collected overnight at RT on apple agar-filled petri plates containing a small smear of live yeast paste (Fleischmann's Dry). Embryos were heat shocked for two hours in a 29°C incubator and allowed to recover at RT for another two hours to allow restoration of axon morphology and microtubule re-polymerization. Embryos were collected from apple juice-agar plates and dechorionated for 7 minutes with 50% bleach. Dechorionated embryos were collected onto a nitex sieve and rinsed with distilled water. Once blotted dry on a kimwipe, the nitex sieve holding the dechorionated embryos was immersed in a scintillation vial containing a fixation solution of 500µl of 37% formaldehyde, 4.5ml of 1X PBS (phosphate buffered saline), and overlayed by 5ml of heptane. Embryos were fixed for 30 minutes at the interface between the heptane and bottom aqueous layer containing the fixative. The heptane at this interface ensures permeabilization of embryos to allow entry of the fixative and subsequent antibodies. The bottom aqueous layer was removed, replenished with fresh methanol and the vial containing the embryos was shaken vigorously for approximately twenty seconds in order to remove the vitelline layer surrounding the embryos. Devitellinized embryos in the bottom methanol layer were transferred to a disposable plastic tube using a Pasteur pipette. Traces of heptane were removed by three methanol washes. Embryos were stored in -20°C for a maximum of two weeks until a large collection was obtained to proceed with antibody staining.

2.8.2 Antibody staining

To proceed with antibody staining, the methanol was replaced with PBT (1X PBS containing 0.1% triton X-100). Embryos were then washed for one hour in PBT on a rotator before incubating in 100µl of PBT containing 10µl of normal goat serum (NGS) for thirty minutes to block nonspecific antibody binding. A primary antibody with specific dilution was added to embryos in blocking solution and was incubated at 4°C overnight. Residual antibody was washed away with PBT 3X for 1 hour. The washed embryos were blocked again in PBT containing NGS for 30 minutes. The secondary antibody (goat anti-mouse IgG conjugated to horseradish peroxidase) was added to the embryos in blocking solution and was incubated for two hours at RT. The secondary antibody was then washed out with PBT for 1 hour on a rotator.

Antibody reactivity was visualized by incubating embryos in 1000µl PBT containing 500µl 0.3 mg/ml diaminobenzadine (DAB). 3µl of 3% hydrogen peroxidase was added and the reaction was allowed to proceed until appropriate staining was achieved. PBT was added to terminate the reaction. Embryos were dehydrated through a series of increasing ethanol concentrations (50%, 70%, 95% and 100%). Embryos were stored at RT in methyl salicylate to preserve their staining. Embryo staging was according to Campos-Ortega and Hartenstein, 1985.

2.8.3 Antibodies

The following antibodies were used: Primary antibody, BP102 (Developmental Studies Hybridoma Bank, DSHB; Carney *et al.*, 1997) to visualize the formation of embryonic CNS axons at a 1:20 dilution. The secondary antibody is anti-mouse IgG. Anti-

Digoxigenin-AP primary antibody was used for *in situ* hybridization (Roche Applied Science).

2.9 Light Microscopy

Embryo fixation and staining were according to standard protocols (Patel, 1994). Embryos were analyzed on a Zeiss Axioskop microscope, and images were captured on a Nikon DXM1200 digital camera and processed using Adobe Photoshop software.

2.10 Statistical Analysis

For each GAL4/UAS pair, a histogram was obtained of the mean, each mean was generated from 2-4 independent measurements, with each measurement performed on stage 15 embryos. Standard deviation was calculated using Microsoft Excel as the square root of the averaged square deviation from the mean. When analyzing the phenotypes associated with either RNAi or overexpression experiments, eight segments out of a total fourteen segments were examined. Penetrance, or the frequency of phenotype, was examined by scoring the number of embryos in the total population exhibiting an abnormal phenotype after staining with a particular antibody. Expressivity, or the severity of the phenotype, was examined by looking at the number of hemisegments that exhibit an abnormal phenotype in each mutant embryo.

RESULTS

3.1 Identification of the mammalian SLMAP homologue in fruit flies

In order to determine if a mammalian SLMAP homologue exists in fruit flies, homology searches were performed using BLASTP algorithm of the National Center for Biotechnology Information (NCBI) (http://www.ncbi.nlm.nih.gov) to compare the rabbit SLMAP amino acid sequence (Accession No. U21157; Wigle *et al.*, 1997) to all sequences present in the database. Homology searches resulted in the identification of a protein sequence in *Drosophila*, related to rabbit SLMAP3 protein with accession No. CG17494 that shares a 28.6% identity over 721 amino acids (48.3% similarity) (Fig. 8). Multiple sequence alignment using Clustal X (1.81) was performed and revealed a percentage identity of 55.9% over 59 amino acid residues at the extreme N-terminus of *D*SLMAP (76.3% similarity) (Fig. 9A). This identity encompasses a fork head associated (FHA) domain corresponding to amino acid 25-58 within the region spanning the first initiating methionine (M1) and 2nd initiating methionine (M2) of the rabbit SLMAP3 protein sequence encoded by exon I. The high percentage identity in this region is indicative of an essential conserved function encoded by the FHA domain. Similarities were also found at the C-terminus, which shares a 25% identity (37.5% similarity) over 32 hydrophobic amino acid residues corresponding to TMD1 encoded by exon XXIII of the rabbit SLMAP3. An 8.8% identity (32.4% similarity) was also identified over 34 hydrophobic amino acid residues corresponding to TMD2 encoded by exon XXIV of SLMAP3 (Fig. 9A), which implies that the *Drosophila* clone may encode a putative hydrophobic TMD at its C-terminus. Furthermore, a hydrophobicity plot

Figure 8. The *Drosophila* SLMAP shares similarity with the mammalian SLMAP3 protein.

A BLAST homology search was performed to identify proteins that share identity with the mammalian SLMAP protein. The *Drosophila* SLMAP amino acid sequences (Accession No. CG17494) showed 48.3% similarity over 721 amino acids with the rabbit SLMAP3 protein (Accession No. U21157)

Identities = 206/721 (28.6%), Similarities = 348/721 (48.3%), Gaps = 124/721 (17.2%)

```
Drosophila   208 AAKIVLLCEPKSHKFETRSILLQPNQDCKVGRLIAKSKAGEGNAIFDCKV   257
                 :|..:..|.|.||.|:.|.:.|  ::..|:||.:|:.:..:.||.|||||
Rabbit         3 SALAIFTCRPNSHPFQERHVYL--DEPIKIGRSVARCRPAQNNATFDCKV    50

Drosophila   258 LSRNHAILWYT-PDGKFWVKDTKSSNGTFINDNKLG-----SDPAELHYG   301
                 ||||||::|:. ..|||:::|||||||||||..:|.     |.|.|:..|
Rabbit        51 LSRNHALVWFDHKTGKFYLQDTKSSNGTFINSQRLSRGSEESPPCEILSG   100

Drosophila   302 DIVKFGVEVIENSRQEVHGCILARVALFLPNGQEA----------ISVEA   341
                 ||::|||:|.||:|:..||||::.:.||||:|.||          :....
Rabbit       101 DIIQFGVDVTENTRKVTHGCIVSTIKLFLPDGMEARLRSDVIHAPLPSPV   150

Drosophila   342 EQMMLTVPNRISFDEVQRLSSFLQEAAQREKSLKAKLSSLQGVLDNTRKN   391
                 :::....|:..| .|:.:||.:||||..||:.|:.||::||.:|..|::.
Rabbit       151 DKVAANTPSMYS-QELFQLSQYLQEALHREQMLEQKLATLQRLLAITQEA   199

Drosophila   392 SAMCWQSMITEDQLLHKINILEKKLQMMEKNIPENALRNEIVKLLEDKTT   441
                 |...||::|.||:||.::.::..:||...||..|::||.|::.|.|||..
Rabbit       200 SDTSWQALIDEDRLLSRLEVMGNQLQACSKNQTEDSLRKELIALQEDKHN   249

Drosophila   442 YQLTAKEALRKVYQERCDAMQMLSKMEMAYATSENECGIL-----RAQVL   486
                 |:.||||:||:|.||:.:.::.||::|.:.:.:::|:||..|     |.|.
Rabbit       250 YETTAKESLRRVLQEKIEVVRKLSEVERSLSNTEDECTHLKEMNERTQE-   298

Drosophila   487 TLKQTLTDFNTRLEELQQ-----EYMEFKKESVRQEQEAKEQESRSLEVL   531
                 .|::....:|..:.|::.     ...|.|:|:::|:.:|:::|      |
Rabbit       299 ELRELANKYNGAVNEIKDLSDKLKVAEGKQEEIQQKGQAEKKE------L   342

Drosophila   532 NGKLTTQELELKELRLQVS----RIHRDLSESDTEHLKERIVLKN-LDTI   576
                 ..|:  .|:|.||..||..    :...|.:......|:|.::.|: .|..
Rabbit       343 QHKI--DEMEEKEQELQAKIEALQADNDFTNERLTALQEHLLSKSGGDCT   390

Drosophila   577 NLDDYDHAQDRAL-----------------NERDDNESSDDDILSVSPAK   609
                 .:.::...|.:.:                 |:....||...|.||.|..|
Rabbit       391 FIHQFIECQKKLIVEGHLTKVVEETKLAKENQARAKESDLSDTLSPSKEK   440

Drosophila   610 NVLSETKKRKLKLSNPDLEEGNYKSNVLRLL----KNSDLGKGEEGSSVL   655
                    |.......::...||.|...|.::|:.|    :.:...:.||.|..:
Rabbit       441 ---SSDDTTDAQMDEQDLNESLAKVSLLKALLEEERKAYRNQVEESSKQI   487

Drosophila   656 KAI------FNGDDEAFECKVKEEEDMANDSVPTEFVSRNTSEIVDHFKN   699
                 :.:      .:.|.|    .::||:|....|...|.:|.....::.|
Rabbit       488 QVLQAQLQRLHMDIE----NLREEKDNEITSTRDELLSARDEILLLH---   530

Drosophila   700 HSSTTHTILEDSAATKLSAPNAESKEKLVDVEENLNIPNALPTEQAIDML   749
                            .||.|.:   :|....:..::|.|.            .:
Rabbit       531 -----------QAAEKAA---SERDTDIASLQEELK------------KV   554

Drosophila   750 QEECDTYKKKTAHLTSEIHFLQGQIELLKKQLEKGVDHNFATNLQEEENS   799
                 :.|.:.::|..:....|:..||...:|..:|.|...... ||.||.|...
Rabbit       555 RAELERWRKAASEYEKEVTSLQSSFQLRCQQCEDQQKEE-ATRLQGELEK   603

Drosophila   800 LPRETLELIDNRDSTEGVWN---EDIATINNPNVENEEELIVYKELLENS   846
                 |.:|              ||   .:..::....||....||...::.|.||
Rabbit       604 LRKE--------------WNVLETECHSLKKENVLLSSELQRQEKELHNS   639

Drosophila   847 ELNNMQLRKEISELHLKHKHI   867
                 :.::::|..::|.|::..|.:
Rabbit       640 QKQSLELTSDLSILQMTRKEL   660
```

Figure 9. Structural Features of *Drosophila* SLMAP.

(A) Multiple sequence alignment of *D*SLMAP with the rabbit SLMAP3 isoform amino acid sequences using CLUSTAL X (1.8) program. The Rabbit SLMAP homologue in fruit flies shares 28.6% identity over 721 amino acid residues with SLMAP3 isoform. However, a higher percentage identity was identified in the fork head associated (FHA) domain (55.9%). A 25% identity (12/32 = 37.5% similarity) was identified between the *Drosophila* TM domain and the rabbit TMD1, whereas TMD2 had a lower identity of 8.8% (11/34 = 32.4% similarity). Coiled-coil regions are shown in green boxes. Conserved residues are shown in blue, identical in red, and similar in green.

(B) Similarity between the *D*SLMAP protein and its closest known relatives as defined by amino acid sequence similarity using BLASTP. The *D*SLMAP protein was found to have a close relative in *A. Gambiae* (mosquito) comprised of all domains but lacks the TM domain. Mammalian SLMAP species, (rabbit, mouse and human) have an alternatively spliced C-terminus TM domain shown to target SLMAP to different membrane systems (Guzzo *et al.*, 2004). The coiled-coil region is found in all species and was shown to be involved in mediating SLMAP homo/heterodimerization(s) in mammals (Guzzo *et al.*, 2004). The fork head associated (FHA) domain, a stretch of amino acids present in several transcription factors, exists at the extreme N-terminus in all species and has been shown to play an important role in localization of SLMAP to the centrosome (Guzzo *el al*; 2004). Structural domains were identified using SMART website (Schultz *et al.*, 1998).

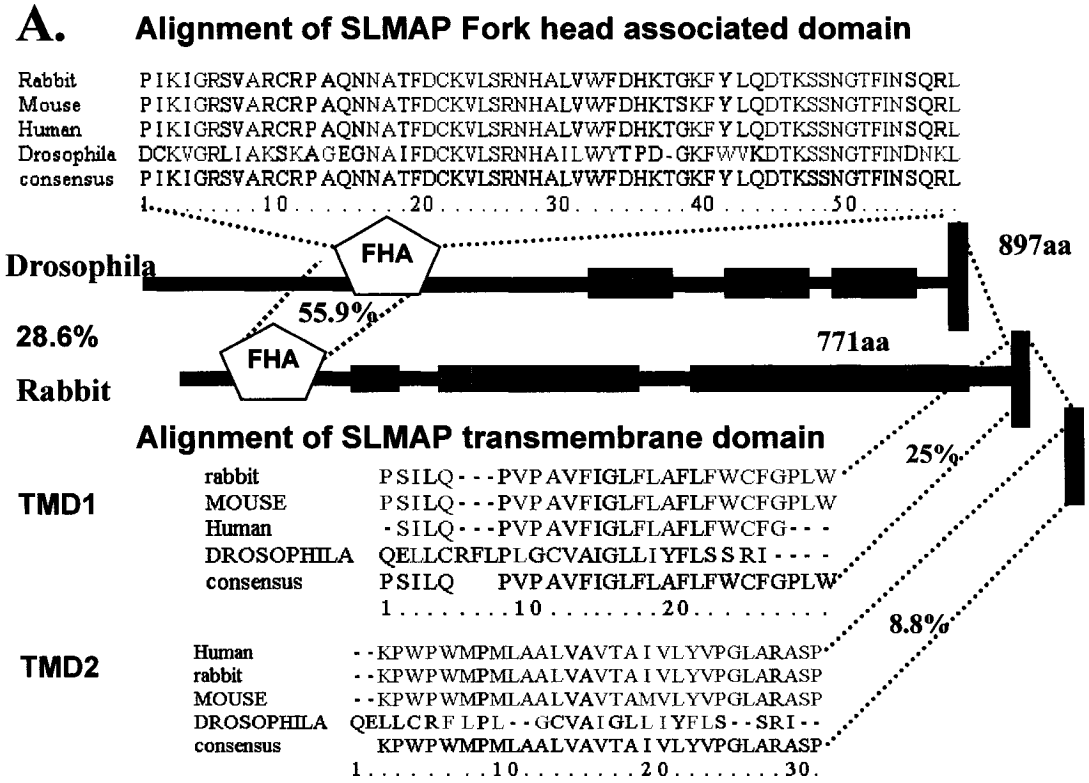
A.
Alignment of SLMAP Fork head associated domain
Rabbit PIKIGRSVARCRPAQNNATFDCKVLSRNHALVWFDHKTGKFYLQDTKSSNGTFINSQRL
Mouse PIKIGRSVARCRPAQNNATFDCKVLSRNHALVWFDHKTSKFYLQDTKSSNGTFINSQRL
Human PIKIGRSVARCRPAQNNATFDCKVLSRNHALVWFDHKTGKFYLQDTKSSNGTFINSQRL
Drosophila DCKVGRLIAKSKAGEGNAIFDCKVLSRNHAILWYTPD-GKFWVKDTKSSNGTFINDNKL
consensus PIKIGRSVARCRPAQNNATFDCKVLSRNHALVWFDHKTGKFYLQDTKSSNGTFINSQRL
1.....10.....20.....30.....40.....50.....
Drosophila
FHA
897aa
55.9%
28.6%
771aa
FHA
Rabbit
Alignment of SLMAP transmembrane domain
25%
TMD1
rabbit PSILQ---PVPAVFIGLFLAFLFWCFGPLW
MOUSE PSILQ---PVPAVFIGLFLAFLFWCFGPLW
Human -SILQ---PVPAVFIGLFLAFLFWCFG---
DROSOPHILA QELLCRFLPLGCVAIGLLIYFLSSRI----
consensus PSILQ PVPAVFIGLFLAFLFWCFGPLW
1.....10.....20.....
8.8%
TMD2
Human --KPWPWMPMLAALVAVTAIVLYVPGLARASP
rabbit --KPWPWMPMLAALVAVTAIVLYVPGLARASP
MOUSE --KPWPWMPMLAALVAVTAMVLYVPGLARASP
DROSOPHILA QELLCRFLPL--GCVAIGLLIYFLS--SRI--
consensus KPWPWMPMLAALVAVTAIVLYVPGLARASP
1.....10.....20.....30.
B.
D. melanogaster
FHA
897aa
A. gambiae
FHA
484aa
C. elegans
FHA
582aa
M. muscus
FHA
874aa
O. cuniculus
FHA
771aa
H. sapiens
FHA
941aa

(TMHMM server, v. 2.0) suggests that a C-terminus stretch of 17 amino acid residues encodes a single putative TM domain in *D*SLMAP. A BLAST homology search aligned the *D*SLMAP protein with other mammalians species such as the mouse, rabbit, and human, all comprised of similar structural features to the ones identified in *D*SLMAP (Fig. 9B). An uncharacterized SLMAP sequence in *C. elegans* was found to be similar to *D*SLMAP; however, it lacks the C-terminus TM domain. Further analysis of *D*SLMAP secondary structure revealed the presence of large coiled-coil regions predicted by the COILS program (Fig. 10A) (Lupas *et al.*, 1991).

In summary, a mammalian SLMAP homologue is identified in *D. melanogaster* that shares a 28.6% identity with SLMAP3 isoform in the rabbit. Further examination of the structural features of *D*SLMAP, revealed the presence of similar domains to those identified in its mammalian counterpart and includes the FHA domain (55.9%), and other domains such as the coiled-coil regions and TMD.

3.2 Genomic organization of *Dslmap*

The elucidation of the genomic structure of *Dslmap* is essential since it may offer valuable insights to understanding the function and regulation of this novel gene. *Dslmap* genomic sequence was analyzed using the Ensembl Genome program which maintains annotation on selected eukaryotic genomes. This analysis revealed a small gene of 7.65 kb located on chromosome 2h in Chunk 2h_33 (Fig. 11A) and corresponds to accession No. CG17494 (LD47843) of *Dslmap* cDNA in the fly database. Computer Sequaid program assisted in the alignment of *Dslmap* cDNA sequence with flybase deposited *Dslmap* genomic sequences. The analysis revealed a *Dslmap* genomic DNA of 7.65 kb comprised of four putative exons and three introns (Fig. 11A). Intron sizes varied from a

Figure 10. Prediction of a coiled-coil secondary structure.

The probability that *D*SLMAP could exist in a coiled-coil conformation was predicted using the COILS analysis program (Lupas *et al.*, 1991) with a window of 28 amino acids. The *D*SLMAP protein was predicted to have three coiled-coil regions interspersed with short non-coiled-coil segments. The coiled-coil prediction for the mammalian SLMAP3 isoform is shown in B.

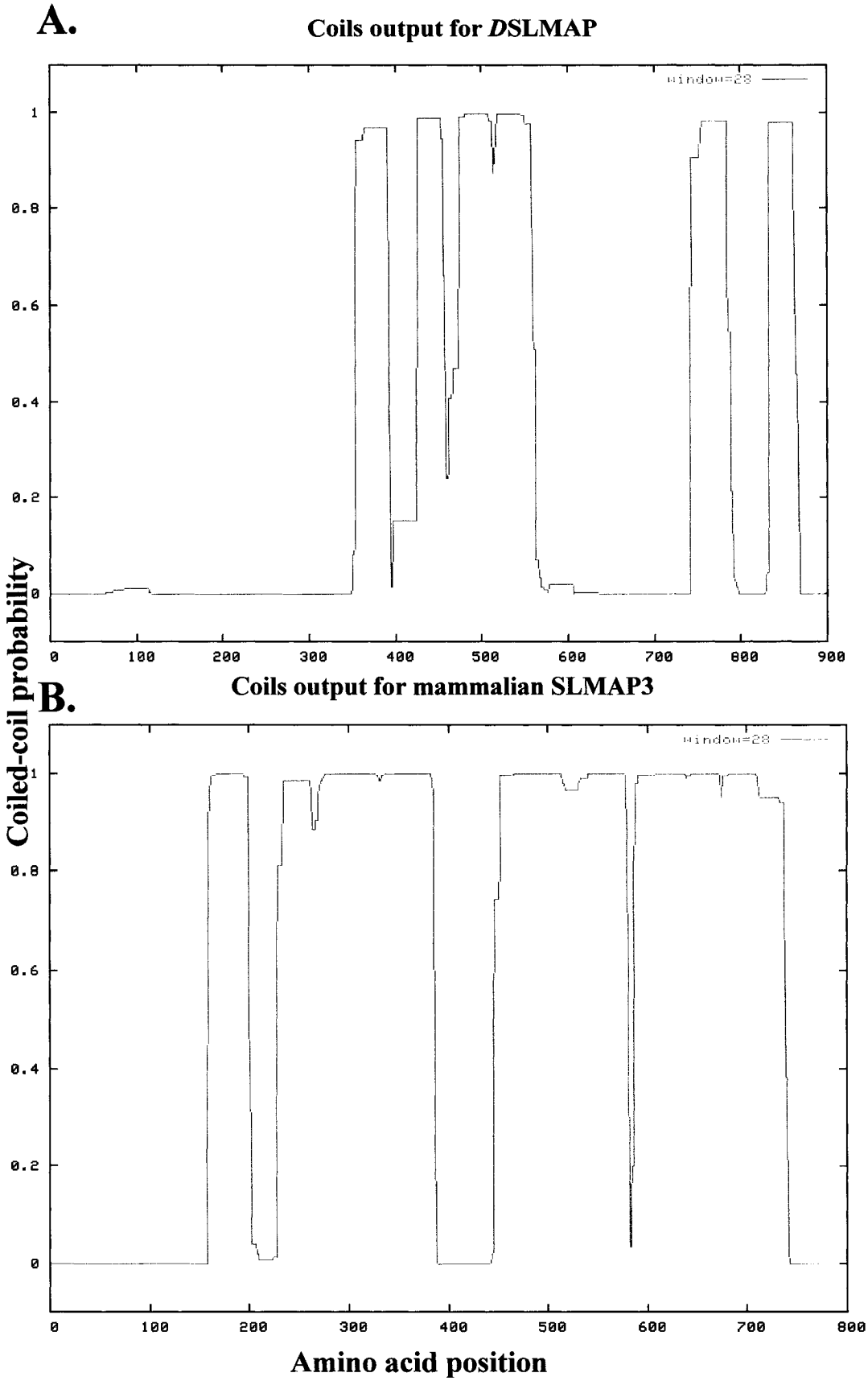
A.
Coils output for DSLMAP
window=28
1
0.8
0.6
0.4
0.2
0
0
100
200
300
400
500
600
700
800
900
B.
Coils output for mammalian SLMAP3
window=28
Coiled-coil probability
1
0.8
0.6
0.4
0.2
0
0
100
200
300
400
500
600
700
800
Amino acid position

Figure 11. Genomic Organization of *Dslmap.*

Panel A is a graphic representation of the genomic structure of *Dslmap*. The schematic illustrates that the *Dslmap* gene is composed of 4 exons and three introns spanning 7.65 kb of genomic DNA. Exon I and intron I reside in the 5' untranslated region. Exon II contain the fork head associated domain (FHA), and the ATG initiation site. A large intron II of 3.0 kb separates the 2^{nd} and 3^{rd} exon. Exon III encodes a coiled-coil motif. In the 3′ untranslated region part of exon IV resides, and encodes both a coiled-coil motif and a putative transmembrane (TM) domain. Panel B summarizes the intron-exon junctions of *Dslmap* as predicted by alignment of *Dslmap* cDNA with its genomic DNA using Sequaid program. All of the exon-intron boundaries conform to the consensus splice donor and acceptor sites (gt-ag).

A.

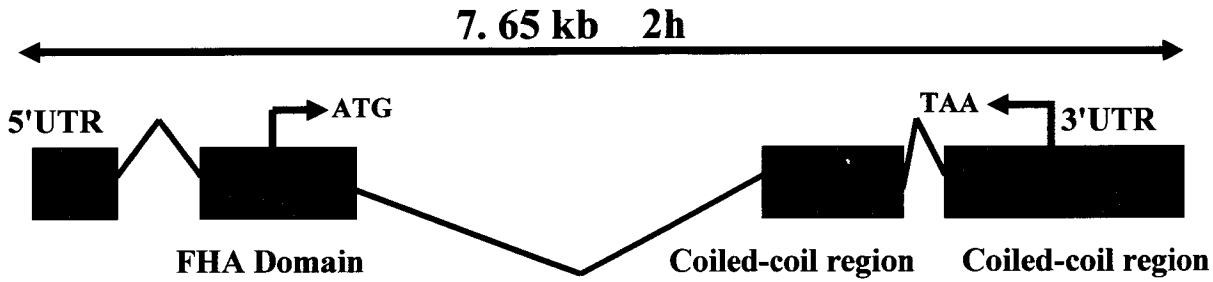

B.

No.	Size (bp)	Exon	Intron No.	Intron Size (bp)	Class	Exon	No.
						GCTTTTTTC	I
I	189	AATTCCAAG**gt**aagccaa	1	568	0	ccccc**aaag**GTTTGTTTT	II
II	1313	CGAAACGAG**gt**aagtccc	2	2988	1	cttcaat**ag**ATTGTAAAG	III
III	561	AAAAAAAG**Ggt**aatgctt	3	59	0	taattct**ag**AAGCTAAAA	IV
IV	1378	TTAACATCG					

Note: Exon-intron boundaries conform to the consensus splice donor and acceptor sites (**gt-ag**).

very short intron III (59bp), an intermediate intron I (568bp) to a very large intron II (2.9kb). *Dslmap* exons ranged in size from the shortest 189-bp (exon I) to the largest 1.37 kb (exon IV) (Fig. 11B). Sequence data for each intron-exon boundary conformed to the canonic consensus donor (GT) and acceptor (AG) splice sites described by Mount (1982) and is depicted in Fig. 11B. Each class of intron (0, 1 and 2) is represented within the *Dslmap* genomic sequences (Fig. 11B). Each exon is flanked by either class 0 introns (introns I and III) which occurs between codons or class 1 introns (intron II), which interrupt the coding between the first and second base of the codon (Mount, 1982).

In the 5'untranslated region, Exon I and intron I reside whereas part of exon IV resides in the 3′ untranslated region. The exon-intron junctions of *Dslmap* are very simple (Fig. 11B) in comparison to the much larger and more complex exon-intron structure of mammalian SLMAP which is composed of twenty four exons and introns spanning over 122 kb of genomic DNA. Exon II of *Dslmap* encodes the fork head associated domain and contains the ATG initiation site. Exon III and IV encode coiled-coil motifs, and exon IV encodes the putative transmembrane domain. There is a large intron of 3.0 kb separating the second and third exons.

3.3 Expression of *Dslmap* during embryonic development

In order to determine the expression pattern of *Dslmap*, *in situ* hybridization was performed with DIG labeled riboprobes and DNA probes of three different regions of the *Dslmap* cDNA. The mRNA was expressed ubiquitously at various stages of embryonic development (stages 5-17) as illustrated by whole mount *in situ* hybridization (Fig. 12). Expression of *Dslmap* mRNA was first detected in stage 5, cellular blastoderm (Fig. 12A). During this stage, cellularization occurs rapidly by means of the introgression of

Figure 12. *Dslmap* expression during embryonic development.

Whole mount *in situ* hybridization was performed using DIG-labeled riboprobes and DNA probes of *Dslmap* cDNA at various stages of embryonic development. *Dslmap* mRNA transcripts expression in wild type w^{1118} embryos at different stages of embryogenesis revealed: (A) *Dslmap* has an early component present at stage 5. (B) At gastrulation stage 11, *Dslmap* transcripts dominate in the mesoderm (black arrow), head mesoderm (arrowhead), and midgut primordium (white arrow) in sagittal view embryo. (C) A sagittal stage 15 embryo showing *Dslmap* transcripts in brain hemispheres (arrowhead), neuroectoderm (black arrow), and hindgut (white arrow). (D) At stage 17 of embryonic development, *Dslmap* is expressed in the brain hemispheres (arrowhead) and in the hindgut (arrow). Right column represent negative control using *Dslmap* sense riboprobe. Anterior is to the left. Scale bar = 100μm.

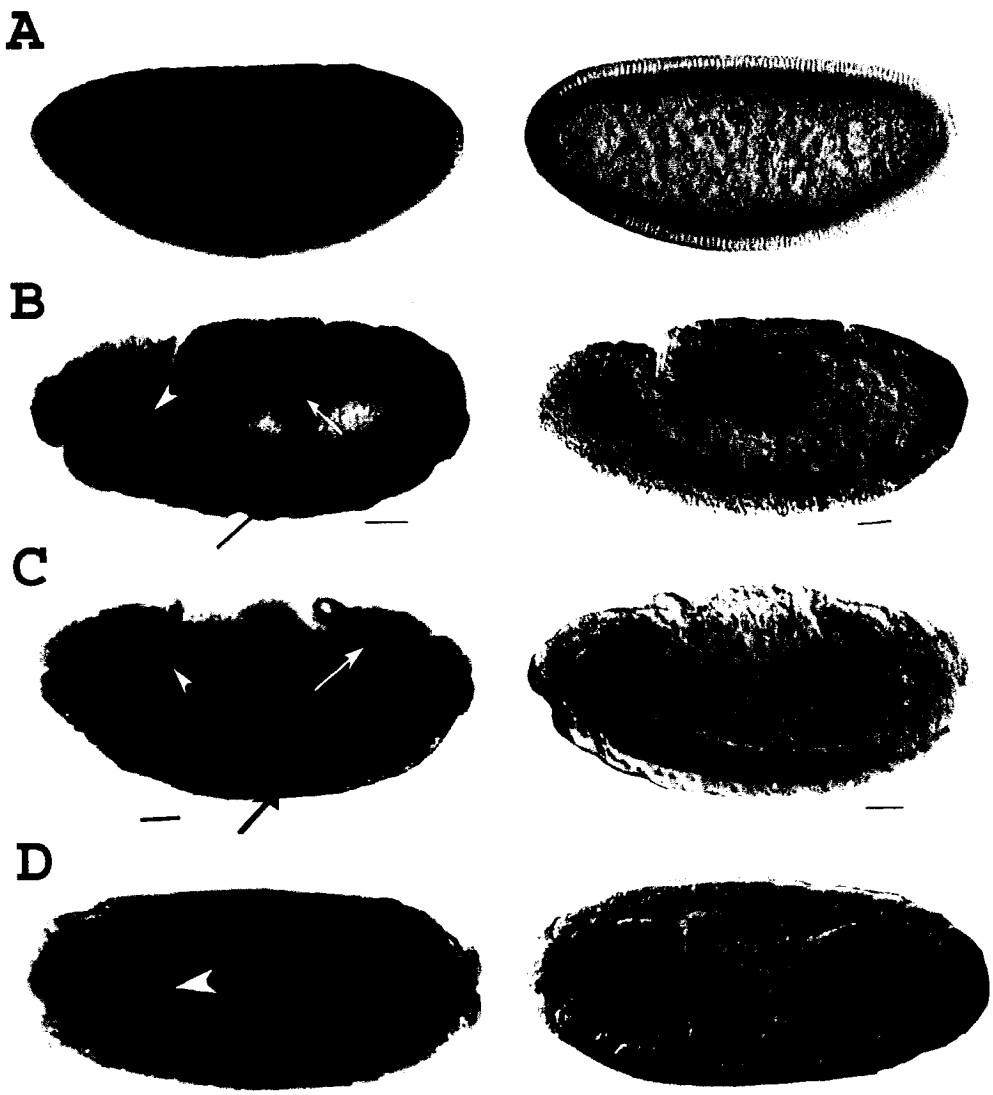
A
B
C
D

membrane furrows to separate single blastoderm nuclei. As development progresses, *Dslmap* transcripts appears at gastrulation stage of embryonic development, and are visible in the mesoderm of an elongating germ band embryo (Fig. 12B, black arrow), midgut (Fig. 12B, white arrow), and head mesoderm (Fig. 12B, arrowhead). During stage 15 of embryonic development, *Dslmap* transcripts become enriched in the neuroectoderm (Fig. 12C, black arrow), supraesophageal ganglion (brain) (Fig. 12C, arrowhead), and hindgut (Fig. 12C, white arrow). At the final stage 17 of embryonic development, *Dslmap* is still noticeable in the brain hemispheres (Fig. 12D, arrowhead) and hindgut (Fig. 12D, arrow).

The controls used in this experiment included a sense RNA riboprobe of three different regions of *Dslmap* cDNA (Fig. 12, right column in A, B, C and D), showing no hybridization signal. A positive control for the *in situ* hybridization reaction is an antisense RNA probe for X-linked nuclear protein (*XNP*), a gene known to be expressed in the CNS (Sun *et al.*, 2006) (Fig. 13E, red arrow). The positive control for the DNA probe was *Jing*, expressed in the CNS (Sedaghat *et al.*, 2002) (Fig. 13A arrow and arrowhead) and tracheal pits (Fig. 13 B and C arrowhead).

In situ hybridization has led us to conclude that *Dslmap* mRNA transcripts are expressed ubiquitously and at an early stage of embryonic development.

Figure 13. *In situ* hybridization for CNS markers.

RNA riboprobe and DNA probes were constructed for amplified regions of *XNP* and *Jing*, both used as positive controls for *in situ* hybridization. *Jing* is known to be expressed in the CNS and was confirmed by *in situ* hybridization which revealed expression in the brain hemispheres and ventral nerve cord (A, arrowhead and arrow respectively). *Jing* was also shown to be expressed in tracheal pits (B, C, and D arrowheads). *XNP* is also known to be expressed in the CNS and was confirmed by *in situ* hybridization which shows expression in the ventral nerve cord (E, red arrow).

Positive control for DNA probe, *Jing*

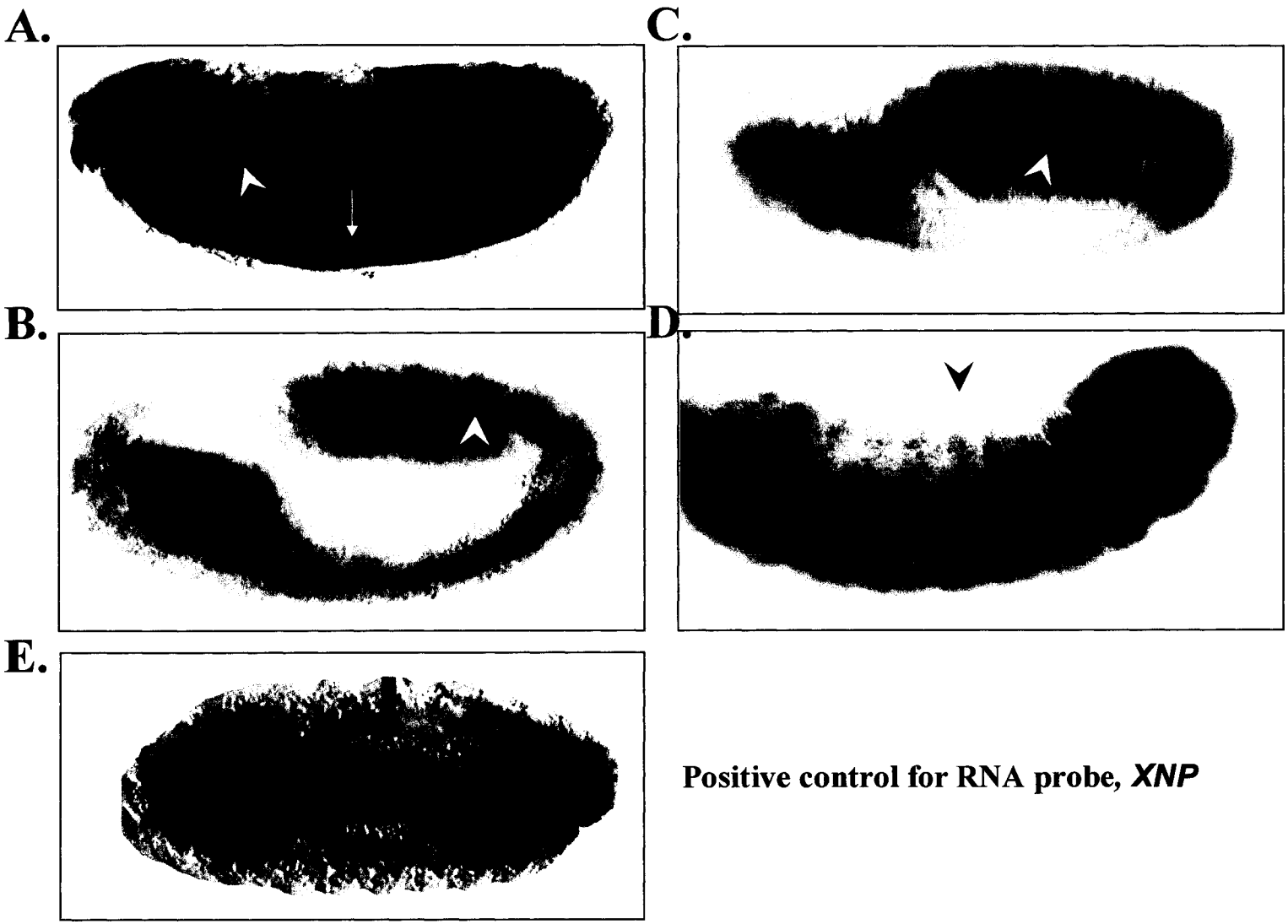

Positive control for RNA probe, *XNP*

3.4 Down-regulation of *D*SLMAP to generate reduction-of-function phenotypes

Based on the *in situ* hybridization results, it appears that *Dslmap* is expressed ubiquitously and at early stages of embryogenesis indicating that it may serve a developmental role. In order to determine this role at the embryonic stage, a reverse genetic approach was applied to generate reduction-of-function phenotypes. RNAi technique (Lee & Carthew, 2003) was employed and three potential RNAi constructs were generated comprised of inverted repeats of three different regions of the *Dslmap* cDNA. One RNAi construct was used for micro-injection into stage 1 or 2 embryos to generate transgenic RNAi lines.

3.4.1 Generation of inverted repeats for RNAi constructs

To construct an IR transgene using the pWIZ vector, a DNA fragment corresponding to each of the three regions of interest in *Dslmap* cDNA was inserted twice as a PCR fragment upstream and downstream of a 74-nucleotide second intron of the white gene in pWIZ vector. Directional primers with inserts in opposite orientations on each side of the white intron were used (Fig. 14). The presence of the white intron spacer greatly facilitated cloning of the inverted repeats. The intron is flanked by *EcoRI, BglII, NotI, XhoI, SpeI,* and *AvrII* sites on the 5′ side and by *NheI, MluI,* and *XbaI* sites on the 3′ side. The entire cassette is downstream of the UAS enhancer–promoter and upstream of the SV40 transcription termination site.

Several criteria were considered while choosing the right region for subcloning including: the size of the fragment, which was between 300 and 1000 base pairs in

length, as this triggers stronger silencing by binding more efficiently to its complementary strands than shorter fragments. Second, the DNA fragment corresponded to a single complete exon from the target gene, since exons usually contain sequences that facilitate the translational processing of transcripts. Third, the fragment did not contain any restriction sites used in the PCR primers and last, conserved domains that might cause global silencing were avoided.

Three RNAi constructs with the desired orientations were generated, two head-head and one tail-tail corresponding to regions 1, 2 and 3 respectively (Fig. 15B). All three constructs were confirmed by restriction digest and sequencing (Fig. 16).

3.4.2 Generation of RNAi lines

Once the RNAi constructs were generated, 50μg of Qiagen purified DNA of one construct pertaining to Region3-*Dslmap*-pWIZ was injected (*Drosophila* Transgenic Services) into stage 1 or 2 w^{1118} having white eye color (Fig. 7 materials and methods). Seven RNAi lines were obtained that required a labor intensive process called pair-wising which requires two months to complete and consists of crossing one individual male with red eye to one individual virgin female with red eye. This process was repeated for the progeny of each of the seven pair-wised RNAi lines and continued for the next 3-4 generations until all individual flies from each line exhibited a uniform red eye color phenotype indicating homozygosity. The presence of the red-eyed flies further confirmed the successful insertion of the *Dslmap* IR due to the presence of mini white gene in the vector.

Figure 14. Generation of *Dslmap* inverted repeats constructs.

A procedure for generating RNAi constructs using the pWIZ vector. The target fragment of three different regions of the *Dslmap* cDNA were amplified by PCR using *XbaI* primers on both sides of the 1st insert and directional primers for the 2nd insert. The PCR product was inserted twice by two ligation steps into the *AvrII* and *NheI* sites of pWIZ. CIP, a calf intestinal phosphatase was used to dephosphorylate the 5′ ends of the pWIZ vector prior to ligation. Recombinants were selected in the desired orientation, such that after the second ligation step, inserts are in opposite orientations on either side of the white intron. IRs were generated for all three regions that are head–head or tail–tail repeats.

Generation of *Dslmap* inverted repeat (IR) for RNAi experiments

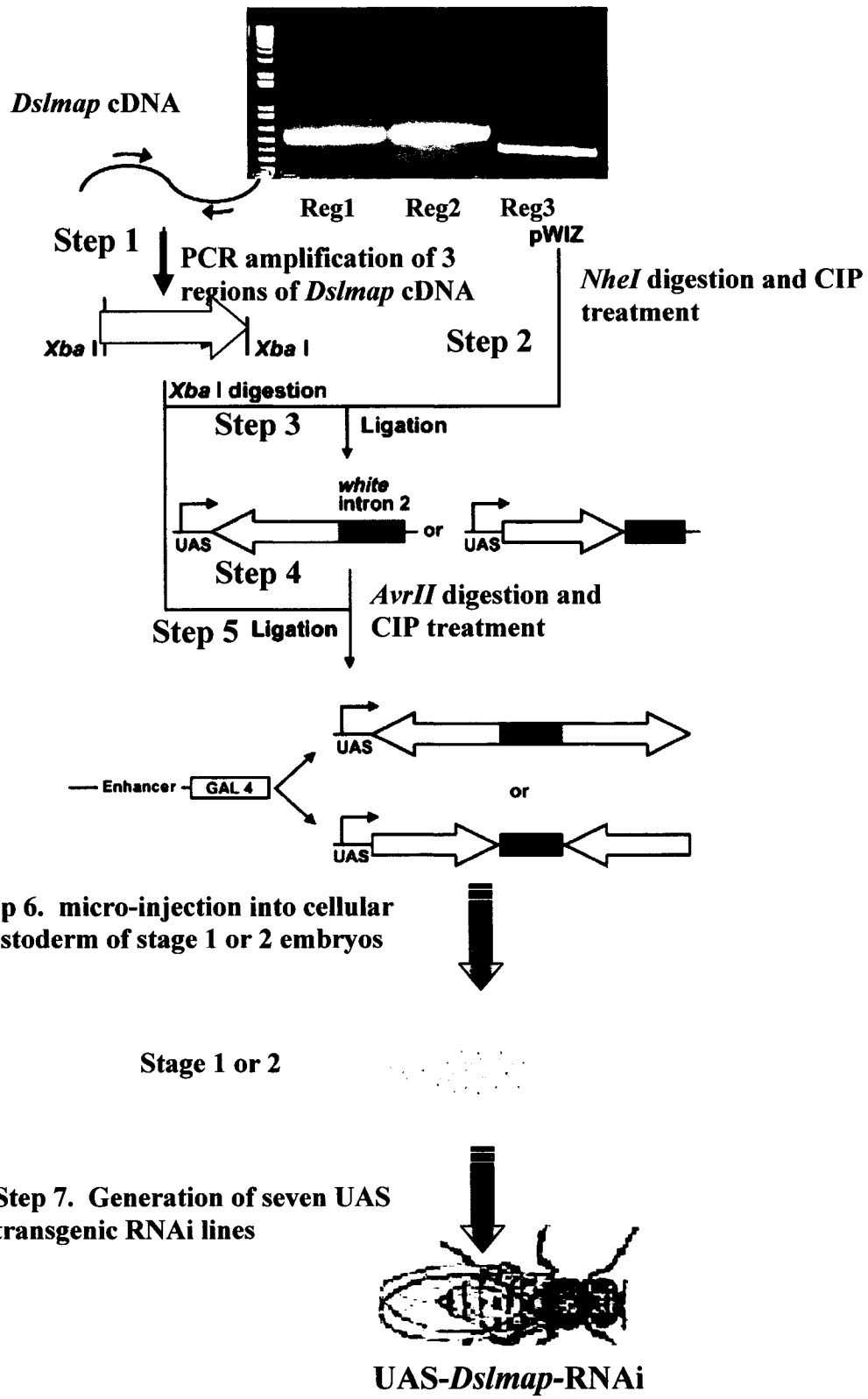

Figure 15. Structures of the RNAi constructs.

In panel A, Schematic representation of the pWIZ vector (Lee and Carthew, 2003). The pWIZ vector was constructed by placing the 74-bp second intron of the white gene into the pUAST transformation vector (Lee and Carthew, 2003). The intron is flanked by unique multiple cloning sites on the 5′ and 3′ ends to facilitate cloning. This vector was used to subclone *Dslmap* IR. Panel B, Three RNAi constructs generated using pWIZ vector including: Region 1 (520-bp), Region 2 (530-bp) and Region 3 (374-bp).

A.

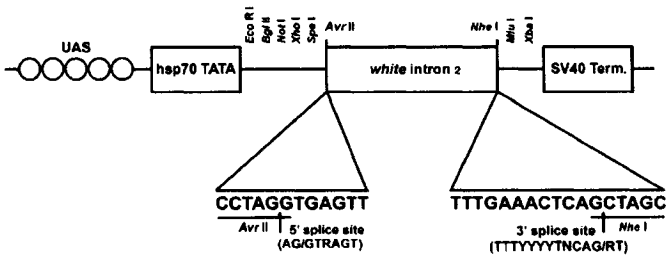

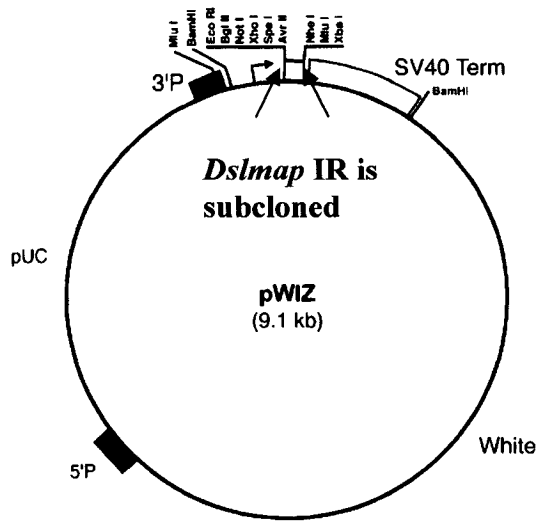

White intron zipper (pWIZ) RNAi vector

Lee and Carthew, 2003

B. **Structures of the three RNAi constructs**

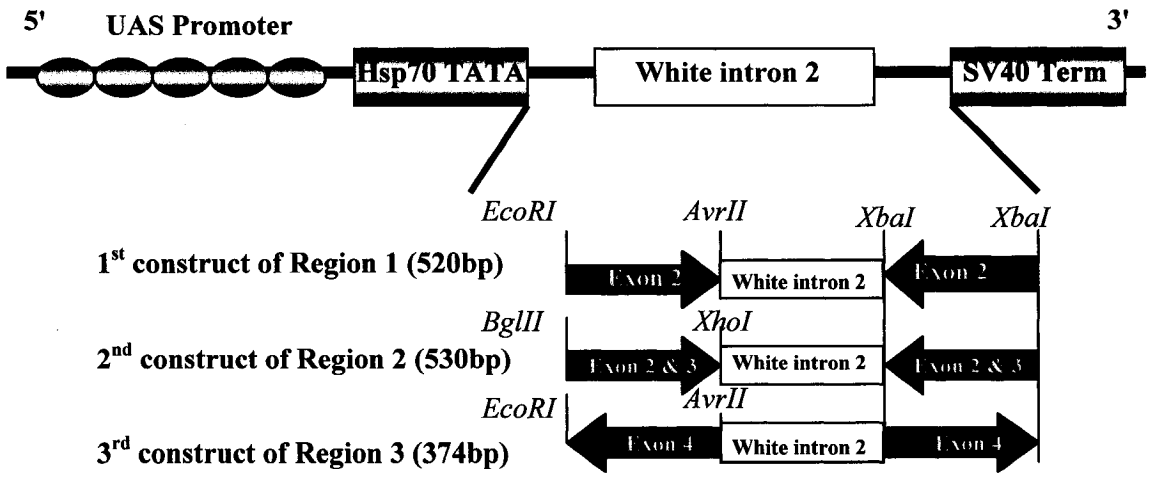

All three regions are free of conserved domains and restriction sites that are used in the PCR primers

Figure 16. Confirmation of the RNAi constructs.

All three constructs were confirmed by restriction digest with appropriate restriction enzymes and sequencing. In panel A, the RNAi construct of region 1 was confirmed by restriction digest of five colonies using *EcoRV*. All five colonies released 854-bp fragment of region 1 (orange arrow). The RNAi construct of region 2 was also confirmed by restriction digest with *EcoRI* which releases a 200-bp fragment (lower band, blue arrow). Panel B displays RNAi construct of region 3. This was also confirmed by restriction digest with *AftII* which releases a 250-bp fragment (lower band, blue arrow).

A.

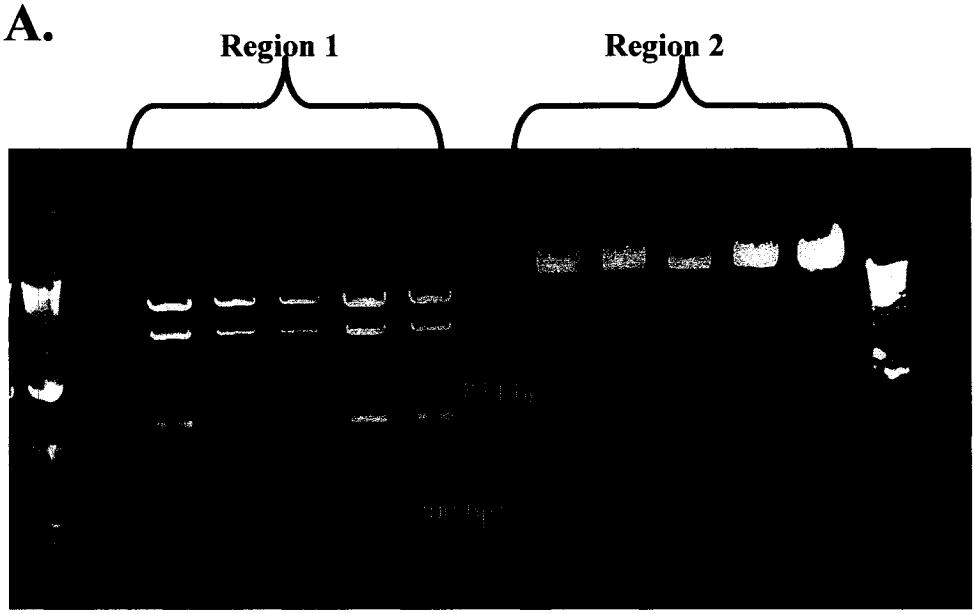

Region1+pWIZ
***EcoRV* digest**

Region 2+pWIZ
***EcoRI* digest**

B.

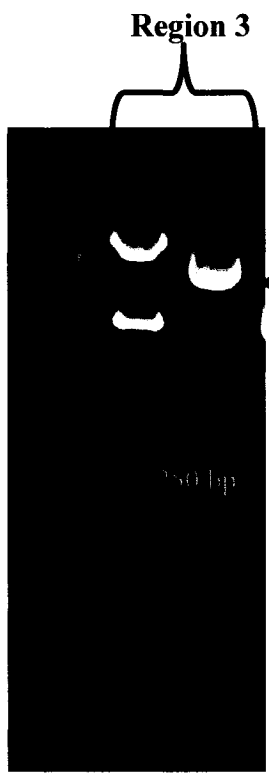

Region 3+pWIZ
No digest

Region 3+pWIZ
***AftII* digest**

3.4.3 Targeted activation of RNAi *in vivo*

Targeted RNAi uses the same rationale as conventional RNAi in which double stranded RNA from a gene is used to disrupt the function of that gene (Fire *et al.*, 1998). However, in studies presented here, gene disruption is targeted to specific cells using the GAL4/UAS binary system (Brand and Perrimon, 1993). Each of the seven homozygous RNAi lines carrying the *Dslmap* IR is called a responder line and is controlled by the presence of the UAS element which contains five optimized GAL4 binding sites (Fig 17). Since transcription of the responder RNAi lines requires the presence of GAL4, the absence of GAL4 in these responder lines maintains them in a transcriptionally silent state. To activate their transcription, the RNAi responder lines were crossed to flies expressing GAL4 in a particular pattern, termed the driver. In order to determine the efficiency of the RNAi technique, we needed to examine the levels of *Dslmap* mRNA expression in the activated RNAi lines, which is predicted to have a decrease in *Dslmap* expression. *In situ* hybridization was performed on stage 13 embryos using a ubiquitous driver, termed *arm*-GAL4 which revealed that 73.4% of stage 13 embryos carrying the transgene and the Gal4 driver have reduction of *Dslmap* mRNA transcripts as shown by decreased staining (Fig. 18 C and D). In comparison, 87.5 % of w^{1118} controls carrying the driver or the transgene alone and showed intense staining indicating high levels of *Dslmap* expression (Fig. 18 A and B). Of the seven transgenic RNAi lines, three were chosen for subsequent analysis based on the levels of *Dslmap* transcript expression as shown by *in situ* hybridization experiment.

Figure 17. Targeted activation of RNAi lines.

The GAL4/UAS binary system in *Drosophila*. Each Gal4 driver has a unique transcriptional pattern; in this case, *arm*-Gal4 was used to ubiquitously activate the responder *Dslmap* gene which is fused to five Gal4 binding sites arrayed in tandem (5X UAS, red circles). Upon crossing the two lines, *arm*-Gal4 driver and the *Dslmap*-IR-pWIZ responder line, the Gal4 protein, directly binds to the Upstream Activating Sequence (UAS) element and drive the expression of *Dslmap* located downstream from the UAS element in tissues where Gal 4 is expressed.

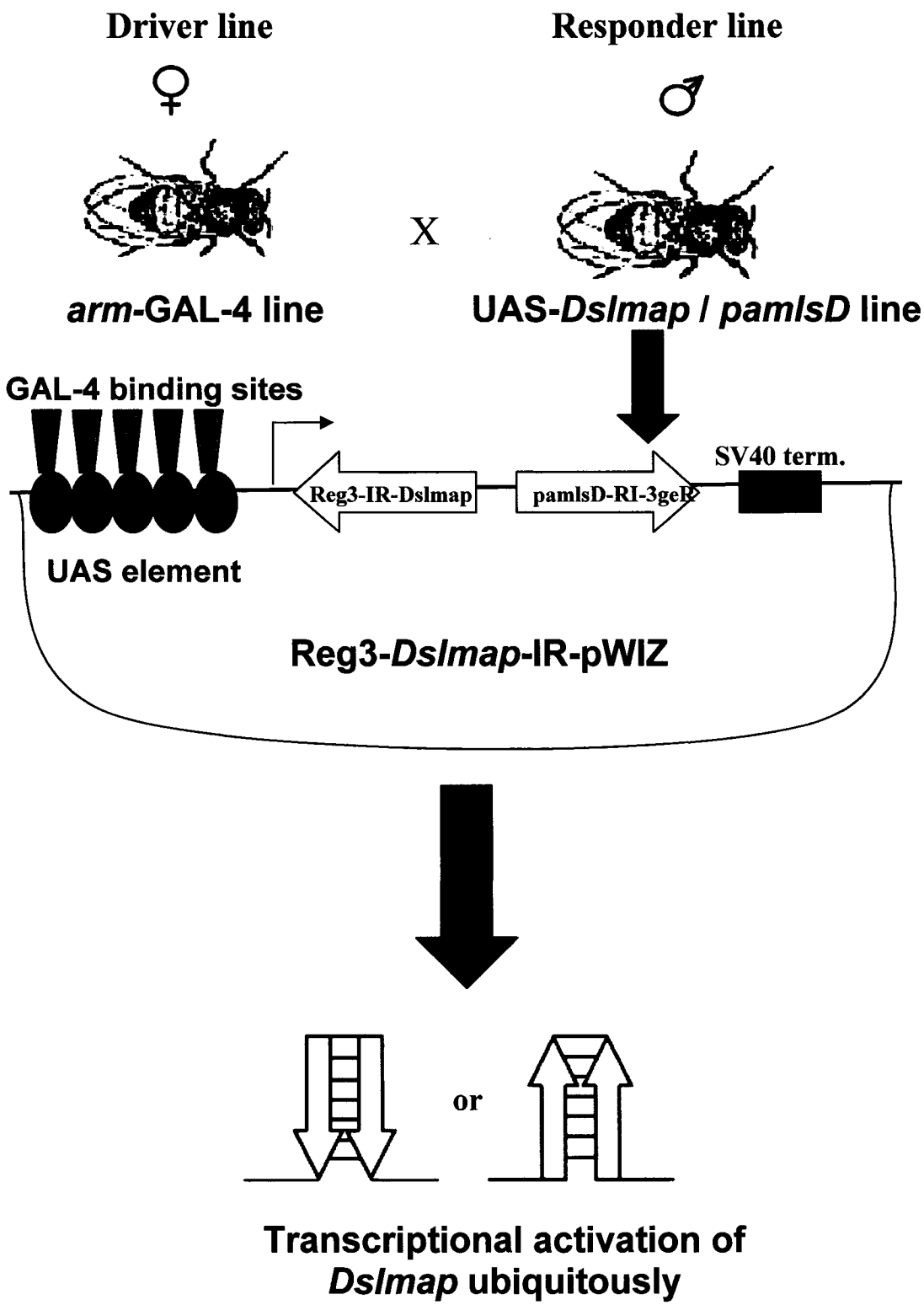
Driver line
Responder line
X
arm-GAL-4 line
UAS-DsImap / pamIsD line
GAL-4 binding sites
Reg3-IR-DsImap
pamIsD-RI-3geR
SV40 term.
UAS element
Reg3-DsImap-IR-pWIZ
or
Transcriptional activation of
DsImap ubiquitously

Figure 18. *Dslmap* mRNA transcript levels in activated RNAi lines.

(A-D) *In situ* hybridization performed on stage 13 embryos. (C & D) A significant reduction of *Dslmap* mRNA was observed in comparison to the much darker staining observed in controls (A & B). This was accomplished using a ubiquitous *arm*-Gal-4 driver. (E) Represents a quantitative analysis revealing only 26.6 % of stage 13 embryos carrying the transgene and the Gal-4 gene express *Dslmap* transcripts in comparison to 87.5% of w^{1118} controls carrying the Gal-4 or the transgene alone. Anterior to the left; A & C; sagittal view, B & D; dorsal view, Scale bar = 100μm.

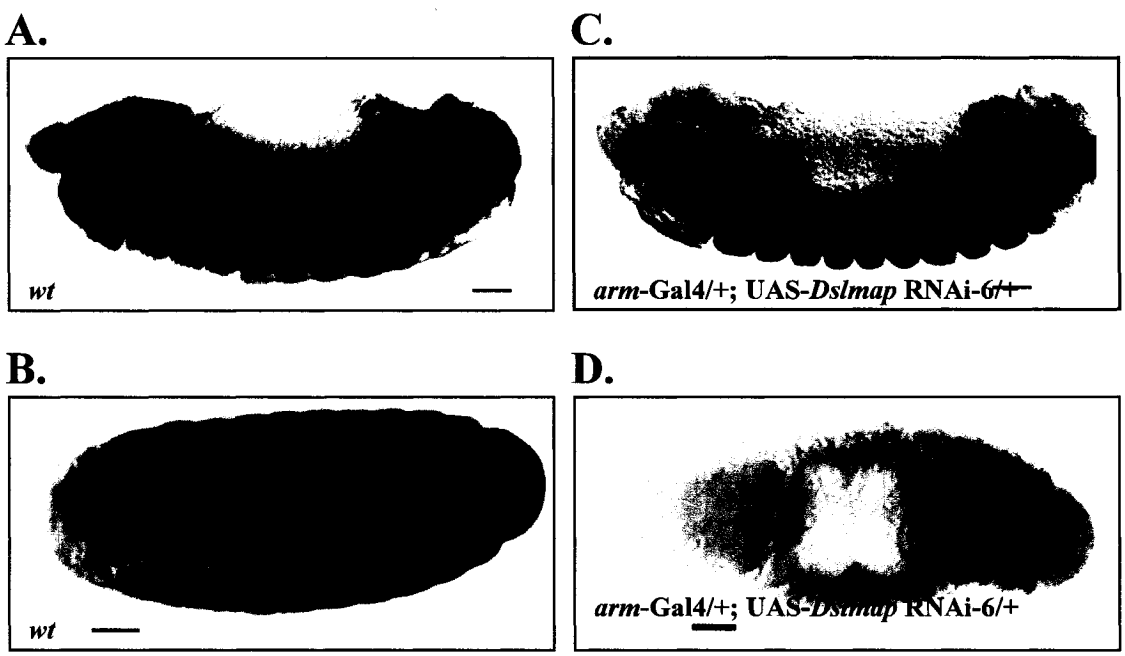
A.
C.
wt
arm-Gal4/+; UAS-Dslmap RNAi-6/+
B.
D.
wt
arm-Gal4/+; UAS-Dslmap RNAi-6/+

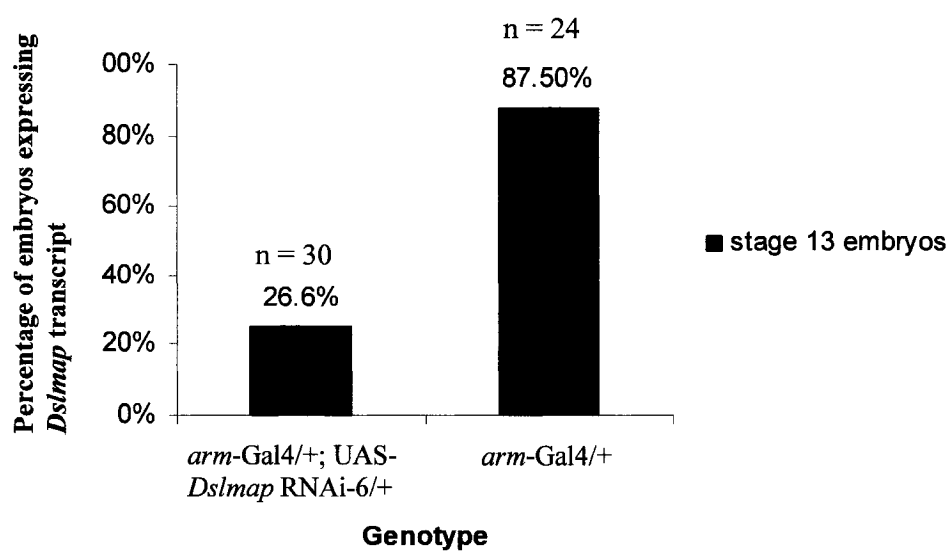
E.
Percentage of embryos expressing Dslmap transcript
00%
80%
60%
40%
20%
0%
n = 24
87.50%
n = 30
26.6%
stage 13 embryos
arm-Gal4/+; UAS-Dslmap RNAi-6/+
arm-Gal4/+
Genotype

3.4.4 *In vivo* effects of *Dslmap* RNAi

Once we determined that the levels of *Dslmap* transcripts were reduced following activation of the RNAi lines, we proceeded to determine if the RNAi effect on development could be manipulated in a tissue specific manner. We examined the effects of activating RNAi on the CNS system since the *in situ* hybridization data indicated a robust expression in fly embryos. Three RNAi lines (Lines 1, 6 and 10) were generated and examined using two CNS drivers: a pan-neuronal driver, termed *elav*-Gal4 (Rogina and Helfad, 2004) and a Glial driver, *Gcm*-Gal4 (Sears *et al.*, 2003) to activate RNAi in neurons and glia respectively.

3.4.5 Neuronal specific down-regulation of *Dslmap*

The *Drosophila* embryonic nervous system has a ladder like structure (Schmidt *et al.*, 1997) consisting of two lateral longitudinal axons (Fig. 19A, arrowhead) connecting individual segments which are interconnected by an anterior and posterior commissures (Fig. 19A, downward and upward arrows, respectively). This can be visualized with mAb BP102, an excellent marker for the pattern of commissures and connectives. *Dslmap* was down regulated in the CNS after crossing three RNAi lines to virgins of *elav*-Gal4, a pan-neuronal driver (Rogina and Helfad, 2004). Embryos were collected every 4-5 hours, and then heat shocked for 2 hours at 29°C as this was shown to have a stronger effect on Gal4 activity (Duffy, 2002). After heat shocking, the embryos were allowed to recover and aged at room temperature until the desired stage was obtained. Collected embryos were fixed according to the protocol described in the materials and methods and stored in methanol at -20°C until later use. Embryos were stained with monoclonal antibody BP102.

Down-regulation of *Dslmap* in neurons of stage 15 embryos revealed obvious defects in the organization of the axonal scaffold (Fig. 19, A-H). Commissural axons were either partially fused or less distinct (B, F, & G, arrows), completely fused (C, D, & E, arrows), and / or missing (H, arrow). Defects were also observed in the longitudinal connectives extending to adjacent neuromeres, and consisted of reduction or breakage (F & G, arrowheads), or absence (B, C, E, & H, arrowheads). Furthermore, disorganization in the longitudinal tracts was also seen (D, arrowhead).

A quantitative analysis was carried out to determine the percentage of embryos and hemisegments (i.e., single side of a segment) exhibiting the above defects in the commissures and longitudinal connectives following antibody staining with BP102. Two RNAi lines were examined closely for quantification of CNS axonal defects and revealed 18.8% (n=138) of stage 15 embryos carrying the transgene and *elav*-gal4 driver exhibiting defects in the ventral nerve cord segments (Penetrance). Defective hemisegments were present in 46.6% of all 208 scored segments in defective embryos (Expressivity) (Fig. 20, table and graph). Activated ln10 exhibited a 14% penetrance (n=86) and 62.5% of segments were defective (n=96) (Fig. 20, table and graph). Controls used in the RNAi experiment included w^{1118} embryos carrying the driver or the transgene alone. Controls did not have any of the specific defects identified in the activated RNAi lines.

In summary, the use of the RNAi technique was shown to be an effective method to down-regulate *Dslmap* in the neurons using the pan-neuronal *elav*-Gal4 driver as was evidenced by the quantitative deficits in the longitudinal and commissural axons.

Figure 19. *Dslmap* is critical for the developing CNS.

Pan-neural expression of *Dslmap* RNAi affects axonal patterning (B-I). Ventral view of the ventral nerve cord (VNC) of stage 15 embryos stained with BP102 (A-I) and shown with anterior up. (A) Control embryo heterozygous for *elav*-Gal4 and w^{1118}. Thick longitudinal connectives connect each hemisegment (arrowhead). The downward and upward arrows denote the anterior and posterior commissures, respectively. (B-H) Defects in axonal scaffold after down-regulating *Dslmap* in neurons consisted of partially fused or less distinct (B, F, & G, arrows), completely fused (C, D, & E, arrows), and / or missing (H, arrow). The axons of the longitudinal connectives also exhibited some reduction or breakage (F & G, arrowheads), and absence (B, C, E, & H, arrowheads). (I) Down-regulation of *Dslmap* in glia using *Gcm*-Gal4 also revealed similar neuronal defects. Defects in commissural axons resemble those observed in neuronal down-regulated lines and include: thickness in commissural regions where the anterior and posterior commissures are in close proximity and are not well separated (I, arrow). Defects in the longitudinal axons were also observed and consist of thin or absent longitudinal tracts (I, arrowheads). Only stage 15 embryos were examined and eight segments out of 14 were quantified. Collected embryos were heat shocked for 1hour at 29°C, then allowed to recover at room temperature for 2 hours and aged for an extra 5 hours to obtain the required stage. Scale bar = 100μm.

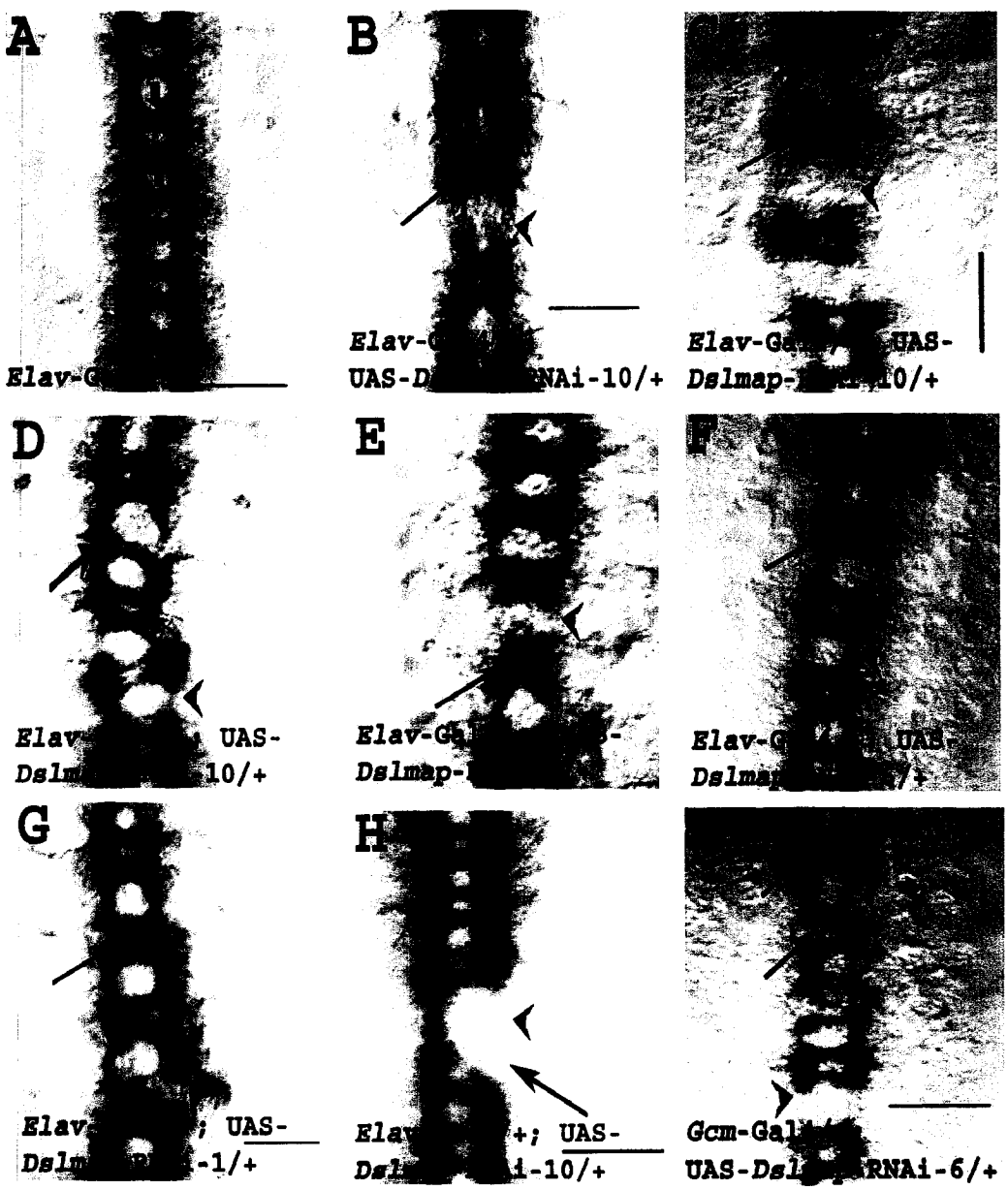
A
Elav-G
B
Elav-G
UAS-D NAi-10/+
Elav-Ga UAS-
Dslmap- 10/+
D
Elav UAS-
Dslm 10/+
E
Elav-Ga -
Dslmap-
F
Elav-G UAS-
Dslma /+
G
Elav ; UAS-
Dslm -1/+
H
Elav +; UAS-
Dsl i-10/+
Gcm-Gal
UAS-Dsl RNAi-6/+

Figure 20. Quantitative analysis of the effects of *Dslmap* RNAi.

Two RNAi lines were examined carefully for axonal defects. In A, quantification of stage 15 embryos of both Line 10 and 6 revealed a low penetrance for targeted neuronal activation using *elav*-Gal4. However, the percentage of defective segments in defective embryos was much higher (expressivity: ln10 = 62.5% & ln6 = 46.6%). Activation of the RNAi lines using a Glial driver, *gcm*-Gal4 revealed a much higher penetrance for line 6 (42.4%), and a similar expressivity (45.1%). Panel B, shows a graphical representation of the quantification presented in A. Penetrance was calculated for embryos exhibiting defects in total population for each RNAi line whereas expressivity was counted as the percentage of defective hemisegments in defective embryos. Only stage 15 embryos were quantified and eight segments were examined. Controls were free of any RNAi activation. Error bars represent standard deviation.

A

Genotype	Stage	Total embryos	Defects	%	Total hemi-segments	Defective hemi-segments	%
				Penetrance			Expressivity
In6/*elav* Gal4	15	138	26	18.8	208	97	46.6
In6/w^{1118}	15	140	0	0			
In10/*elav*-Gal4	15	86	12	14	96	60	62.5
In10/w^{1118}	15	120	0	0			
In6/*gcm*-Gal4	15	66	28	42.4	224	101	45.1
***gcm*-Gal4/ w^{1118}**	15	135	0	0			

B

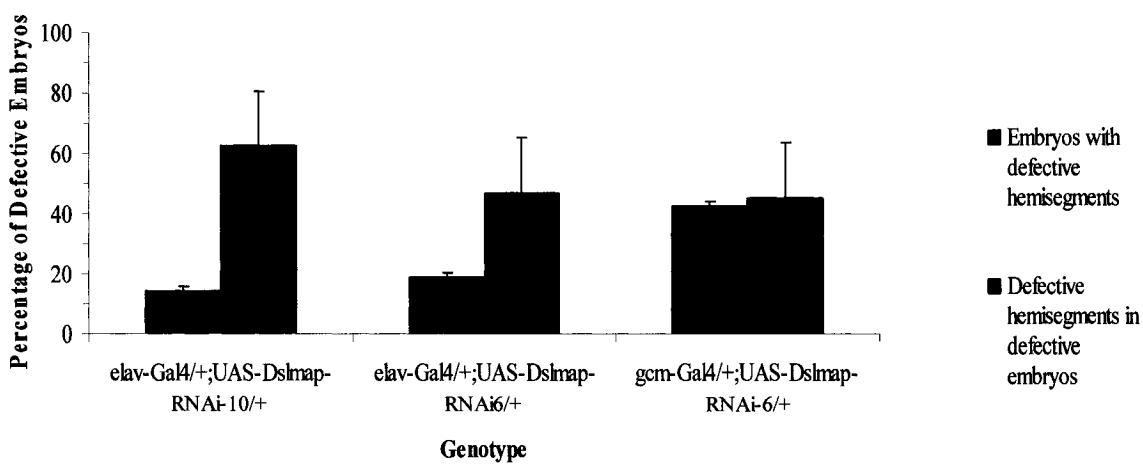

We have determined the effect of *Dslmap* down-regulation on the neuronal component of the CNS but since SLMAP is ubiquitously expressed, it may also have a role in glial functions. Glial cells are known to provide a supportive role for the neurons by insulating them and providing them with trophic and nutritive factors (Parker and Auld, 2004). In addition, reciprocal interactions between glia and neurons are essential in dictating the CNS structure, and in assisting the proper bundling and ensheathment of axons (Sepp and Auld, 2003).

3.4.6 Glial down-regulation of *Dslmap*

In view of the important role that the glia serves, we investigated whether *Dslmap* down regulation in the glia serve a function in CNS development. A *Gcm*-Gal4 glial driver was used to activate RNAi lines in order to examine the requirement for *Dslmap* in this function. Embryos were then stained with BP102 antibody to examine the integrity of the CNS axons. One *Dslmap* RNAi line (ln 6) was expressed using the *Gcm*-Gal4 driver based on the range of phenotypes obtained with the pan-neuronal driver. Activation of ln6 with *Gcm*-Gal4 revealed commissures that are thicker than normal (Fig. 19 I, arrows), as well as reduction and breaks in the longitudinal connectives (Fig.19 I, arrowheads). Quantification analysis of the data indicated a more penetrant phenotype of 42.4% (Fig. 20) whereas 45% of defective segments exhibited defects similar to those observed with pan-neuronal *elav*-Gal4 driver but more severe and frequent.

The RNAi technique was able to efficiently down-regulate *Dslmap in vivo* in both neurons and glia, which resulted in a disruption of the commissural and longitudinal

axonal scaffold. Targeted down-regulation of *Dslmap* in neurons and glia revealed similar axonal defects although glial phenotypes were more frequent and severe in nature.

3.5 Overexpression of *Dslmap*

An alternative approach to RNAi which can be equally informative for regulating the activity of *Dslmap in vivo* is overexpression. The full length *Dslmap*-UAS plasmid was established as described in the materials and methods section. The pUAST vector contains a UAS promoter comprised of five optimized sites for the binding of the GAL4 protein (when crossed to the Gal4 driver line), a heat shock protein 70 TATA site essential for the transcription of the GAL4 protein, a multiple cloning site and an SV40 transcription termination site (Fig. 21, A & B). The completed UAS-*Dslmap* construct was confirmed by sequencing and restriction digests (Fig. 22 A). 50 μg of UAS-*Dslmap* plasmid was injected into stage 1 or 2 embryos in a similar fashion to the RNAi constructs (see Fig. 7 in materials and methods).

Twelve transgenic UAS lines were obtained from transgenic services that required a pair-wising process similar to the one employed in RNAi lines to generate homozygous flies with red eyes only. Two lines showing expression of *Dslmap* in seven segments using the *paired*-Gal4 line were chosen for subsequent studies (Lines 2 & 12). *In situ* hybridization was performed to determine if *Dslmap* is overexpressed using a *paired*-Gal4 driver, which specifically drives expression in seven segments due to the expression pattern of *paired* gene. The results confirms that *Dslmap* overexpression is in fact induced in seven segments (Fig. 22B), and furthermore these results confirm the specificity of the RNA riboprobe used in *In situ* hybridization studies.

Figure 21. Generation of *Dslmap* overexpression construct.

In panel A, pUAST transformation vector (Brand and Perrimon, 1993) was used to sub-clone the full length *Dslmap* (3.02 kb) cDNA downstream of a UAS promoter element (Brand and Perimon, 1993). In panel B, the full length *Dslmap* cDNA flanked at both ends with *EagI* primers was digested, blunt-ended and PCR purified then ligated into *KpnI* digested, CIP and blunt treated pUAST vector. Ligation was performed at room temperature for two hours. Fermentas Blunting kit and enzymes were used.

A. **pUAST Overexpression Construct**

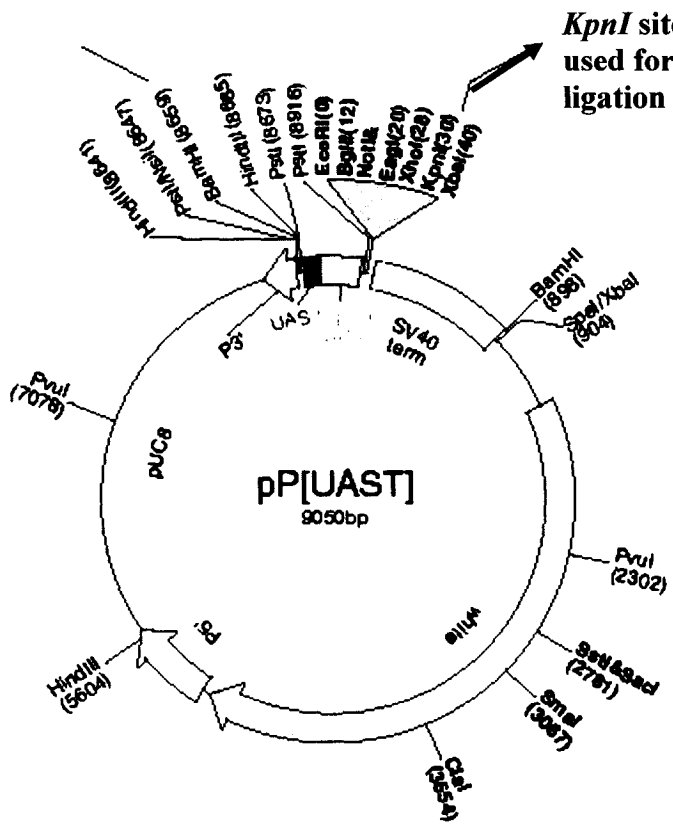

Brand and Perrimon, 1993

B. **UAS-*Dslmap* construct**

Figure 22. Confirmation of *Dslmap* overexpression.

In panel A, the UAS-*Dslmap* construct was confirmed by restriction digest with two restriction enzymes: *KpnI* and *XhoI* which release a 2.0 kb and 1.2 kb fragments respectively. In panel B, stage 10 embryo of an activated UAS line revealed expression of *Dslmap* in seven segments confirming that overexpression is induced; furthermore it proves the specificity of the riboprobe. Six UAS lines were examined for the induction of *Dslmap*, and four showed positive results but two were chosen for further analysis and revealed strong expression in seven segments (open arrow) upon activation with *paired*-Gal 4 driver. Scale bar = 100μm.

A.

B. **Activation of UAS line in 7 segments using *paired*-Gal4 driver**

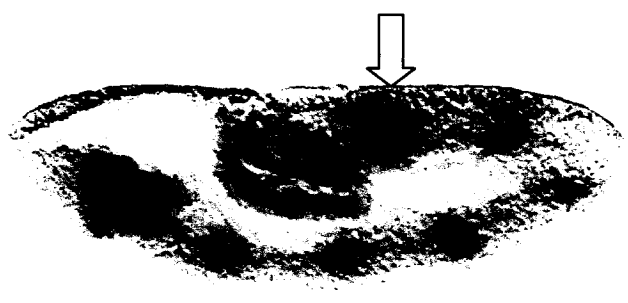

3.5.1 Overexpression of *Dslmap* perturbs commissural and longitudinal axonal scaffold formation

CNS drivers including glial (*gcm*-Gal4) and pan-neuronal (*elav*-Gal4) were also used to overexpress *Dslmap* in the CNS. Activation of two UAS lines in glia (B,F) and neurons (C-E) resulted in axonal defects consisting of weak longitudinal tracts (Fig. 23, B-F, arrowheads) that results from failure of the longitudinals to extend in an anterior-posterior direction. Some segments exhibited fused or less distinct commissures (Fig. 23, B, C, & E, arrows) and/or absent commissures (Fig. 23, D & F arrows). The last defect consisting of the absent commissure was frequently observed in both glial and neuronal overexpression in which one segment located in the middle of the midline was absent and accompanied with disorganized longitudinal connectives. Quantitative analysis revealed that neuronal activation of lines 2 and 12 resulted in 15.7% and 20.1% of defective embryos respectively (Fig. 24, table and graph). A slightly higher penetrance was observed for glial activation of line 2 (23.5%). 55.5% and 35.0% of hemisegments were defective in the neuronal activated lines 2 and 12 respectively, whereas the glial activated line 2 revealed a slightly lower expressivity (20.1%) (Fig. 24). In conclusion, these results support a role for *Dslmap* in both neurons and glia and are consistent with those of the RNAi experiments with the exception of one specific phenotype consisting of the absence of one segment localized to the middle of the ventral cord. The penetrance for the neuronal activated RNAi and UAS lines were very similar. However, the glial activated lines revealed higher penetrance.

Figure 23. Axonal defects due to *Dslmap* overexpression.

Overexpression of *Dslmap* in neurons and glia using *Elav*-Gal4 and *Gcm*-Gal4 respectively, resulted in axonal scaffold defects ranging from absent or fused commissures to weak longitudinal tracts. (A) Control embryo heterozygous for *elav*-Gal4 and w^{1118}. Thick longitudinal connectives connect each hemisegment (arrowhead). The downward and upward arrows, denotes the anterior and posterior commissures respectively. (B) Overexpression of *Dslmap* in glia resulted in weak or broken longitudinal tracts (arrowheads), and the space between the anterior and posterior commissural axons is smaller (arrow). (C) After neuronal activation of UAS line 12, the commissures are less distinct (arrows), and the longitudinals are weak in three segments (arrowhead). (D) In the neuronal overexpressed embryo of line 2, longitudinal tract in one segment appears to be weak (arrowhead), whereas the commissural axon in one segment appear to be absent (arrow). (E) After neuronal activation of UAS line 2, commissures are fused in two segments (arrows), and longitudinals are weak (arrowheads). (F) The commissures in one segment is missing (arrow), accompanied with weaker longitudinal tracts (arrowhead) in glial activated UAS-*Dslmap*. Scale bar = 100μm.

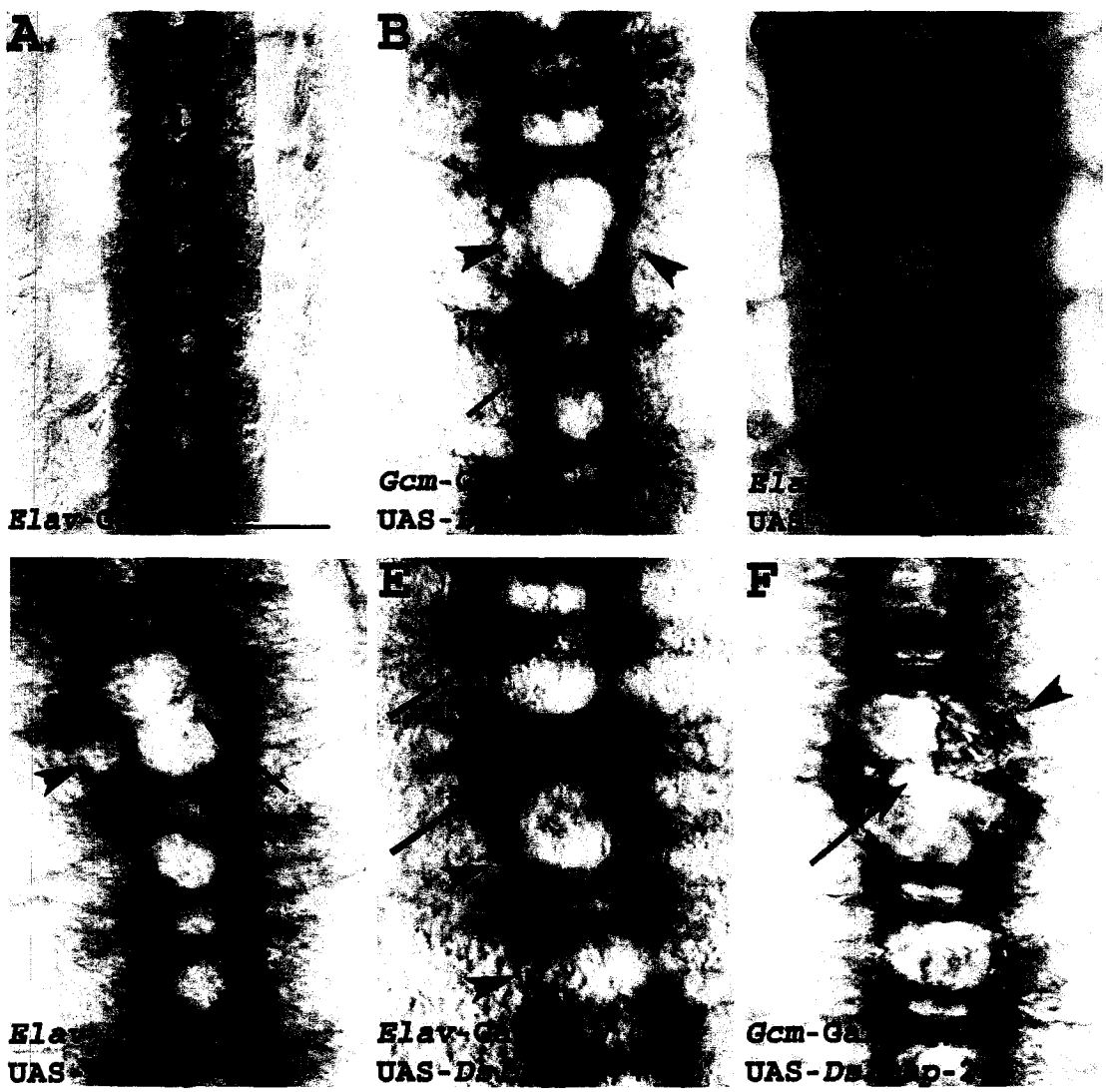
A
B
Elav-G
Gcm-G
UAS-
Ela
UA
Ela
UAS-
E
Elav-G
UAS-Da
F
Gcm-Ga
UAS-Da p-2

Figure 24. Quantitative analysis of *Dslmap* overexpression defects.

Two UAS lines were examined carefully for axonal defects using glial and neuronal drivers. In panel A, quantification of stage 15 embryos of both lines 2 and 12 exhibited a low penetrance of axon defects after targeted neuronal activation using the *elav*-Gal4 driver. However, the percentage of defective segments in embryos was much higher in UAS line 2 in comparison to a slightly lower one in line 12 (ln2 = 55.4% & ln12 = 35%). Activation of one UAS line using *gcm*-Gal4 revealed a similar penetrance to the neuronally activated UAS lines. However, the expressivity was much lower (20.1%). In panel B, graphical representation of numerical values presented in A. Penetrance was calculated for the number of embryos exhibiting defects in the total population for each UAS line whereas expressivity was counted as the percentage of defective hemisegments per embryo. Only stage 15 embryos were scored and eight segments were examined. Controls were free of any RNAi activation. Error bars represent standard deviation.

A

		Penetrance			Expressivity		
Genotype	**Stage**	**Total embryos**	**Defects**	**%**	**Total hemi-segments**	**Defective hemi-segments**	**%**
ln2/*elav*-Gal4	15	134	21	15.7	168	93	55.4
ln2/w^{1118}	15	100	0	0			
ln12/*elav*-Gal4	15	50	10	20	80	28	35
ln12/w^{1118}	15	120	0	0			
***gcm*-Gal4/ln2**	15	170	40	23.5	320	67	20.1
***gcm*-Gal4/w^{1118}**	15	135	0	0			

B

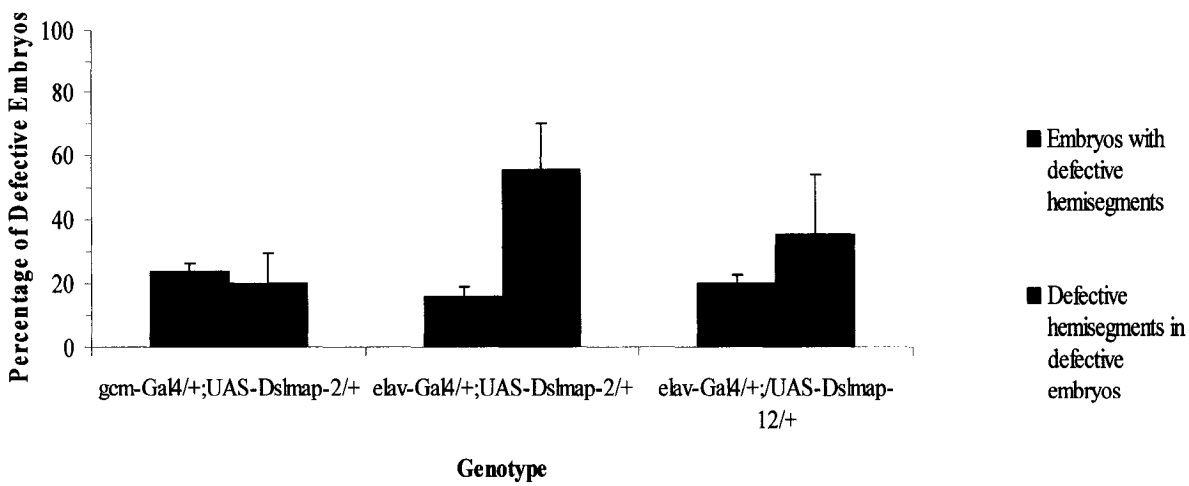

DISCUSSION

We have identified a novel coiled-coil tail-anchored membrane protein in fruit flies referred to as *Dslmap* (corresponding to accession No. CG17494 in flybase). *Dslmap* represents the mammalian SLMAP homologue whose function remains to be defined. Genetic manipulation employing *in vivo* approaches to alter *Dslmap* expression in the developing CNS of *Drosophila* embryos revealed a critical role in axonal morphology. In the present study, we report that the *Dslmap* gene is encoded by four exons that span 7.65 kb of genomic DNA sequence. Analysis of *D*SLMAP structural features revealed the presence of a putative FHA domain at the extreme N-terminus encompassing 59 amino acids. Three coiled-coil regions were also predicted using the COILS program (Lupas *et al.*, 1991). The hydrophobicity plot and SMART programs predicted a single putative TM domain at the extreme C-terminus encoded by 17 amino acids. *In situ* hybridization experiments revealed an early and a ubiquitous expression of *Dslmap* during embryogenesis.

A single gene mapped to the short arm of human chromosome 3 encodes SLMAP, which undergoes alternative splicing to generate tissue specific isoforms. The relatedness between fly SLMAP and the rabbit SLMAP3 isoform was predicted using the BLAST algorithm and revealed 28.6 % identity (48.3% similarity) over 721 amino acid residues. The domain organization of *D*SLMAP was also found to be similar to its mammalian counterpart and is comprised of a FHA domain with a significant identity (55.9%) to the rabbit SLMAP3 isoform. This high identity is significant because the FHA domain in mammalian SLMAP3 isoform is essential for centrosomal targeting (Guzzo *et al.*, 2004) which is crucial for various nuclear processes. The FHA domains have been

characterized in a number of proteins with diverse roles, including transcription factors (Kim *et al.*, 2002), kinases and phosphatases (Li *et al.*, 1999), and kinesin (Lee *et al.*, 2003). However, there are some proteins lacking this domain that are known to be targeted to the centrosome such as centrosomin (Heuer *et al.*, 1995). Centrosomin possess other structural features that might have an essential role in its localization to the centrosome, including three leucine zipper motifs and several coiled-coil domains (Heuer *et al.*, 1995). Analysis of *D*SLMAP secondary structure revealed the presence of large regions of coiled-coil structures lacking leucine zipper motifs. The coiled-coil regions are known to mediate protein-protein interactions (Landshulz *et al.*, 1988; Lupas *et al.*, 1991), and are identified in many transcription factors (Wang *et al.*, 2001). Coiled-coil regions are also found in many other classes of proteins including ion channels (McCormack *et al.*, 1991), glucose transporter glycoproteins (Thorens *et al.*, 1988), P transposases (Simonelig and Anxolabehere, 1991) and heat shock factors (Rabindran *et al.*, 1991; Sarge *et al.*, 1991). The specialized leucine-rich coiled-coil regions in mammalian SLMAP are essential for SLMAP oligomerization and were shown to mediate SLMAP-SLMAP interactions (Guzzo *et al.*, 2004). The presence of multiple coiled-coil regions in SLMAP of both flies and vertebrates further confirms the relatedness of SLMAP between the two species, and suggests that *Dslmap* either oligomerizes with itself (Guzzo *et al.*, 2003) or with other proteins to carry out its function. A stretch of 19 hydrophobic amino acid residues present at the extreme carboxyl terminal of *D*SLMAP was predicted using a hydrophobicity plot to encode a single putative TM domain sharing identity with two alternatively spliced TM domains in rabbit (25% to TMD1 and 8.8% to TMD2). The function of the TM domain in *Dslmap*

remains to be defined. However, we know from its mammalian homologue that the TM domain is essential for targeting SLMAP to different membrane systems. Guzzo *et al.*, (2004) demonstrated that the TMD1 targets SLMAPs to the ER whereas TMD2 targets SLMAPs to the mitochondria.

The *Dslmap* gene is encoded by only four exons that span approximately 7.65 kb of DNA genomic sequence in comparison to the much larger mammalian SLMAP gene that has twenty-four exons spanning over approximately 122 kb of genomic DNA. Furthermore, the *Dslmap* intron-exon boundary is much simpler than its mammalian counterpart, and the intron sizes in *Dslmap* vary from 59-bp to 2.9 kb in comparison to the mammalian gene. Exon I in mammalian SLMAP encodes the FHA domain and the first initiating methionine (ATG1; M1), whereas the FHA domain and the ATG initiation site in *Dslmap* are encoded by exon II. Other features such as the coiled-coil regions in *Dslmap* are encoded by both exon III and exon IV, and a single TM domain is encoded by the last exon IV. By comparison, the two mammalian TM domains reside within the extreme carboxyl terminus of SLMAP3 and are encoded by exon XXIII and XXIV. Another important structural feature of *Dslmap* is the presence of several protein kinase recognition sites, many of these are known to regulate the functions of proteins through phosphorylation. The presence of such sites in *Dslmap* implies that phosphorylation may be an important mechanism in the regulation of *Dslmap* activity. This idea is supported by the observation that many centrosomal proteins are phosphorylated in order to carry out their functions (Kuriyama and Nislow, 1992). Similar sites were also found in mammalian SLMAP through a PROSITE sequence scan, which predicted the presence of the following consensus sites for casein kinase II phosphorylation, protein kinase C

phosphorylation, N-glycosylation and N-myristoylation. In conclusion, both *Dslmap* and mammalian SLMAP share similar structural features that include the FHA domain, coiled-coil regions and a hydrophobic TM domain at the extreme C-terminus, which may imply a similar function between the two species.

The expression of *Dslmap* using whole-mount *in situ* hybridization revealed a ubiquitous expression at various stages of embryonic development including, the earliest stage 5 of cellular blastoderm. This is similar to its mammalian counterpart, which has an early and ubiquitous expression in cardiac tissue, smooth muscle, liver, pancreas, kidney, spleen, and brain (Wigle *et al.*, 1997). *Dslmap* on the other hand, was also shown to be expressed in the mesoderm, midgut, hindgut, brain hemispheres and ventral nerve cord. Tissue specific expression and the existence of multiple structural domains in *Dslmap* suggests that this protein may play multiple cellular roles, and therefore may serve to regulate membrane biology, consistent with its hypothesized roles in membrane biology and cell function.

There are a number of proteins, such as Ephrins in *Drosophila* that share an overall low similarity in amino acid sequence with their homologues in other species (8% similarity to human ephrinB1, 7% similarity to the *C. elegans* ephrin vab-2 and only 3% to human ephrinA1) (Bossing and Brand, 2002), and yet despite these differences they perform similar functions with regards to midline guidance due to a much higher identity shared in structural domains such as the extracellular domain of ephrins (41% to human ephrin A1) and (42% to human ephrin B1) (Bossing and Brand, 2002). Another example of conserved genes between flies and vertebrates is the newly identified pro-survival Bcl-2 protein homologue in flies, referred to as *Buffy*, which shares a low overall identity of

19% but a 56% similarity to a 239 amino acid region of human Bcl-2 (Quinn *et al.*, 2003). However, despite the low identity, *Buffy* shares essential conserved domains with its homologue including a C-terminus hydrophobic anchor which is believed to have an essential role in mammalian Bcl-2 (Nguyen *et al.*, 1993; Lithgow *et al.*, 1994). This suggests an important point with regards to using the *Drosophila* model system and that is, for a given protein to have a significant and an essential role in development, it is not necessary for it to share an overall high identity at the amino acid level, instead the importance of a given protein stems from the structural features associated with it. In the case of *Dslmap*, these essential features are comprised of a putative hydrophobic C-terminus anchor, and the FHA domain.

To determine the functional role of the novel *Dslmap* gene, targeted RNAi and overexpression studies were performed coupled with the use of the GAL4/UAS binary system. This system has been used successfully to investigate the function of many genes (Korey and MacDonald, 2003; Hay *et al.*, 1997). Using this system, *Dslmap* was down-regulated using two different CNS drivers, a pan-neuronal *elav*-Gal4 and a glial *Gcm*-Gal4 driver. The CNS system was chosen due to expression of *Dslmap* in the brain hemispheres and in the ventral nerve cord. This expression pattern resembles that of rat SLMAP, which is also expressed in the neonatal hippocampus, Mueller glia, and migratory neurons (Wigle, 1997). Furthermore, there are many similarities in nervous system development between flies and vertebrates that could imply similarities in higher functions (Arendt and Nubler-Jung, 1997, 1999). Similarities in the nervous system between the two species include the generation of neuronal and glial precursors from the neuroectoderm. Both vertebrates and *Drosophila* employ the same basic strategies and

similar cell-to-cell signaling mechanisms for the initial determination of glia cells, the guidance of growth cones, the migrational patterns of glia and neurons, the ensheathment of axons and the survival of both glia and neurons (Campbell and Perterson, 1993; Rothberg *et al.*, 1990). In addition, both vertebrates and insects have conserved molecules such as netrins and receptor protein tyrosine kinases that are essential for the chemoattraction of commissural axons and axon pathfinding (Mitchell *et al.*, 1996; Wilson *et al.*, 1993; McLaughlin and O'Leary, 1999; Holder and Klein, 1999).

RNAi experiments revealed similar phenotypes for both glial and neuronal activated RNAi lines. All three RNAi lines exhibited a consistent spectrum of axonal phenotypic defects in the CNS of stage 15 embryos. Defects ranged from fused or absent commissures to reduced, broken or absent longitudinal connectives. Interestingly, gain-of function phenotypes of *Dslmap* resemble those of reduction-of-function. However, one segment in particular appeared to be missing and was constantly located in the middle of the ventral nerve cord. The similarities of defects in both RNAi and overexpression techniques suggest that *Dslmap* may have a direct role in the formation of commissures. Furthermore, it indicates that the correct amount of *Dslmap* is important in CNS development. The reduction-of-function of *Dslmap* by RNAi could be more advantageous than gain-of-function by overexpression since overexpressing a protein may result in defects that would not occur under normal protein levels. However, this was not the case using our techniques since the defects appeared to be similar in both RNAi and overexpression. The resulting phenotypes associated with the reduction of *Dslmap*, demonstrated that this protein is essential for the formation of an intact ventral nerve cord. In wild-type embryos, the axons of the ventral nerve cord normally form a

ladder-like structure, revealed by BP102 antibody (Goodman and Doe 1993). Consecutive segments of the CNS (referred to as neuromere) are connected by two lateral longitudinal connectives, whereas each side of the axon scaffolds is interconnected by the anterior and posterior commissures. Within the CNS, each neuromere contains three basic types of axonal pathways; most CNS axons extend along a commissural pathway and cross the midline in the anterior and posterior commissures (Araújo and Tear, 2003). The ipsilaterally projecting axons extend on one side of the CNS only, and never cross the midline, whereas the motor neurons extend out to the periphery either on their own side of the CNS or after crossing the midline (Araújo and Tear, 2003). Here, the reported phenotypes revealed that two axonal pathways were perturbed, as defects are observed in the longitudinal connectives and in the commissural pathways. The phenotypes detected exhibited low penetrance in both RNAi and overexpression, but were more expressive in defects that varied between different lines.

We propose that the phenotypic defects found in the CNS of activated RNAi lines are due to a reduction in *D*SLMAP protein which possibly affects multiple functions that pertain to certain structural features such as the coiled-coil regions and the FHA domain. The coiled-coil region may be ideal for protein-protein interactions (Blazek *et al.*, 2005). The coiled-coil motif is a common structural feature, which confers protein stability by directing subunit oligomerization. It is also found in proteins that withstand considerable cellular stress such as motor proteins (Rose and Meier, 2004). Intermolecular coiled-coil motifs are also known to mediate the assembly of integral membrane components (Chapman *et al.*, 2001). The coiled-coil motifs have also been shown to be involved in intramolecular interactions with the fork head associated domain (Lee *et al.*, 2004). The

interactions mediated by the coiled-coil regions might have a potential role in the function of *Dslmap,* where a decrease of this protein may result in reduction of interactions maintained by the coiled-coil regions, which would in turn affect *Dslmap* homodimerization.

Another important structural property of SLMAP is being a tail-anchored membrane protein via hydrophobic amino acid residues at the C- terminus facilitating the integration of this protein into different membrane systems (Guzzo *et al.*, 2004). This property might help in understanding some of the defects observed in the CNS. A variety of proteins conserved in both vertebrates and invertebrates perform essential roles in neuronal development. While a number of these proteins are diffusible molecules acting at long range such as *netrins* and *wnt5* (Zou *et al.*, 2004), other axon guidance molecules are membrane-associated and function in a cell contact mediated fashion (Palmer and Klein, 2003). An example of these proteins include Ten a, Ephrin, and Synaptogamin (Ngernsiri *et al.*, 2005; Holder and Kelin., 1999; Littleton *et al.,* 1993; Bossing and Brand., 2002). In order for these proteins to function, they need to be membrane bound to efficiently cluster and activate their receptors. This theory that the tail-anchoring property of *Dslmap* might have a critical role in CNS development is confirmed by the presence of commissural defects that could be explained by the lack of key molecules controlling attractive and repulsive interactions at the midline that are necessary for guiding axons across the midline to the contralateral side and preventing them from recrossing (Tessier-Lavigne and Goodman, 1996). De-regulation of *Dslmap* consequently caused misrouting of axons, leading to a fused or less distinct appearance of commissures observed with BP102 staining. Mutations in molecules regulating axon

crossing of the midline reported similar defects in commissures. Among these molecules are Netrins and Slit ligands (Mitchell *et al.*, 1996 & Kidd *et al.*, 1999) and their respective receptors, frazzled and the robos (Kolodzieg *et al.*, 1996 & Kidd *et al.*, 1998). The RNAi and overexpression lines activated with a pan-neuronal driver exhibited defects resembling those found in glial activated lines suggesting that *Dslmap* may have an important role in both glia and neurons. Glia and neurons participate in extensive reciprocal interactions at the midline that are essential for the formation and separation of the two distinct segmental commissures (Sepp and Auld, 2003; Hummel *et al.*, 1999). Therefore, when *Dslmap* is down regulated in glia, neuronal defects such as fused commissures are also evident which further support an essential interaction between glia and neurons for the developing CNS. In turn, we predict that down regulating *Dslmap* in neurons might also result in glial defects, which would further suggest that glia and neurons are co-dependent for neurogenesis.

The variability in the expressivity of defective phenotypes between different transgenic lines might be caused by the varying efficiency of RNAi mediated silencing, which varies between different lines (Kennerdell and Carthew, 2000). This is considered one of the drawbacks of the RNAi technique in which silencing of *Dslmap* was frequently variable, with only a fraction of embryos exhibiting complete silencing. Such variability was reported by Bonini and Fortini (2003) when it was observed that using the same Gal4 line to activate different transgenic lines of the same UAS transgene gave different phenotypes termed strong, medium and weak. The variation in the strength of RNAi effects between different transformant lines carrying the same expressed IR transgene was observed at the level of target mRNA abundance, as it was tested with *in*

situ hybridization revealing a pooled population of activated embryos exhibiting a great reduction in mRNA levels. It is assumed that these differences are due to position effects, depending on the point of transgene insertion in the genome. The severity of the silencing response in activated lines is not only sensitive to the level of expressed IR (Fortier and Belote, 2000; Piccin *et al.*, 2001) but also to temperature (Duffy, 2002). This could apply to the variability of defects observed in activated lines, since they were only heat shocked only for 1 hour at 29°C and then allowed to recover at room temperature. Fortier and Belote (2000) tested the effect of temperature on the degree of silencing using three independent GAL4 lines and found that the silencing induced by the IR of tranformer-2 was temperature dependent and the effects were more severe at 29°C and absent at 22°C. One possibility for this temperature dependence is that GAL4 is more active at 29°C than at lower temperatures (Duffy, 2002). This is not surprising since the Gal4 protein is isolated from *Saccharomyces cerevisiae,* which is typically grown at approximately 30°C.

The data presented in this work revealed that a coiled-coil tail-anchored membrane protein exists in fruit flies and shares a significant similarity to mammalian SLMAP3 isoform. Structural features such as the highly conserved fork head associated domain (55.9%) and the presence of a putative transmembrane domain and coiled-coil regions suggest that SLMAP may serve multiple cellular roles. *In situ* hybridization on whole mount embryos showing ubiquitous expression of *Dslmap* at various stages of embryonic development is indicative of the importance of *Dslmap* in embryonic development in flies. In agreement with the function of tail-anchored membrane proteins, *Dslmap* through its hydrophobic residues at the extreme carboxyl terminus may

serve a role in targeting *Dslmap* to different neuronal compartments. The other possibility is that *Dslmap* could serve as a receptor on axons interacting with axonal guidance molecules through its extensive coiled-coil regions.

REFERENCES

Abell, B. M., Jung, M., Oliver, J.D., Knight, B.C., Tyedmers, J., Zimmermann R., and High, S. 2003. Tail-anchored and signal-anchored proteins utilise overlapping pathways during membrane insertion. *J. Biol. Chem* 278 (8), 5669-5678.

Adams, M. D., Celniker, S. E., Holt, R. A., Evans, C. A., Gocayne, J. D., Amanatides, P. G., Scherer, S. E., Li, P. W., Hoskins, R. A., and Galle, R. F. 2000. The genome sequence of *Drosophila melanogaster*. *Science* 287, 2185-2195.

Ahmad, A., Nagamatsu, N., Kouriki, H., Takami., Y and Nakayama, T. 2001. Leucine zipper motif of chicken histone acetyltransferase-1 is essential for in vivo and in vitro interactions with the p48 subunit of chicken chromatin assembly factor-1. *Nucleics Acids Res.* 29(3), 629-637.

Altschul, S.F., Gish, W., Miller, W., Myers, E.W., and Lipman, D. J. 1990. Basic Local Alignment Search Tool (BLAST) server. *J. Mol. Biol.* 215, 403-410.

Aplin, A.C., and Kaufman, T.C. 1997. Homeotic transformation of legs to mouth parts by proboscipedia expression in *Drosophila* imaginal discs. *Mech. Dev.* 62,51–60.

Araújo, S.J., and Tear, G. 2003. Axon guidance mechanisms and molecules: lessons from invertebrates. *Nat. Rev. Neurosci.* 4, 910-922.

Arendt, D. and Nubler-Jung, K. 1997. Dorsal or ventral: similarities in fate maps and gastrulation patterns in annelids, arthropods and chordates. *Mech. Dev.* 61, 7-21.

Arendt, D. and Nubler-Jung, K. 1999. Comparison of early nerve cord development in insects and vertebrates. *Development* 126, 2309-2325.

Bajjalieh, S.M. 1999. Synaptic vesicle docking and fusion. *Curr Opin Neurobiol.* 9(3):321-8.

Bernstein, E., Caudy A. A., Hammond, S. M. and Hannon, G. J. 2001. Role for a bidentate ribonuclease in the initiation step of RNA interference. *Nature* 409, 363–366.

Blazek, D., Barboric, M., Kohoutek, J., Oven, I., and Peterlin B. M. 2005. Oligomerization of HEXIM1 via 7SK snRNA and coiled-coil region directs the inhibition of P-TEFb. *Nucleic Acids Res.* 33(22), 7000-7010.

Bonini, N.M., and Fortini, M.E. 2003. Human neurodegenerative disease modeling using Drosophila. *Annu. Rev. Neurosci.* 26, 627–656.

Bossing, T., and Brand, A. 2002. Ephrin, a transmembrane ephrin with a unique structure, prevents interneuronal axons from exiting the Drosophila embryonic CNS. *Development* 129, 4205-4218.

Brand, A.H., and Perrimon, N. 1993. Targeted gene expression as a means of altering cell fates and generating dominant phenotypes. *Development* 118, 401–415.

Brand, A.H., and Perrimon, N. 1994. Raf acts downstream of the EGF receptor to determine dorsoventral polarity during *Drosophila* oogenesis. *Genes Dev.* 8,629–639.

Buckland, R., and Wild, F. 1989. Leucine zipper motifs extend. *Nature* (London). 338:547.

Burkhard, P., Strelkov, S. V., and Stetefeld, J. 2001. Coiled coils: a highly versatile protein folding motif. *Trends Cell Biol.* 11, 82–88.

Campbell, R. M. and Peterson, A. C. 1993. Expression of a *lacZ* transgene reveals floor plate cell morphology and macromolecular transfer to commissural axons. *Development* 119, 1217-1228.

Campos-Ortega, A.J., and Hartenstein,V. 1985. The embryonic development of *Drosophila melanogaster*. Springer-Verlag, New York.

Carroll, P.M., Dougherty, B., Macdonald, P.R., Browman, K., and FitzGeral, K. 2003. Model systems in Drug discovery: chemical genetics meets genomics. *Pharmacol. Ther.* 99, 183-220.

Coburn, G.A., and Cullen, B.R. 2003. siRNAs: a new wave of RNA-based therapeutics. *J. Antimicrob. Chemother.* 51(4), 753-756.

Cory, S., and Adams, J.M. 2002. The Bcl2 family: regulators of the cellular life-or-death switch. *Nat. Rev. Cancer* 2,647–656.

Duffy, J.B. 2002. GAL4 system in Drosophila: a fly geneticist's Swiss army knife. *Genesis* 34, 1–15.

Durocher, D., and Jackson, S.P. 2002. The FHA domain. *FEBS Lett.* 513, 58-66.

Durocher, D., Taylor, I.A., Sarbassova, D., Haire, L.F., Westcott, S.L., Jackson, S.P., Smerdon, S.J., and Yaffe, M.B. 2000. The molecular basis of FHA domain: phosphopeptide binding specificity and implications for phosphor-dependent signaling mechanisms. *Mol. Cell* 6, 1169-1182.

Dzitoyeva, S., Dimitrijevic, N., and Manev, H. 2001. Intra-abdominal injection of double-stranded RNA into anesthetized adult Drosophila triggers RNA interference in the central nervous system. *Mol. Psychiatry* 6, 665-670.

Dzitoyeva, S., Dimitrijevic, N., and Manev, H. 2003. γ-Aminobutyric acid B receptor 1 mediates behavior-impairing actions of alcohol in Drosophila: Adult RNA interference and pharmacological evidence. *Proc. Natl. Acad. Sci.* USA. 100, 5485-5490.

Dzitoyeva, S., Dimitrijevic, N., and Manev. H. 2003. Identification of a novel Drosophila gene, beltless, using injectable embryonic and adult RNA interference (RNAi). *BMC Genomics* 4,33.

Elmayan, T., Balzergue, S., Béon, F., Bourdon, V., Daubremet, J., Guenet, Y., Mourrain, P., Palauqui, J.C., Vernhettes, S., Vialle, T., Wostrikoff, K., and Vaucheret, H. 1998. Arabidopsis mutants impaired in cosuppression. *Plant Cell* 10, 1747-1758.

Enerly, E., Larsson, J., and Lambertsson A. 2002. Reverse genetics in *Drosophila*: From sequence to phenotype using *UAS*-RNAi transgenic flies. *Genesis* 34,152–155.

Engel, J. 1996. Domain organizations of modular extracellular matrix proteins and their evolution. *Matrix Biol.* 15, 295-299.

Fire, A., Xu, S., Montgomery, M. K., Kostas, S. A., Driver, S. E. and Mello, C. C. 1998. Potent and specific genetic interference by double-stranded RNA in Caenorhabditis elegans. *Nature* 391, 806-811.

Fischer, J.A., Giniger, E., Maniatis, T., and Ptashne, M. 1988. GAL4 activates transcription in *Drosophila. Nature* 332, 853–856.

Fortier, E., and Belote, J.M. 2000. Temperature-dependent gene silencing by an expressed inverted repeat in *Drosophila. Genesis* 26,240–244.

Giordano, E., Rendina, R., Peluso, I., and Furia, M. 2002. RNAi triggered by symmetrically transcribed transgenes in *Drosophila melanogaster. Genetics* 160, 637–648.

Goentoro, L.A., Yakoby, N., Goodhouse, J., Schupbach, T., and Shvartsman, S.Y. 2005. Quantitative analysis of the GAL4/UAS system in Drosophila oogenesis. *Genesis* 44, 66-74.

Gönczy, P., Echeverri, C., Oegema, K., Coulson, A., Jones, S.J., Copley, R.R, Duperon, J., Oegema, J., Brehm, M., Cassin, E., Hannak, E., Kirkham, M., Pichler, S., Flohrs, K., Goessen, A., Leidel, S., Alleaume, A.M., Martin, C., Özlü, N., Bork, P., and Hyman, A.A. 2000. Functional genomic analysis of cell division in C. elegans using RNAi of genes on chromosome III. *Nature* 408, 331-336.

Goodman, C.S. and. Doe, C.Q. 1993. Embryonic development of the Drosophila central nervous system. Cold Spring Harbor Laboratory Press, New York. pp. 1131-1206.

Greenwald, I. 1998. LIN-12/Notch signaling: lessons from worms and flies. *Genes Dev.* 12, 1751-1762.

Guzzo, R.M. 2003. Sarcolemmal Membrane Associated Proteins: Structure-Function Analysis and Localization Studies. *Ph.D. thesis.* University of Ottawa. p. 25, 171, 181.

Guzzo, R. M., Salih, M., Moore, E., and Tuana, B. C. 2005. Molecular properties of cardiac tail-anchored membrane protein SLMAP are consistent with structural role in arrangement of excitation-contraction coupling apparatus. *Am. J. Physiol. Heart Circ. Physiol.* 288, H1810- H1819.

Guzzo, R. M., Sevinc, S., Salih, M., and Tuana, B.C. 2004. A novel isoform of sarcolemmal membrane-associated protein (SLMAP) is a component of the microtubule organizing centre. *J. Cell Sci.* 117, 2271-2281.

Guzzo, R. M., Wigle, J., Salih, M., Moore, E., and Tuana, B. C. 2004. Regulated expression and temporal induction of the tail-anchored sarcolemmal-membrane-associated protein is critical for myoblast fusion. *Biochem. J.* 381, 599-608.

Hannon, G. 2002. RNA interference. *Nature* 418, 244-251.

Hay, B. A., Maile, R., and Rubin, G. M. 1997. P element insertion-dependent gene activation in the *Drosophila* eye. *Proc. Natl. Acad. Sci. USA.* 94, 5195-5200.

Heuer, J., Li, K., and Kaufman, T. 1995. The Drosophila homeotic target gene centrosomin(cnn) encodes a novel centrosomal protein with leucine zippers and maps to a genomic region required for midgut morphogenesis. *Development* 121, 3861-3876.

Hofmann, K., and Baron, M. Shading of multiple alignment files. BOXSHADE server (version 3.21).

Holder, N. and Klein, R. 1999. Eph receptors and ephrins: effectors of morphogenesis. *Development* 126, 2033-2044.

Hummel, T., Schimmelpfeng, K., and Klämbt, C. 1999a. Commissure formation in the embryonic CNS of *Drosophila*: I Identification of the required gene functions. *Dev. Biol.* 208, 381-398.

Hummel, T., Schimmelpfeng, K., and Klämbt, C. 1999b. Commissure formation in the embryonic CNS of *Drosophila*: II Function of the different midline cells. *Development* 126,771-779.

Irvine, K. D. 1999. Fringe, Notch, and making developmental boundaries. C*urr. Opin. Genet. Dev.* 9, 434-441.

Kakidani, H., and Ptashne, M. 1988. GAL4 activates gene expression in mammalian cells. *Cell* 52, 161-167.

Kalidas, S., and Smith, D.P. 2002. Novel genomic cDNA hybrids produce effective RNA interference in adult *Drosophila*. *Neuron* 33, 177–184.

Keleman, K., and Dickson, B.J. 2001. Short- and long-range repulsion by the Drosophila Unc5 netrin receptor. *Neuron* 32(4), 605-17.

Kennedy, T. E., Serafini, T., de la Torre, J.R and Tessier-Lavigne, M. 1994. Netrins are diffusible chemotropic factors for commissural axons in the embryonic spinal cord. *Cell* 78, 425–435.

Kennerdell, J.R., and Carthew, R.W. 1998. Use of dsRNA-mediated genetic interference to demonstrate that *frizzled* and *frizzled 2* act in the Wingless pathway. *Cell* 95,1017–1026.

Kennerdell,J.R., and Carthew, R.W. 2000. Heritable gene silencing in Drosophila using double-stranded RNA. *Nat. Biotechnol.* 18,896–898.

Ketting, R. F., Fischer, S. E., Bernstein, E., Sijen, T., Hannon, G. J., and Plasterk, R. H. 2001. Dicer functions in RNA interference and in synthesis of small RNA involved in developmental timing in *C. elegans*. *Genes Dev.* 15, 2654–2659.

Kidd, K., Brose, K., Mitchell, K.J., Fetter, R.D., Tessier-Lavigne, M., Goodman, C.S. and Tear, G. 1998. Roundabout controls axon crossing of the CNS midline and defines a novel subfamily of the evolutionary conserved guidance receptors. *Cell* 92, 205-215.

Kidd, T, Bland, K.S. and Goodman, C.S. 1999. Slit is the midline repellent for the robo receptor in *Drosophila*. *Cell* 96,785-794.

Kidokoro, Y. 2003. Roles of SNARE proteins and synaptotagmin I in synaptic transmission: studies at the Drosophila neuromuscular synapse. *Neurosignals* 12(1), 13-30.

Kim, M., Ahn, J.W., Song, K., Paek, K.H., and Pai, H.S. 2002. Forkhead-associated domains of the tobacco NtFHA1 transcription activator and the yeast Fhl1 forkhead transcription factor are functionally conserved. *J. Biol. Chem.* 277(41), 38781-38790.

Klambt, C., and Goodman, C.S. 1991a. The diversity and pattern of glia during axon pathway formation in the *Drosophila* embryo. *Glia* 4, 205-213.

Klämbt, C., Jacobs, J.R, and Goodman, C.S. 1991. The midline of the Drosophila central nervous system: A model for the genetic analysis of cell fate, cell migration, and growth cone guidance. *Cell* 64, 801-815.

Knecht , V., and Grubmüller, H. 2003. Mechanical Coupling via the Membrane Fusion SNARE Protein Syntaxin 1A: A Molecular Dynamics Study. *Biophys. J.* 84,1527-1547

Knight, S.W., and Bass, B. L. 2001. A role for the RNase III enzyme DCR-1 in RNA interference and germ line development in *Caenorhabditis elegans*. *Science* 293, 2269–2271.

Kolodzieg, P.A., Timpe, L.C., Mitchell, K.J., Fried, S.R., Goddman, C.S., Jan, L.Y., and Jan, Y.N. 1996. *frazzled* encodes a *Drosophila* member of the DCC immunoglobulin subfamily and is required for CNS and motor axon guidance. *Cell* 87, 197-204

Korey, C.A. and MacDonald, M.E. 2003. An over-expression system for characterizing *Ppt1* function in *Drosophila*. *BMC. Neuroscience* 4, 30.

Kuriyama, R., and Nislow C. 1992. Molecular components of the mitotic spindle. *Bioessays* 14(2), 81-88.

Kweon, D. H., Kim, C.S., and Shin, Y.K. 2003. Insertion of the Membrane-proximal Region of the Neuronal SNARE Coiled Coil into the Membrane. *J. Biol. Chem.* 278(14),12367-12373.

Lam, G., and Thummel, C.S. 2000. Inducible expression of double-stranded RNA directs specific genetic interference in Drosophila. *Curr. Biol.* 10, 957-963.

Landschulz, W.H., Johnson, P.F., and McKnight, S.L. 1988. The leucine zipper: a hypothetical structure common to a new class of DNA binding proteins. *Science* 240(4860), 1759 – 1764.

Laughon, A., Driscoll, R., Wills, N., and Gesteland, R.F. 1984. Identification of two proteins encoded by the Saccharomyces cerevisiae GAL4 gene. *Mol. Cell Biol.* 4, 268–275.

Laughon, A., and Gesteland, R.F. 1984. Primary structure of the Saccharomyces cerevisiae GAL4 gene. *Mol. Cell. Biol.* 4, 260–267.

Lee, J.R., Shin, H., Choi, J., Ko, J., Kim, S., Lee, H.W., Kim, K., Rho, S.H., Lee, J.H., Song, H.E., Eom, S.H., and Kim, E. 2004. An intramolecular interaction between the FHA domain and a coiled coil negatively regulates the kinesin motor KIF1A. *EMBO J.* 23, 1506-1515.

Lee, J.R., Shin, H., Ko, J., Lee, H., and Kim, E. 2003. Characterization of the movement of the kinesin motor KIF1A in living cultured neurons. *J. Biol. Chem.* 278(4), 2624-2629

Lee, W.C., Yoshihara, M., and Littleton, T. 2004. Cytoplasmic aggregates trap polyglutamine-containing proteins and block axonal transport in a *Drosophila* model of Huntington's disease. *Proc. Natl. Acad. Sci. USA.* 101(9), 3224-3229.

Lee, Y.S., and Carthew, R.W. 2003. Making a better RNAi vector for Drosophila: Use of intron spacers. *Methods* 30, 322-329.

Li, C., Hu, Y., Mayr, M., and Xu, Q. 1999. Cyclic Strain Stress-induced Mitogen-activated Protein Kinase (MAPK) Phosphatase 1 Expression in Vascular Smooth Muscle Cells Is Regulated by Ras/Rac-MAPK Pathways. *J. Biol Chem.* 274(36), 25273-25280

Li, J., Lee, G., Van Doren, S.R., and Walker, J.C. 2000. The FHA domain mediates phosphoprotein interactions. *J. Cell Sci.* 113, 4143-4149.

Lithgow, T.R., Van Driel, R., Bertram, J.F., and Strasser, A. 1994. The protein product of the oncogene Bcl-2 is a component of the nuclear envelope, the endoplasmic reticulum and the outer mitochondrial membrane. *Cell Growth Differ.* 5(4), 411–417.

Littleton, J.T., Bellen, H.J., and Perin, M.S. 1993. Expression of synaptotagmin in *Drosophila* reveals transport and localization of synaptic vesicles to the synapse. *Development* 118,1077-1088.

Littleton, J.T., and Ganetzky, B. 2000. Ion channels and synaptic organization: Analysis of the *Drosophila* genome. *Neuron* 26,35-43.

Lloyd, T. E., Verstreken, P., Ostrin, E. J.,. Phillippi, A., Lichtarge, O, and Bellen, H. J. 2000. A genome-wide search for synaptic vesicle proteins in *Drosophila*. *Neuron* 26,45-50.

Lupas, A., Van, D.M., and Stock, J. 1991. Predicting Coiled Coils from Protein Sequences. *Science* 252, 1162-1164.

Martinek, S., and Young, M.W. 2000. Specific Genetic Interference With Behavioral Rhythms in Drosophila by Expression of Inverted Repeats. *Genetics*. 156,1717–1725.

Matzke, M., Matzke, A.M., and Kooter, J.M. 2001. RNA: Guiding Gene Silencing. *Science* 293(5532), 1080-1083.

McCormack, K., Tanouye, M.A., Iverson, L. E., Lin, J.-W., Ramaswami, M., McCormack, T., Campanelli, J. T., Mathew, M. K. and Rudy, B. 1991. A role for hydrophobic residues in the voltage dependent gating of Shaker K+ channels. *Proc. Natl. Acad. Sci. USA*. 88, 2931-2935.

McLaughlin, T. and O'Leary, D. D. 1999. Functional consequences of coincident expression of EphA receptors and ephrin-A ligands. *Neuron* 22(4): 636-639.

Misquitta, L., and Paterson, B.M. 1999. Targeted disruption of gene function in Drosophila by RNA interference (RNA-i): A role for *nautilus* in embryonic somatic muscle formation. *Proc. Natl. Acad. Sci.* 6,1451–1456.

Mitchell, K.J., Doyle, J.L., Serafini, T., Kennedy, T.E., Tessier-Lavigne, M., Goodman, C.S., and Dickson, B.J. 1996. Genetic analysis of Netrin genes in Drosophila: Netrins guide CNS commissural axons and peripheral motor axons. *Neuron* 17,203-215.

Mount, S.M. 1982. A catalogue of splice junction sequences. *Nucleic Acids Res.* 10(2), 459-472.

Nagel, A.C., Maier, D., and Preiss, A. 2002. Green fluorescent protein as a convenient and versatile marker for studies on functional genomics in *Drosophila*. *Dev. Genes. Evol.* 212, 93–98.

Napoli, C., Lemieux, C., and Jorgensen, R. 1990. Introduction of a chimeric chalcone synthase gene into petunia results in reversible cosuppression of homologous gene in trans. *Plant Cell* 2,279-289.

Nguyen, M., Millar, D.G., Yong, W.V., Korsmeyer, S.J., and Shore, G.C. 1993. Targeting of Bcl-2 to the mitochondrial outer membrane by a COOH-terminal signal anchor sequence. *J. Biol. Chem.* 268, 25265–25268.

Nykänen, A., Haley, B., and Zamore, P.D. 2001. ATP requirements and small interfering RNA structure in the RNA interference pathway. *Cell* 107, 309–321.

Oshima, Y. 1982. Regulatory circuits for gene expression: the metabolism of galactose and phosphate. In: *The molecular biology of the yeast Saccharomyces, Metabolism and Gene expression*, Edited by Strathern, J.N., Jones, E.W., and Broach, J.R. Cold Spring Harbor Laboratory, Cold Spring Harbor, New York. pp. 159-180.

Palauqui, J.C., Elmayan, T., Pollien, J.M., and Vaucheret, H. 1997. Systemic acquired silencing: transgene-specific post-transcriptional silencing is transmitted by grafting from silenced stocks to non-silenced scions. *EMBO J.* 16, 4738–4745.

Palmer, A. and Klein, R. 2003. Multiple roles of ephrins in morphogenesis, neuronal networking, and brain function. *Genes Dev.* 17, 1429–1450.

Patel, N. H. 1994. Imaging neuronal subsets and other cell types in whole-mount *Drosophila* embryos and larvae using antibody probes. *Methods Cell Biol.* 44, 445-487.

Penny, E.B., and McCabe, B.D. 2005. All neuropathies great and small. *Clin. Invest.* 115(11), 2968–2971.

Piccin, A., Salameh, A., Benna, C., Sandrelli, F., Mazzotta, G., Zordan, M., Rosato, E., Kyriacou, C.P., and Costa, R. 2001. Efficient and heritable functional knock-out of an adult phenotype in *Drosophila* using a GAL4-driven hairpin RNA incorporating a heterologous spacer. *Nucleic Acids Res.* 29,55–55.

Pike, B.L., Hammet, A., and Heierhorst, J. 2001. Role of the N-terminal Forkhead-associated Domain in the Cell Cycle Checkpoint Function of the Rad53 Kinase. *Biol. Chem.* 276(17), 14019-14026.

Presente, A., Shaw, S., Nye, J., and Andres. A. 2002. Transgene-Mediated RNA interference Defines a Novel Role for Notch in Chemosensory Startle Behavior. *Genesis* 34,165-169.

Procopio, W., Pelavin, P., Lee, W., and Yeilding, N. M. 1999. Angiopoietin-1 and -2 Coiled-Coil Domains Mediate Distinct Homo-oligomerization Patterns, but Fibrinogen-like Domains Mediate Ligand Activity. *J. Biol Chem.* 274 (42), 30196-30201.

Quinn, L., Coombe, M., Mills, K., Daish, T., Colussi, P., Kumar S and Richardson, H. 2003. Buffy, a Drosophila Bcl-2 protein, has anti-apoptotic and cell cycle inhibitory functions. *EMBO J.* 22, 3568-3579.

Rabindran, S.K., Giorgi, G. Clos, J. and Wu, C. 1991. Molecular cloning and expression of a human heat shock factor. *Proc. Natl. Acad. Sci.* 88, 6906-6910.

Reichhart, J.M., Ligoxygakis, P., Naitza, S., Woerfel, G., Imler, J.L., and Gubb, D. 2002. Splice activated *UAS* hairpin vector gives complete RNAi knockout of single or double target transcripts in *Drosophila melanogaster*. *Genesis* 34,160–164.

Rhoads, D.D., and Routa, D.J. 1989. A software used for aligning sequences and locating restriction sites. Molecular Genetic Laboratory at the Center for Cancer Research. *Sequaid version 3.81*. Kansas state university, USA.

Robinson, L. J., and Martin, T. 1998. Docking and fusion in neurosecretion. *Curr. Opin. Cell Biol.* 10(4), 483-492.

Roessel, P.V., Hayward, N.M., Barros, C.S., and Brand, A.H. 2002. Two-color GFP imaging demonstrates cell autonomy of GAL4-driven RNA interference in *Drosophila*. *Genesis* 34,170–173.

Rogina, B., and Helfand, S.L. 2004. Sir2 mediates longevity in the fly through a pathway related to calorie restriction. *Proc. Natl. Acad. Sci. USA.* 101(45), 15998-16003.

Roman, G. 2004. The genetics of Drosophila transgenics. *BioEssays.* 26, 1243–1253.

Rose, A., and Meier, I. 2004. Scaffolds, levers, rods and springs: diverse cellular functions of long coiled-coil proteins. *Cell. Mol. Life. Sci.* 61(16), 1996-2009.

Rothberg, J. M., Jacobs, J. R., Goodman, C. S. and Artavanis-Tsakonas, S. 1990. *slit*: an extracellular protein necessary for development of midline glia and commissural axon pathways contains both EGF and LRR domains. *Genes Dev.* 4, 2169-2187.

Rubin, G. M., Yandell, M. D., Wortman, J. R., Gabor Miklos, G. L., Nelson, C. R., Hariharan, I. K., Fortini, M. E., Li, P. W., Apweiler, R., and Fleischmann W. 2000. Comparative genomics of the eukaryotes. *Science* 287, 2204-2215.

Ruiz, M.T., Voinnet, O., and Baulcombe, D.C. 1998. Initiation and maintenance of virus-induced gene silencing. *Plant Cell* 10, 937-946.

Sarge, K.D., Zimarino, V., Holm, K., Wu, C., and Morimoto, R. I. 1991. Cloning and characterization of two mouse heat shock factors with distinct inducible and constitutive DNA binding ability. *Genes Dev.* 5, 1902-1911.

Schindelholz, B., Knirr, M., Warrior, R., and Zinn, K. 2001. Regulation of CNS and motor axon guidance in Drosophila by the receptor tyrosine phosphatase DPTP52F. *Development* 128,4371–4382.

Schmid, A., Schindelholz, B., and Zinn, K. 2002. Combinatorial RNAi: a method for evaluating the functions of gene families in *Drosophila. Trends Neurosci.* 25,71–74.

Schmidt, H., Richert, C., Bossing, T., Vef, O., Urban, J., and Technau, G.M. 1997. The embryonic central nervous system lineages of *Drosophila melanogaster*. II. Neuroblast lineages derived from the dorsal part of the neuroectoderm. *Dev. Biol.* 189, 186-204.

Schultz, J., Milpetz, F., Bork, P., and Ponting,C. 1998. SMART: Simple Modular Architecture Research Tool: Identification of signaling domains. *Proc. Natl. Acad. Sci.USA* 95(11), 5857-5864.

Sears, H.C., Kennedy, C.J., and Garrity, P.A. 2003. Macrophage-mediated corpse engulfment is required for normal Drosophila CNS morphogenesis. *Development* 130, 3557-3565.

Sedaghat, Y., Miranda, W.F., and Sonnenfeld, M.J. 2002. The jing Zn-finger transcription factor is a mediator of cellular differentiation in the Drosophila CNS midline and trachea. *Development* 129(11), 2591-2606.

Sepp, K., and Auld, V. J. 2003. Reciprocal interactions between neurons and glia are required for *Drosophila* nervous system development. *Neuroscience* 23, 8221– 8230.

Serafini, T., Colamarino, S.A., Leonardo, E.D., Wang, H., Beddington, R., Skarnes, W.C., and Tessier-Lavigne, M. 1996. Netrin-1 is required for commissural axon guidance in the developing vertebrate nervous system. *Cell* 87, 1001–1014.

Simonelig, M., and Anxolabehere, D. 1991. A P-element of *Scaptomyza pallida* is active in *Drosophila melanogaster. Proc. Natl. Acad. Sci.USA.* 88, 6103-6107.

Simpson, P. 1997. Notch signaling in development: on equivalence groups and asymmetric development potential. *Curr. Opin. Genet. Dev.* 7, 537-542.

Sollner, T., Whiteheart, S. W., Brunner, M., Erdjument-Bromage, H., Geromanos, S., Tempst, P. and Rothman, J. E. 1993. SNAP receptors implicated in vesicle targeting and fusion. *Nature* 362, 318-324.

Soutschek, J., Akinc, A., Bramlage, B., Charisse, K., Constien, R., Donoghue, M., Elbashir, S., Geick, A., Hadwiger, P., Harborth, J., John, M., Kesavan, V., Lavine, G., Pandey, R.K., Racie, T., Rajeev, K.G., Rohl, I., Toudjarska, I., Wang, G., Wuschko, S., Bumcrot, D., Koteliansky, V., Limmer, S., Manoharan, M., and Vornlocher, H.P. 2004. Therapeutic silencing of an endogenous gene by systemic administration of modified siRNAs. *Nature* 432, 173-178.

Storey, K.G., Selleck, M.A., and Stern, C.D. 1995. Neural induction and regionalisation by different subpopulations of cells in Hensen's node. *Development* 121(2), 417-428.

Sun, X., Morozova, T., and Sonnenfeld, M. 2006. Glial and neuronal functions of the Drosophila homolog of the human SWI/SNF gene ATR-X (DATR-X) and the jing zinc-finger gene specify the lateral positioning of longitudinal glia and axons. *Genetics* 173(3), 1397-1415.

Sun, Z., Hsiao, J., Fay, D.S., and Stern, D.F. 1998. Rad 53 FHA domain associated with phosphorylated Rad9 in the DNA damage checkpoint. *Science* 281, 272-274.

Tessier-Lavigne, M., and Goodman, C.S. 1996. The molecular biology of axon guidance. *Science* 274, 1123-1133.

Thakur, A. 2003. RNA interference revolution. *J. Biotechnol.* 6(1).

Thompson, J.D., Higgins, D.G., and Gibson, T.J. 1994. CLUSTAL W: improving the sensitivity of progressive multiple sequence alignment through sequence weighting, position-specific gap penalties and weight matrix choice. *Nucleic Acids Res.* 22(22), 4673-4680.

Thorens, B., Sarkar, H. K., kaback, H. R. and Lodish, H. 1988. Cloning and functional expression in bacteria of a novel glucose transporter present in liver, intestine, kidney and b-pancreatic islet cells. *Cell* 55, 281-290.

Tufan, C., Akdogan, I., and Adiguzel, E. 2004. Shell-less culture of the chick embryo as a model system in the study of developmental neurobiology. *Neuroanatomy* 3, 8–11.

van der Krol, A.R., Mur, L.A., Beld, M., Mol, J.N.M., and Stuitje, A.R. 1990. Flavonoid genes in petunia: addition of a limited number of gene copies may lead to a suppression of gene expression. *Plant Cell* 2,291-299.

Voinnet, O., Vain, P., Angell, S., and Baulcombe, D.C. 1998. Systemic spread of sequence-specific transgene RNA degradation in plants is initiated by localized introduction of ectopic promoterless DNA. *Cell* 95,177–187.

Wang, Y., Devereux, W., Woster, P.M., and Casero, A. 2001. Cloning and characterization of the mouse polyamine-modulated factor-1 (mPMF-1) gene: an alternatively spliced homologue of the human transcription factor. *Biochem J.* 359, 387-392.

Warrick, J. M., Chan, H.Y., Gladys L., Board, G., Chai, Y., Henry L., Paulson., and Bonini, N.M. 1999. Suppression of polyglutamine-mediated neurodegeneration in Drosophila by the molecular chaperone HSP70. *Nat. Genet.* 23, 425 – 428.

Wattenberg, B., and Lithgow, T. 2001. Targeting of C-Terminal (Tail)-Anchored Proteins: Understanding how Cytoplasmic Activities are anchored to Intracellular Membranes. *Traffic* 2, 66–71.

Webster, N., Jin, J. R., Green, S., Hollis, M. and Chambon, P. 1988. The yeast UAS_G is a transcriptional enhancer in human hela cells in the presence of the GAL4 *trans*-activator. *Cell* 52, 169–178.

White, M.K., and Weber, M.J. 1989. Leucine-zipper motif update. *Nature* 340, 103-104.

Wielowieyski, P.A., Sevinc, S., Guzzo, R., Salih, M., Wigle, J. T. and Tuana, B.C. 2000. Alternative Splicing, Expression, and Genomic Structure of the 3' Region of the Gene Encoding the Sarcolemmal-associated Proteins (SLAPs) Defines a Novel Class of Coiled-coil Tail-anchored Membrane Proteins. *J. Biol. Chem.* 275, 38474-38481.

Wigle, J.T. 1997. Molecular Cloning, Characterization and Expression of a Novel Family of Tail-Anchored Membrane Proteins from the Myocardium. *Ph.D.Thesis*. University of Ottawa. pp. 83-87.

Wigle, J.T., Demchyshyn, L., Pratt, M. A., Staines, W.A., Salih, M. and Tuana, B.S. 1997. Molecular cloning, expression, and chromosomal assignment of sarcolemmal-associated proteins. *J. Biol. Chem.* 272, 32384-32394.

Wilson, C., Goberdhan D.C.I., and Steller H. 1993. *Dror*, a potential neurotrophic receptor gene, encodes a *Drosophila* homolog of the vertebrate Ror family of Trk-related receptor tyrosine kinases. *Proc. Natl. Acad. Sci.* 90, 7109-7113.

Wolpert, L. Principles of Development. Edited by Beddington, R., Jessell, T., Lawrence, P., Meyerowitz, E., and Smith, J. 2002. Oxford press *(2^{nd} Edition)* pp.49.

Wolpert Wu, J.Y., and Rao, Y. 1999. Fringe: defining borders by regulating the notch pathway. *Curr Opin Neurobiol.* 9, 537–543.

Xue, M., and Zhang, B. 2002. Do SNARE proteins confer specificity for vesicle fusion? *Proc. Natl. Acad. Sci. USA.* 99(21), 13359-133.

Yang, Y., Gehrke,S., Haque, E., Imai, Y., Kosek,J., Yang, L., Beal, M.F., Nishimura, I., Wakamatsu, K., Ito, S., Takahashi, R., and Lu, B. 2005. Inactivation of Drosophila DJ-1 leads to impairments of oxidative stress response and phosphatidylinositol 3-kinase/Akt signaling. *Proc. Natl. Acad. Sci. USA.* 102(38), 13670-13675.

Zhou, L., Schnitzler, A., Agapite, J., Schwartz, L.M., Steller, H., and Nambu, J.R. 1997. Cooperative functions of the reaper and head involution defective genes in the programmed cell death of *Drosophila* central nervous system midline cells. *Proc. Natl. Acad. Sci. USA.* 94,5131–5136.

Zou, Y. 2004. Wnt signaling in axon guidance. *Trends Neurosci.* 27(9).